Computational modeling of mechanobiology in intact and healing rat Achilles tendon

Notermans, Thomas

2021

Document Version:
Publisher's PDF, also known as Version of record

Computational modeling of mechanobiology in intact and healing rat Achilles tendon

Thomas Notermans

LUND
UNIVERSITY

DOCTORAL DISSERTATION

by due permission of the Faculty of Engineering, Lund University, Sweden.
To be defended in Segerfalksalen BMC A10, Sölvegatan 17, Lund

June 18th 2021 at 14.00

Faculty opponent
Professor Jeffrey W. Holmes

Cover artwork by Thomas Notermans depicting finite element model predictions for heterogeneous tissue production during tendon healing.

Department of Biomedical Engineering
Lund University
P.O. Box 118, SE-221 00 Lund
Sweden

ISBN: 978-91-7895-915-0 (print)

ISBN: 978-91-7895-916-7 (pdf)

ISRN-nr: LUTEDX/TEEM-1124-SE

Report No. 2/21

Printed in May 2021 by Tryckeriet i E-huset, Lund, Sweden

Public defence

June, 18th, 2021, 14.00 in Segerfalksalen
BMC A10, Lund University, Sölvegatan 17, 222 42 Lund, Sweden

Supervisors

Prof. Hanna Isaksson
Department of Biomedical Engineering, Lund University

Dr. Hanifeh Khayyeri
Department of Biomedical Engineering, Lund University

Faculty opponent

Prof. Jeffrey W. Holmes
Departments of Biomedical Engineering, Surgery and Medicine
University of Alabama, Birmingham, Alabama, USA

Board of examination

Prof. Toni Arndt
Department of Sport and Health Sciences
Swedish School of Sport and Health Sciences, GIH, Sweden

Prof. Jonas Stålhand
Department of Management and Engineering
Linköping University, Linköping, Sweden

Associate Prof. Darcy Wagner
Department of Experimental Medical Science
Lund University, Lund, Sweden

Deputy member: Prof. Aylin Ahadi
Department of Mechanical Engineering
Lund University, Lund, Sweden

Deputy member: Associate Prof. Frida Sandberg
Department of Biomedical Engineering
Lund University, Lund, Sweden

Organization LUND UNIVERSITY Department of Biomedical Engineering Box 118, 211 00 Lund, Sweden	**Document name** DOCTORAL DISSERTATION **Date of issue** June 18, 2021
Author: Thomas Notermans	Sponsoring organization

Title: Computational modeling of mechanobiology in intact and healing rat Achilles tendon

Abstract

Tendons fulfill an important musculoskeletal function by enabling energy-efficient force transmission between muscles and bones. The tendon is a collagen-rich connective tissue that adapts to mechanical loading through mechanobiological processes. The tendon contains a hierarchical collagen fiber structure that displays complex mechanical behaviour by storing and dissipating energy. Current understanding of how tendon properties adapt to short and long-term mechanical loading is limited, but is key to prevent tendon disease and design optimal rehabilitation protocols after tendon rupture. Recently, an increasing amount of small animal experiments have investigated how intact and healing tendons adapt *in vivo* upon different mechanical loading regimens. Yet, limited numerical models have investigated tendon mechanobiology; even though existing modeling tools from other research fields are available and the amount of experimental data for validation is growing.

The aim of this thesis was to investigate the mechanobiology of intact and healing tendon by utilizing and developing advanced numerical models. First, a 3D finite element framework was used to determine the constitutive viscoelastic material properties of intact healthy tendons in rats. The material properties were fitted to experimental data from rats that were subjected to two loading regimens, i.e. free cage activity (full loading) and reduced loading, for five weeks. The resulting material properties showed strong differences in both elastic and damping properties of the collagen between the rats that were subjected to full or reduced loading.

Using this material model, a finite element mechanobiological healing framework for Achilles tendons was developed. The adaptive healing model investigated how principal strain and cell infiltration can govern tissue regeneration. The tendon model was stimulated with different levels of external loading, mimicking physiological and sub-physiological load levels explored in animal experiments. Model predictions of the spatio-temporal evolution of tissue distribution, collagen alignment and mechanical properties (stiffness, creep behaviour and strain levels) were validated by comparison with experimental measurements from rat Achilles tendon throughout the first four weeks of spontaneous healing after rupture. Interestingly, both strain-dependent and cell density-dependent tissue production were identified as possible explanations for decreased tissue production in the tendon core during healing.

The healing framework was expanded to predict formation of different tissue types during healing. According to established tissue differentiation frameworks in bone fracture healing, different mechanobiological factors were explored to regulate the formation of different tissue types, i.e. tendon-, cartilage-, fat- and bone-like tissue. This framework is the first to reproduce experimental observations of these tissues. It provides several potential mechanisms of mechanobiological regulation of the formation of different tissue types during tendon healing.

In summary, this thesis investigated mechanobiology in intact and healing tendon. An adaptive framework was developed that enabled the prediction of heterogeneous tissue distribution, organization, differentiation, and evolution of mechanical function during tendon healing. The spatial distribution of mechanical stimuli, particularly strain, but also biological stimuli such as cells and oxygen, were identified as potential mechanisms to regulate tendon healing by influencing formation of different tissue types, tissue alignment and the recovery of mechanical properties. Further development and thorough characterization of these models could expand our understanding of mechanobiological, biomechanical or biological processes in intact, diseased or healing tendons. Ultimately, these models could help designing optimal loading regimens to prevent chronic tendon disease or stimulate tendon healing after rupture.

Key words: collagen, finite element model, mechano-regulation, mechanical properties, strain, oxygen, viscoelasticity

Classification system and/or index terms (if any)

Supplementary bibliographical information ISRN: LUTEDX/TEEM-1124-SE Report No. 2/21		**Language:** English
		ISBN: 978-91-7895-915-0 (print) ISBN: 978-91-7895-916-7 (pdf)
Recipient's notes	**Number of pages** 250	Price
	Security classification	

Populärvetenskaplig sammanfattning

Hälsenan förbinder hälbenet med vadmusklerna. Senor består till största del av kollagenfibrer som kan överföra stora krafter. Fibrerna är inbäddade i en mjuk, proteinrik vävnad som innehåller stora mängder vatten. Olyckligtvis har hälsenerupturer blivit allt vanligare till följd av ett ökat intresse för sportaktiviteter hos allmänheten. Trots att det finns många olika behandlingar och rehabiliteringsprotokoll efter en hälsenruptur, är det fortfarande oklart vilken behandling som medför bäst resultat. Detta beror delvis på att vi saknar en djupare förståelse för hur den läkande hälsenan anpassar sig till olika typer av fysisk aktivitet. De olika rehabiliteringsprotokollen, t.ex. immobilisering genom gipsning, passiva ankelrörelser, gång, att springa och/eller hoppa, utsätter senan för olika nivåer av mekanisk belastning. Mekanobiologi är studien om hur fysiska krafter påverkar respons och funktion hos celler och vävnader. För att förstå senans mekanobiologi har djurexperiment undersökt hur senor reagerar på olika belastningsprotokoll. I den här avhandlingen presenteras först en sammanställning av litteratur där både den intakta och den läkande senans mekanobiologi har studerats experimentellt.

Att förstå hur belastning påverkar senans egenskaper är utmanande. I detta avseende är beräkningsmodeller värdefulla verktyg. Idag finns dock endast en handfull olika beräkningsmodeller som kan beskriva de mekanobiologiska processerna i senan. Den här avhandlingens mål var att utveckla beräkningsmodeller för att undersöka hur den friska och den läkande senans egenskaper påverkas av mekanisk belastning. En materialmodell användes för att beskriva de mekaniska egenskaperna hos kollagenfibrerna, den mjuka vävnaden och vattnet inuti senan. Materialmodellen fångade det mekaniska beteendet hos kollagenfibrerna genom att både beskriva senans elastiska och tidsberoende egenskaper. Materialmodellen har använts för att undersöka hur de mekaniska

egenskaperna hos hälsenan ändras när senans belastning från vadmusklerna reduceras under fem veckor. Resultaten visade att både de elastiska och tidsberoende mekaniska beteendena hos kollagenet ändrades i de senor som utsattes för nedsatt belastning.

En ny beräkningsmodell som undersökte spatiala ändringar i senans egenskaper under läkningsprocessen utvecklades för första gången. Modellen användes för att utforska hur lokala deformationer, t.ex. töjning, ger signaler till celler att producera kollagen. Modellen förutspådde väldigt höga töjningar i den inre delen av den läkande senan i jämförelse med de yttre delarna av senan. Den mest lovande modellen förutspådde att kollagenet skulle produceras i de yttre delarna först och inte i den inre delen, där stor töjning hämmade kollagenproduktionen. Intressant nog så stämde det här väl överens med experimentell data. Det finns också andra processer som kan påverka kollagenproduktionen, t.ex. celler som rör sig in i den skadade zonen för att börja reparera senan. Att lägga till den här cellaktiviteten förbättrade modellens förmåga att beskriva de experimentella observationerna av att kollagenet först produceras i senans perifera områden.

Litteratursammanställningen identifierade en ökande mängd bevis på att även fett-, brosk och benliknande vävnader bildas under läkningsprocessen av hälsenor i råttor och möss. Bildningen av dessa vävnadstyper har tidigare undersökts med beräkningsmodeller vid läkning av benfraktur. Till att förutsäga hur olika vävnadstyper bildas beroende på mekanisk belastning implementerades liknande beräkningsmodeller för den läkande senan. Detta möjliggjorde att modellen kunde prediktera bildningen av fett-, brosk och benliknande vävnader, vilket i stort liknande de experimentella observationer som gjorts under senans läkningsprocess. Resultaten antyder att mekanobiologi kan spela en viktig roll i bildningen av olika vävnadstyper under senans läkningsprocess.

Sammanfattningsvis undersökte denna avhandling mekanobiologiska processer i friska och skadade senor med hjälp av beräkningsmodeller. Läkningsprocessen hos senor undersöktes genom att utforska möjliga mekanismer som kan förklara hur den spatiala distributionen av deformation och celler kan påverka heterogen vävnadsproduktion och differentiering. Dessa beräkningsmodeller är viktiga verktyg för att uppnå en ökad förståelse om senans beteende, då experiment är kostsamma, tidskrävande, svåra att genomföra och ofta resulterar i data som är svår att tyda. Ramverket för modellerna som utvecklats i den här avhandlingen, samt ytterligare utveckling av dessa eller liknande modeller, är ett värdefullt bidrag för att identifiera de processer som påverkar senans respons till på belastningsprotokoll. Dessa insikter kommer i sin tur att kunna tillåta utveckling av behandlingar och rehabiliteringsprotokoll för patologiska eller skadade senor.

Abstract

Tendons fulfill an important musculoskeletal function by enabling energy-efficient force transmission between muscles and bones. The tendon is a collagen-rich connective tissue that adapts to mechanical loading through mechanobiological processes. The tendon contains a hierarchical collagen fiber structure that displays complex mechanical behaviour by storing and dissipating energy. Current understanding of how tendon properties adapt to short and long-term mechanical loading is limited, but is key to prevent tendon disease and design optimal rehabilitation protocols after tendon rupture. Recently, an increasing amount of small animal experiments have investigated how intact and healing tendons adapt *in vivo* upon different mechanical loading regimens. Yet, limited numerical models have investigated tendon mechanobiology; even though existing modeling tools from other research fields are available and the amount of experimental data for validation is growing.

The aim of this thesis was to investigate the mechanobiology of intact and healing tendon by utilizing and developing advanced numerical models. First, a 3D finite element framework was used to determine the constitutive viscoelastic material properties of intact healthy tendons in rats. The material properties were fitted to experimental data from rats that were subjected to two loading regimens, i.e. free cage activity (full loading) and reduced loading, for five weeks. The resulting material properties showed strong differences in both elastic and damping properties of the collagen between the rats that were subjected to full or reduced loading.

Using this material model, a finite element mechanobiological healing framework for Achilles tendons was developed. The adaptive healing model investigated how principal strain and cell infiltration can govern tissue regeneration. The tendon model was stimulated with different levels of external

loading, mimicking physiological and sub-physiological load levels explored in animal experiments. Model predictions of the spatio-temporal evolution of tissue distribution, collagen alignment and mechanical properties (stiffness, creep behaviour and strain levels) were validated by comparison with experimental measurements from rat Achilles tendon throughout the first four weeks of spontaneous healing after rupture. Interestingly, both strain-dependent and cell density-dependent tissue production were identified as possible explanations for decreased tissue production in the tendon core during healing.

The healing framework was expanded to predict formation of different tissue types during healing. According to established tissue differentiation frameworks in bone fracture healing, different mechanobiological factors were explored to regulate the formation of different tissue types, i.e. fibrous (like tendon or ligament), cartilage, and bone. This framework is the first to reproduce experimental observations of these tissue. It provides several potential mechanisms of mechanobiological regulation of the formation of different tissue types during tendon healing.

In summary, this thesis investigated mechanobiology in intact and healing tendon. An adaptive framework was developed that enabled the prediction of heterogeneous tissue distribution, organization, differentiation, and evolution of mechanical function during tendon healing. The spatial distribution of mechanical stimuli, particularly strain, but also biological stimuli such as cells and oxygen, were identified as potential mechanisms to regulate tendon healing by influencing formation of different tissue types, tissue alignment and the recovery of mechanical properties. Further development and thorough characterization of these models could expand our understanding of mechanobiological, biomechanical or biological processes in intact, diseased or healing tendons. Ultimately, these models could help designing optimal loading regimens to prevent chronic tendon disease or stimulate tendon healing after rupture.

List of appended papers

This thesis contains a review of the author's work in the field of biomedical engineering. The following selection of the author's publication is referred to in the text by their Roman numerals. Papers I-V are appended at the end of the thesis and have been reproduced with the permission of the copyright holders. In papers I-V, the author of this thesis contributed to the study design and was the main responsible for developing the numerical methods presented and analysing the results. The author of this thesis was the main writer of manuscripts I-V.

I. **T. Notermans**, M. Hammerman, P. Eliasson, H. Isaksson. Tendon mechanobiology in small animal experiments during post-transection healing. Review paper. (under review)

II. **T. Notermans**, H. Khayyeri, H. Isaksson. Understanding how reduced loading affects Achilles tendon mechanical properties using a fibre-reinforced poro-visco-hyper-elastic model. Journal of Mechanical Behaviour of Biomedical Materials, 2019, 96: 301-309

III. **T. Notermans**, P. Tanska, R.K. Korhonen, H. Khayyeri, H. Isaksson. A numerical framework for mechano-regulated tendon repair – simulation of early healing of the Achilles tendon. PLoS Computational Biology, 2021, 17(2): e1008636

IV. **T. Notermans**, H. Khayyeri, H. Isaksson. Predicting the effect of reduced load level and cell infiltration on spatio-temporal Achilles tendon healing. (under review)

V. **T. Notermans**, H. Isaksson. Predicting the formation of different tissue types during Achilles tendon healing: exploring mechano-regulated and oxygen-regulated frameworks. (in preparation)

Other related publications by the author:

VI. H. Khayyeri, M. Hammerman, M.J. Turunen, P. Blomgran, **T. Notermans**, M. Guizar-Sicairos, P. Eliassson, H. Isaksson. Diminishing effects of mechanical loading over time during rat Achilles tendon healing. PLoS one, 2020, 15(12): e0236681

In paper VI, the author of this thesis contributed to mechanical analysis, visualization and reviewing and editing of the manuscript.

Acknowledgements

Four and a half years in Sweden, and here we are. Particularly throughout the last year, it became so clear that the social interactions in- and outside research mean everything. I would like to thank everyone that has contributed to this thesis, and all social and sports activities throughout this journey, in one way or the other.

First of all, I would like to thank my main supervisor Hanna Isaksson for providing great guidance throughout this thesis work. Your eye for detail, high standard, while allowing the freedom to explore both literature and different simulation methods, created an interesting and pleasant work environment for me to perform the research in. I would also like to thank my co-supervisor Hanifeh Khayyeri for guiding me throughout my PhD. You always looked at our problems from a different angle and provided a new and interesting view to the work to improve the research and dissemination. In addition to my official supervisors, I would also like to thank Anna Gustafsson, Lorenzo Grassi, Malin Hammerman, Pernilla Eliasson, Petri Tanska and Rami Korhonen, who provided me with valuable opinions, creative ideas, practical help and co-authorship throughout different parts of the thesis work. Also, thanks to Linda Elowsson Rendin and Anna Löfdahl for allowing me to contribute to your work.

A special thanks to my opponent, Professor Jeff Holmes, and the members of the committee, Professor Toni Arndt, Professor Jonas Stålhand, Associate Professor Darcy Wagner, Professor Aylin Ahadi and Associate Professor Frida Sandberg, for carefully reading and scrutinizing my thesis work. Thank you, Johan Nilsson, for leading my defense and being a great head of department.

A big thanks goes out to all my other colleagues, and friends, in the biomechanics group, Deepak, Elin, Gustavo, Hannicka, Isabella, Joeri, Maria, Mikael, Sophie, Tobias, Yang, that contributed to a great atmosphere at work.

This also goes for all bachelor and master students that stayed at our group throughout the years. Particularly, the intern students from the Netherlands, Leon and Lissa, and the current thesis students, Daniel, Erika and Johanna. I really enjoyed the authentic FIKA experience on a daily basis, with the annual semla tasting as true highlight, but also the conference trips to Dublin, Phoenix, Stockholm and Tahko, and the weekend trips in Kuopio, Öland and Småland. Lorenzo, Elisa, Clara and now also Claudio, thank you for all the pleasant Pizza nights in Billeberga. Anna and the whole Gustafsson family, thanks for the great weekend in Småland and the friendship throughout the years. David, Deepak, Sofie and Joeri, thanks for the best midsommar weekend in Öland. Mikael, Minna and Eljas, thank you for the friendship, BBQs, football with Eljas and the ice skating weekend in Kuopio. Special thanks to Joeri, Floor, Jonathan and Karin, who made this whole PhD journey far easier than expected by providing comradery both in- and outside of work. This was very much appreciated, even more so throughout the last year. A big thanks to Anna, Elin, Isabella, Maria, and Tobias for proofreading, translating, designing and completing the thesis.

Other colleagues in the BMC and E-house, Andreas, Anke, Carl, Carlos, Cecilia, Franzi, Ingrid, Jasper, Jonatan, Klara, Moritz, Per, Peter, Rita, Tirthankar, Tommaso and William. I enjoyed the talks, afterworks, dinners and innebandy. Ingrid, thank you for the pleasant collaboration in the biomechanics course throughout the years.

Then I would also like to thank the BioMEP graduate school program, and particularly all organizers, supervisors and students, for the interesting annual meetings, friendship and support throughout my thesis work. Gustavo, a true friend, and I wish you all the best for the academic journey in Lund and beyond.

I would also like to thank my friends in the Netherlands, my corridor mates in Sparta, and all my friends and fellow football players at FC Helsingkrona (om man vill, och det vill man) and Limhamn Griffins (hass).

Finally, I would like to thank my loving family, Pap & Mam, Remy & Sarah, Opa & Oma, Oma, Ria & Paul, for supporting me. I would particularly like to thank Janine for supporting me, caring for me and being with me, every day throughout my whole PhD, while being so far away. We made it, together, and I can't wait to continue our life together in the Netherlands. Also, a big thanks to the Grolleman family, Johan & Henriëtte, Daniëlle & Rob, Opa & Oma, Guus, Ziggy & Flow, who always take great care of me, provide great support and friendship, and have given me another home.

List of abbreviations

ADAMT	a desintegrin and metalloproteinase with thrombospondin motifs
BMP	Bone morphogenic protein
COX	Cyclooxygenase
CR	Creep
ECM	Extracellular matrix
ENDO	Endochondral
FCA	Free cage-activity
FE	Finite element
FF	Fluid flow
HIF	Hypoxia-inducible factor
HS	Hydrostatic stress
LG	Lateral gastrocnemius
LOX	Lysyl oxidase
MG	Medial gastrocnemius
MMP	Matrix metalloprotease
NRMSE	Normalized root-mean-squared error
OSS	Octahedral shear strain
OXY	Oxygen

PE	Principal strain
PGE	Prostaglandin E
PP	Pore pressure
RUNX	Runt related transcription factor
SAXS	Small angle X-ray scattering
SCX	Scleraxis
SLRP	Small leucine-rich proteoglycans
SLS	Standard linear solid
SOX	SRY-box
SOL	Soleus
SR	Stress-relaxation
TAZ	Transcriptional co-activator with PDZ binding motif
TIMP	Tissue inhibitor of matrix metalloprotease
VEGF	Vascular endothelial growth factor

Contents

Paper I - Tendon mechanobiology in small animal experiments during post-transection healing.
Paper II - Understanding how reduced loading affects Achilles tendon mechanical properties using a fibre-reinforced poro-visco-hyper-elastic model.
Paper III - A numerical framework for mechano-regulated tendon repair – simulation of early healing of the Achilles tendon.
Paper IV - Predicting the effect of reduced load level and cell infiltration on spatio-temporal Achilles tendon healing.
Paper V - Predicting the formation of different tissue types during Achilles tendon healing: exploring mechano-regulated and oxygen-regulated frameworks.

1 Introduction

The Achilles tendon is a soft connective tissue that transmits load between three calf muscles and the calcaneus bone. Several studies reported increasing incidence of acute tendon ruptures throughout the last 50 years (Figure 1.1) [1-5]. Typically, men are more prone to Achilles tendon ruptures [2, 3, 5, 6]. Particularly men aged 30-40 years old comprise the highest risk group [3]. Another recent study found that Achilles tendon ruptures occurred mostly in men aged 20-39 years and in women aged 40-59 years, and they observed the largest increase in incidence rate for men and women aged 40-59 years old [5]. On the other hand, a study identified an increase in tendon rupture for all age groups [4]. The increase in tendon ruptures is mainly contributed to increasing participation in sports [4, 5]. Following rupture, the risk of re-rupturing the same tendon or rupturing the contralateral tendon is substantial. A study found a 7.1% risk of re-rupture at 8 weeks following non-operative treatment with functional rehabilitation [6]. Another study estimated that upon Achilles tendon rupture there was a 5-6.5% risk of rupturing the contralateral Achilles tendon and a 2.7-13.6% risk of re-rupturing the same Achilles tendon [7]. This study also found that age (30-39 years old) was a risk group for contralateral rupture.

Even though Achilles tendon rupture is quite frequent, there is no consensus on the optimal treatment after a rupture. One of the first clinical questions is whether to suture-repair the rupture tendon or not. Many reports have shown no or limited differences between surgical and non-surgical treatment [8, 9]. Additionally, minimally invasive treatments and open surgery have been found to lead to similar healing outcomes [10]. Typically, surgical treatment increases the risk of complications [11] and less-invasive therapies have improved over the last decades [10]. Consequently, surgical treatment is becoming less frequent [1, 2]. One study in Denmark observed an over 50% decrease in surgical treatment between 1994 and 2013 [1]. The rehabilitation regimen following the initial treatment could

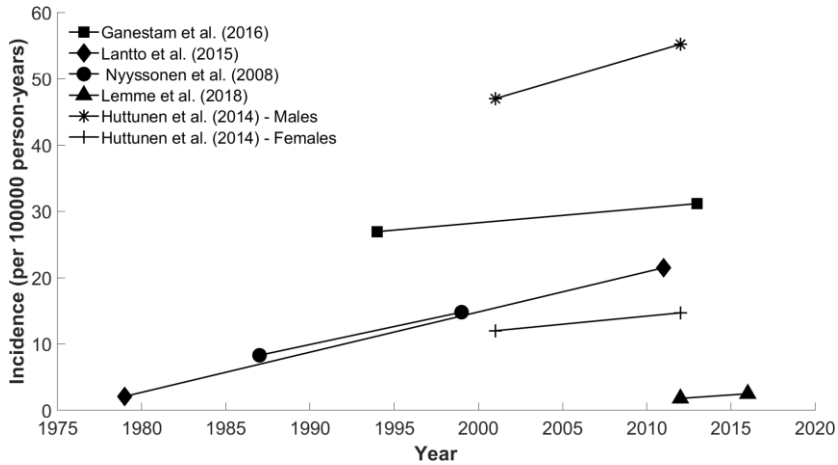

Figure 1.1. Evolution of the incidence rate of Achilles tendon rupture throughout the last 50 years. All studies showed an increase in incidence rate through time. The studies represent data from Denmark [1], Finland [3, 4], Sweden [2] and the US [5].

play a key role in determining the healing outcome [8]. For instance, early mobilization combined with ankle motion had positive effects on tendon healing compared to cast immobilization [12]. Besides the different types of rehabilitation activities, also the timing of treatments could play an important role in determining the healing outcome. However, several reviews have reported similar healing outcomes for early or late functional mobilization [13] or full weightbearing [9]. In summary, there is a wide range of possible treatments following Achilles tendon rupture and no consensus exists on the optimal rehabilitation regimen to stimulate tendon healing. One important reason for this is that our understanding of how tendon healing is affected by different levels and types of mechanical loading protocols, e.g. (im)mobilization, passive movements, training or exercise, is very limited.

It is well known that soft connective tissues such as tendons, cartilage and ligaments respond and adapt to mechanical loading. *Mechanobiology*, is an umbrella term that describes how the tissue adapts to external mechanical loading [14, 15]. In recent years, an increasing interest in tendon mechanobiology has led to a rapid advancement and insights into unraveling how the tendon responds to different external loads in both healthy and ruptured tendon. These experiments typically characterize how tendon composition, structure and mechanical properties develop and change as a function of different levels of external

mechanical loading. However, the complex data coming from these mechanobiological experiments is often challenging to interpret.

Computational modeling can be a valuable tool for gaining insight in tendon mechanobiology [16]. Numerical frameworks can help identifying mechanobiological mechanisms underlying complex features observed in experimental data. Although elaborate adaptive frameworks have investigated mechano-regulated healing and degeneration in other tissue, e.g. bone [17] and cartilage [18], very few computational models have investigated mechanobiological processes underlying intact tendon adaptation or tendon healing after rupture. Only recently, two studies have investigated how mechanical loading can affect tendon healing after rupture [19, 20]. These interesting works address different mechanobiological processes governing tendon healing by predicting the *temporal* evolution of tendon properties as a function of mechanical loading. Yet, these studies do not address the heterogeneity, i.e. the *spatial* distribution, of different tendon properties during healing, and do not investigate different mechanisms that may be involved in tendon heterogeneity. Interestingly, recent experimental studies have shown that tendon properties are heterogeneously distributed throughout healing [21]. Identifying possible (mechano)biological mechanisms underlying these spatial variations may be key to fully understand the benefits or drawbacks of mechanical loading in tendon healing. Additionally, a multitude of publications has shown the presence of cartilage-like [22, 23], bone-like [24] and fat-like [21] tissue properties throughout tendon healing. The occurrence of these different tissue types could be a result of tissue differentiation. Tissue differentiation in soft connective tissues, is the process where mesenchymal stem cells differentiate into more specialized tissue cells, such as fibroblasts, chondrocytes, osteocytes and adipocytes that subsequently produce fibrous-, cartilage-, bone- and fat-like tissue. There is ample experimental evidence that mechanical loading can play a key role in the formation of different tissue types during healing [25-27]. Utilizing existing adaptive bone healing frameworks [17] can be a valuable methodology to investigate how mechanobiology can play a role in tissue differentiation and the formation of different tissue types during healing. A better understanding of tendon mechanobiology, particularly during healing, can be an important tool for developing rehabilitation regimens to stimulate tendon healing.

2 Aim and design of the study

The overall aim of the thesis was to investigate mechanobiological mechanisms in intact and healing tendons after rupture by using and developing adaptive computational models.

The specific objectives were:

- To further validate an existing material model for intact tendon and to assess the mechanobiological adaption in viscoelastic mechanical properties upon a period of reduced daily loading (Study II).
- To develop a mechanobiological framework for describing collagen production, reorientation and mechanical properties during tendon healing after rupture (Study III).
- To characterize and validate the developed framework by investigating the effect of reduced load levels and cell infiltration on spatio-temporal predictions of tendon healing (Study IV).
- To explore different mechanobiological mechanisms underlying the formation of different tissue types by combining the developed tendon healing framework with existing mechanobiological tissue differentiation and formation frameworks (Study V).

The different objectives described above were addressed in five scientific studies (**I-V**) depicted in Figure 2.1. Although experimental studies have investigated tendon mechanobiology, only a very limited number of computational investigations have tried to identify principal mechanisms of mechanobiology. Therefore, computational modeling was performed in this thesis to investigate and identify mechanobiological mechanisms in intact and healing tendon. In particular, this thesis utilized an existing material model for tendon tissue and investigated mechanobiological adaptations in intact

tendon. Subsequently, an adaptive framework was developed to identify key mechanobiological processes involved in tendon healing. The spatial distribution of mechanical stimuli and tendon properties has not been extensively studied. To address this aspect, the finite element method was utilized in this work to account for the 3D geometry of tendon and allow the investigation of the spatial distribution of tendon properties and (mechanical) stimuli that may play an important role in tendon mechanobiology. This work addressed the heterogeneity of tendon healing, and investigated different mechanobiological mechanisms that may be involved in tendon heterogeneity. The developed computational framework was combined and validated with recent data from animal experiments on intact [28] and ruptured [21] Achilles tendons.

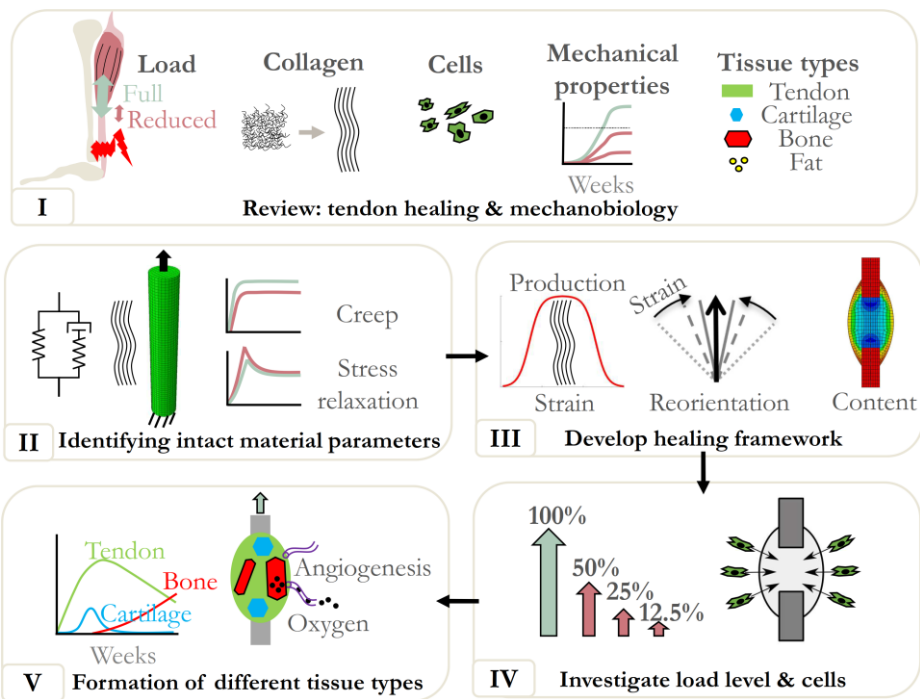

Figure 2.1. Overview of the study design. The Roman numerals I-V refer to the papers appended in the thesis and are linked to the aforementioned objectives.

3 Background

3.1 Tendon composition & structure

Tendon is a load-bearing connective tissue that consists mainly of water (55-70% wet weight) and a highly aligned collagen type 1 matrix (60-85% dry weight) [29]. The collagen matrix is organized in a hierarchical manner ranging from collagen molecules to fascicles (Figure 3.1 and 3.2) [30]. The collagen molecule is a long rod-like structure (1.5 nm diameter, 300 nm length; [31]), which self-assembles [32] into a fibrillar structure (20-280 µm diameter; [33]; 400-800 µm length; [34, 35]). The collagen molecules within the fibrils organize into a staggered arrangement at a characteristic distance (~67nm), called D-spacing [36]. The collagen molecules make a 5° angle compared to the fibril axis and fibrils are long, heterogeneous in size and tightly packed in parallel [37]. The fibril is reinforced by (non)reducible inter- and intrafibrillar crosslinks that strengthen and stabilize the fibril [38, 39]. Bundles of collagen fibrils form collagen fibers (diameter: 1-300 µm; [33]). These fibers display a waviness, also called crimp [40-42]. Large fibre bundles may organize into separate fascicles.

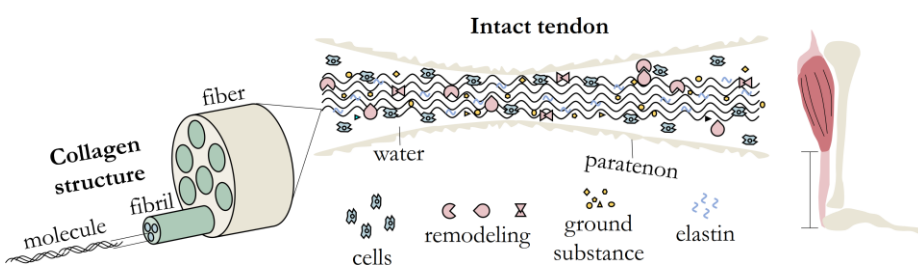

Figure 3.1. The composition and structure of a tendon, displaying its main constituents and the hierarchical collagen structure.

Collagen type 1 is the most abundant protein in the extracellular matrix (ECM). The other 15-40% dry weight consists of 'minor' collagens (type 3, 4, 5, 6, 9, 11, 12, 14) and other ECM proteins such as small leucine-rich proteoglycans (SLRPs; e.g. cartilage oligomeric matrix protein, decorin, biglycan, lumican, fibromodulin, tenascin-c, periostin), large proteoglycans (versican, aggrecan), elastin, matrix metalloproteases (MMPs), tissue inhibitors of matrix metalloproteases (TIMPs), a desintegrin and metalloproteinase with thrombospondin motifs (ADAMT) and lysyl oxidase (LOX) [29]. Matrix proteins such as proteoglycans, e.g. decorin, fibromodulin, lumican, can bind to collagen fibrils [43-48]. Proteoglycans have glycosaminoglycan (GAG) chains that can bind water. However, it is unknown whether these proteoglycans contribute to the mechanical properties of the tendon. It was proposed that proteoglycans transmit and resist interfibrillar load [49], contribute to fibrillar strength and may even facilitate sliding [50, 51]. However, some studies showed that the contribution of proteoglycans to overall tensile strength is marginal [52, 53]. Yet, the exact structure-function relationship for many proteoglycans remains unclear [29, 54].

The tendon consists of different compartments, which contain different cells and proteins [29]. The intrinsic tendon compartment is the actual load-bearing collagen matrix with a low density of tenocytes (tendon fibroblasts; cell mass only 1-3 wt%) [55], which is surrounded by an extrinsic compartment called the paratenon which contains fibroblasts and progenitor cell populations [56, 57]. Intrinsic tendon cells are diverse [58], but have a limited metabolic rate and they show limited capacity to stimulate healing [57, 59, 60]. The extrinsic compartments are connected to the vascular, immune and nerve system [57]. Healthy tendon is relatively avascular [61]. The Achilles tendon consists of three subtendons as it has separate connections to the three calf muscles (Figure 3.2). Recent studies have identified a distinct compartment called the interfascicular matrix that contains elastin, more round cells, more collagen type 3, more proteoglycans and less collagen type 1 [62-64]. Additionally, there is a tendon running adjacent to the Achilles tendon, called the plantaris tendon [65].

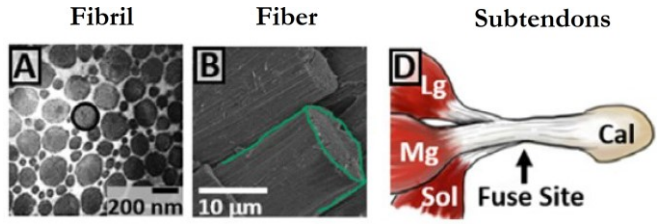

Figure 3.2. The hierarchical structure of rat Achilles tendon, ranging from molecules to three distinct subtendons that are connected to calf muscles (soleus, SOL; lateral and medial gastrocnemius, LG and MG). Republished with permission of John Wiley & Sons - Books, from Comparative multi-scale hierarchical structure of the tail, plantaris, and Achilles tendons in the rat, Anatomical Society of Great Britain and Ireland, 234, 2, 2019; permission conveyed through Copyright Clearance Center, Inc.

3.2 Tendon deformation mechanisms and mechanical properties

The whole tendon displays highly nonlinear stress-strain behaviour (Figure 3.3) [66, 67]. This is particularly true for the so-called toe region at low strains, where the nonlinearity comes from several structural features such as the naturally occurring tendon crimp, observed as a wavy collagen pattern identified at both the fibril and fiber level [41, 42, 68]. Throughout the toe and linear region, there are many structural collagen features that contribute to the overall tendon mechanics [69] such as intra- and inter-fibrillar crosslinks, crimping and helical twist on the fibrillar and fiber level, fibrillar branching that links fibrils together at regular d-period [69], molecular stretching and slippage [70]. Additionally, tendon elongation is governed by sliding at different length-scales, from fibrils to fascicles [30, 71-75]. Multiple studies showed that over 50% of macroscale tendon deformation was due to interfibrillar sliding [72, 76], which could be facilitated by the proteoglycan-rich and water-filled ground substance. All the aforementioned deformation mechanisms contribute to a complex transfer of macroscopic tissue level strains to the smaller length scales of the matrix (fiber, cell, fibril, molecule level), also referred to as strain transfer [77]. These strains may not be distributed evenly throughout the tendon tissue. Tensile tests on tendon fascicles showed heterogeneous strain distributions within the tendon fascicle [71]. For example, the minimum and maximum longitudinal strains were found to be 20% and 300% compared to the mean longitudinal strain, respectively.

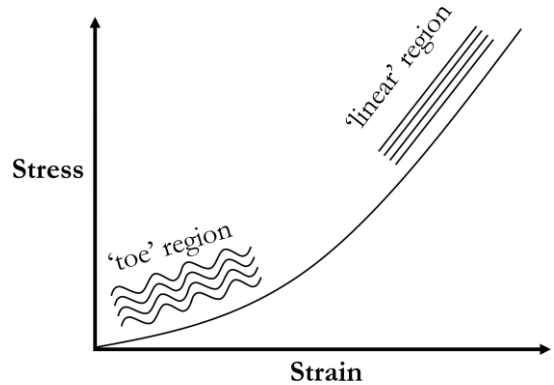

Figure 3.3. The typical nonlinear stress – strain response displayed by tendon tissue upon tensile loading resulting from various structural features, such as the wavy fiber structure, that contributes to the toe region, whereas alignment and straightening of collagen upon further tensile loading lead to a rather linear response.

What is also known, is that collagen has an excellent intrinsic elastic resilience [72]. It was hypothesized that the matrix in between fascicles, the so-called interfascicular matrix, contributes to recoil and elastic properties [78]. Elongation within the toe-region has been described to be fully elastic, yet elongation beyond it may damage the tendon structure and the waviness may be lost [40]. Upon stretching, microscopic failure occurs between 6-10% macroscopic strain, and macroscopic failure between 8-10% strain [15]. During fatigue loading, a similar progression of microscopic damage evolves into macroscopic damage [79].

Tendon displays viscoelastic properties which may be contributed to the interaction between collagen and ground substance, i.e. proteoglycans and water [71, 80, 81]. Tendon viscoelasticity is characterized by stress-relaxation, creep, and hysteresis behaviour [82]. Additionally, tendon displays a strain rate-dependent stiffness, such that stiffness and load-bearing increase at higher strain rates [55, 83]. Moreover, tendon has been shown to have a large Poisson's ratio (>0.5), which potentially contributes to compressive forces in the tendon substance [71]. Proteoglycans may release water under compression, thereby contributing to stress-relaxation behaviour [84]. This mechanism may explain why fluid is squeezed out of the tendon during tensile loading [85, 86]. Overall, these multiscale tissue properties are known to vary, e.g. with tissue type, age and cross-linking density [52, 87-91].

3.3 Tendon mechanobiology

Tendon cells and tissue respond and adapt to altered levels of physical activity [14, 92, 93]. Physical training can affect tissue properties such as strength, stiffness, collagen and proteoglycan content, weight, cross-sectional area, fibril diameter, fibril density and alignment [92]. Yet, different degrees of mechanical loading can affect the tendon differently. Freedman et al. (2015)[93] described how moderate loading can induce mostly positive effects whereas over- and unloading may induce unwanted changes. Positive effects of moderate loading are increases in collagen production, cross-sectional area, tenogenic differentiation and tensile strength. On the other hand, over- and unloading may induce unwanted changes like collagen degradation, decreases in tensile strength, collagen organization, increased inflammatory markers and potential transdifferentiation into non-tendon tissue types. Different levels of load may also induce the production of different collagen types. For example, moderate loading may induce production of collagen type 1, overloading may induce collage type 3 production (as seen during the development of chronic tendon disease), whereas compressive loading may induce a more cartilage-like phenotype by inducing collagen type 2 [14].

To study mechanobiology of tendon, different experimental techniques have been used for small animal models to subject the Achilles tendon to different levels of mechanical load (Figure 3.4). The default loading regimen is free cage activity where the Achilles tendon is subjected to full physiological mechanical loading during gait and all normal activities of the animal. The loading of the Achilles tendon may be reduced through induction of paralysis by intramuscular Botox treatment [94], tail suspension [95] or immobilization by cast [96] or orthosis [97]. The Achilles tendon may also be subjected to training-like exercise through treadmill running [95]. These types of experiments have been widely used to investigate the effect of exercise and immobilization on tendon in rats and mice.

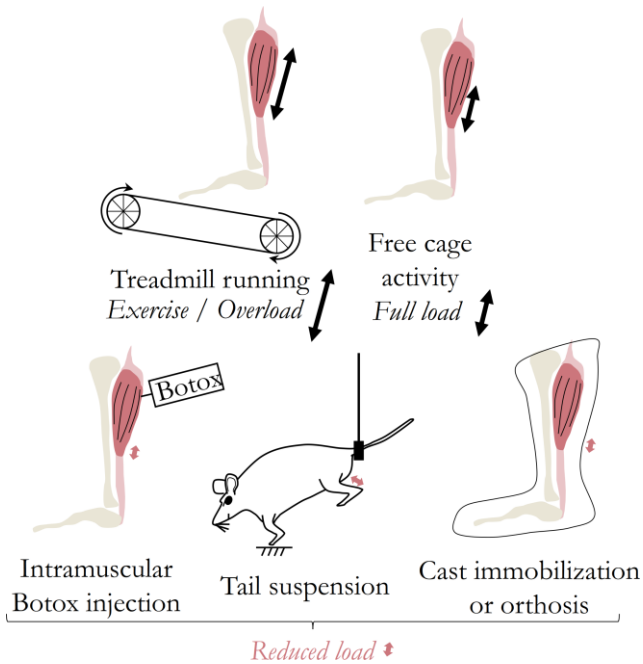

Figure 3.4. Overview of different experimental techniques utilized in small animal studies to investigate the effect of different loading regimens on the evolution of tendon properties in intact and healing tendon. The arrows indicate the load level. These techniques may also be combined to cause a further reduction in load level.

Mechanical loading typically improves biosynthesis. For example, daily treadmill running increased the number and size of collagen fibrils, and cross-sectional area within one week of running in mice [98, 99]. However, prolonged treadmill running reduced the mean diameter of the fibrils to values below the control group. A longer study in rats showed that twelve weeks of daily treadmill running caused increased collagen type 3 production, no change in collagen type 1, decreases in various other proteins (fibromodulin, biglycan, MMPs, TGF-b1), and increased stiffness and ultimate stress [100]. Twenty weeks endurance training in the Senegal bushbaby did not affect the strength of the Achilles tendon, but did increase the strength of patellar and extensor digitorum longus tendon [101]. These results display how the mechanobiological adaptation can lead to complex changes of the tendon structure and composition. Additionally, it also exemplifies that prolonged physical exercise may induce more catabolic (degradation) changes, opposed to initial anabolic changes, in different structural and compositional properties.

Different techniques for achieving reduced mechanical loading and the duration of reduced loading may affect the tendon in different ways. Three weeks of hindlimb suspension resulted in a decreased modulus and peak stress of the Achilles tendon [102]. After three weeks of stress deprivation in rabbit patellar tendon, degenerative changes (increased cross-sectional area, decreased ultimate strength, stiffness) were observed [103, 104]. Five to six weeks of reduced loading affected the weight, modulus, collagen content, collagen dispersion, and different viscoelastic properties (creep, stress-relaxation, hysteresis) in an intramuscular Botox-unloading model in rat Achilles tendon [28, 94]. Nine weeks of joint immobilization of the knee did not affect the collagen mass but increased collagen turnover in the rabbit patellar tendon [105]. Ten weeks of stress-shielding barely affected viscoelastic properties in a mouse patellar tendon model [106], whereas these stress-shielded tendons displayed a more uniform distribution of smaller diameter fibrils, lacking the presence of large diameter fibrils observed in normal tendon [107]. These different animal studies display the complexity of identifying general changes in tendon properties upon different methods and durations of reduced loading.

These mechanobiological changes of tissue properties result from the response of the cell to mechanical loading. On the cell level, several reviews have described the complex nature of mechanotransduction pathways [14, 93, 108]. Mechanical stimulation by strain can regulate collagen production in tendon cells. For *in vitro* experiments with rat fibroblasts, collagen (type 1 and 3) gene-expression increases with increasing strain magnitude up to 15% applied strain, but it remains unclear whether collagen gene-expression and content remain elevated for high strain levels (Figure 3.5). In addition to its effects on collagen synthesis, tendon cells subjected to 8% strain displayed upregulated pro-inflammatory signaling and other matrix proteins or enzymes, e.g. COX-2, PGE2 and MMP-1 [109, 110].

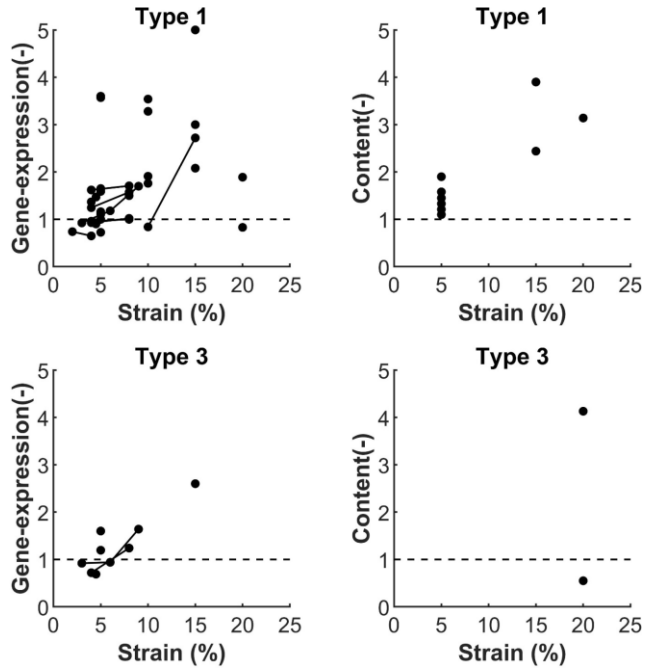

Figure 3.5. Summary of strain-dependent collagen (type 1 and 3) gene-expression and content in *in vitro* experiments in rat fibroblasts. All values are normalized to static treatment (no mechanical stimulation). The data was obtained from the following literature: [111-127].

3.4 Tendon healing in rodents after rupture (I)

Tendon healing is a complex process that aims to repair the damaged tissue. For an overview of different aspects of tendon healing, see Figure 3.6. A critical part of tendon healing is the production and restoration of the collagen matrix, which is responsible for load bearing, such that the tendon can fulfil its function as soft connective tissue. Tendon healing displays classical wound healing characteristics, such as an initial acute inflammatory phase that lasts a few days. The early healing process depends heavily on surrounding tissues providing blood supply, immune cells, nerve system and fibroblastic cells [57]. Throughout healing the tendon is filled with different cell populations [128]. Pro-inflammatory markers are upregulated for a week and markers for angiogenesis are upregulated for at least 2 weeks [129]. Loading during the first days of healing was found to upregulate inflammatory markers [130].

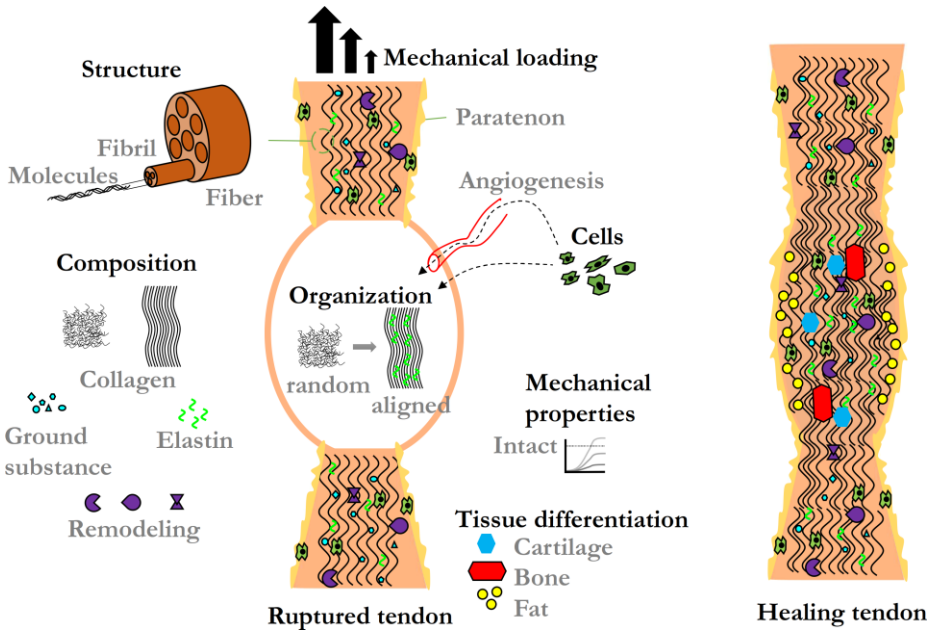

Figure 3.6. Overview of the tendon healing process.

After a few days of healing the reparative phase starts. This phase is characterized by significant cell infiltration and proliferation, as well as ECM production. During early tendon healing, a preliminary matrix is produced that consists mainly of collagen type 3. This network will restore mechanical integrity of the tendon, but it can also potentially accommodate cell behaviour, e.g. cell migration and mechanotransduction [131, 132]. Throughout healing, collagen production shifts from predominantly type 3 to type 1, e.g. [133]. In terms of collagen structure, collagen fibril diameters do not return to intact levels within eight weeks of healing [22]. One study described that the healing tendon has increased elastin content compared to the intact tendon [134], potentially affecting the elastic fiber formation and elastic behaviour of the tendon.

In terms of collagen organization, the majority of alignment occurs within the first four weeks of healing [135-137], yet the collagen remains more disorganized than in the intact tendon, up to 16 weeks of healing [138, 139]. The collagen organization, however, improved with increasing dorsiflexed angle during cast immobilization [140]. In terms of other ground substance proteins, gene expression of MMPs peak at two to four weeks of healing, while tissue inhibitors of MMPs peak earlier, i.e. one to two weeks of healing. Gene expression of different proteoglycans varies (upregulated: aggrecan, biglycan and versican,

downregulated: decorin and fibromodulin) throughout the first weeks of healing [129]. However, histological staining of proteoglycans showed that proteoglycan content peaked at eight weeks in the healing tendon and was significantly decreased at 17 weeks again [139].

Throughout tendon healing, the size and mechanical properties of the tendon evolve as a function of external mechanical loading. Most structural mechanical properties (e.g. stiffness, peak force and work) return to intact values within two to four weeks of healing (Figure 3.7). Oppositely, material properties (e.g. Young's modulus and peak stress) do not return to intact values (Figure 3.7). One study showed that geometrical properties of the healing tendon, e.g. cross-sectional area and gap distance, typically increase with loading [95]. Aligned with this finding, unloading or immobilization appears to "slow down" the recovery of nearly all material properties (Figure 3.7). Yet, there is limited characterization of important mechanical properties such as viscoelastic properties (creep, stress-relaxation, hysteresis), and fatigue (cycles to failure) during tendon healing.

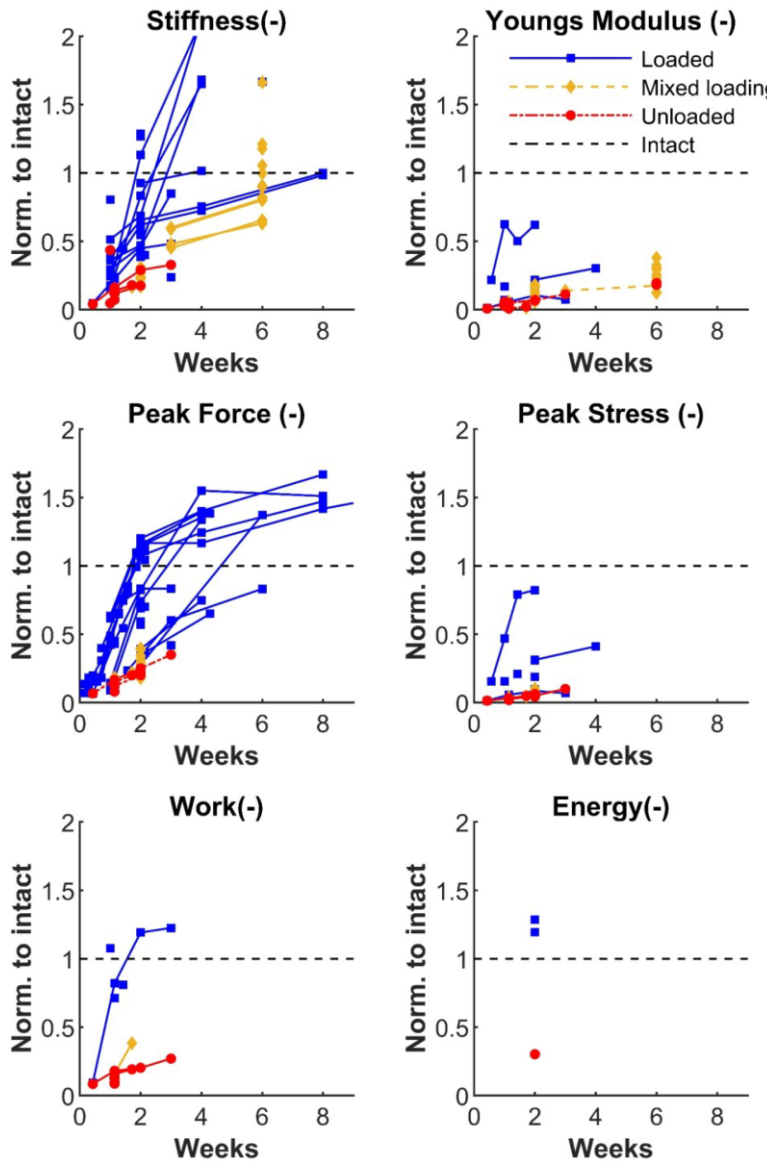

Figure 3.7. Evolution of mechanical properties in rodent studies investigating Achilles tendon healing. The experimental data is subdivided in animals that were subjected to: free cage activity (loaded), constant form of unloading (e.g. Botox injection, tail suspension, or cast immobilization) or a mix of the aforementioned loading scenarios (mixed loading). The intact-normalized data in this figure is based on the following references for loaded [21, 23, 95, 141-163], mixed loading [95, 96, 140, 164-168], unloaded [21, 149, 150, 164, 165, 167-170].

Cells play an important role in repairing the ruptured tendon. Cell proliferation and cell density peak at around one to two weeks of healing [171-175] and decrease thereafter, but remain elevated for several weeks. A wide range of cell types have been observed, e.g. immune cells (macrophages, neutrophils, mast cells), fibroblast-like cells (epitenon, myofibroblasts), tendon stem/progenitor cells, bone-marrow derived cells [128], fat-like, cartilage-like [21] and bone-like cells [24]. There has been an increasing amount of literature reports on aberrant formation of different tissue types during healing, including cartilage-, bone- and fat-like tissues and corresponding cells and gene-expression. Recently, Huber et al., (2020)[25] found that joint immobilization could prevent bone-like tissue formation. They proposed that joint immobilization could induce a decrease in fiber alignment and cell spreading, hereby decreasing TAZ signaling and inducing adipocyte differentiation. Oppositely, fiber alignment, cell spreading and TAZ signaling increase upon loading, potentially inducing bone-like tissue formation. Similarly, bone volume after six weeks of healing was highest for loaded tendon [26], yet partial immobilization decreased fibrocartilage formation [27] and bone volume [26] compared to full immobilization.

Recently, a few experimental studies have identified heterogeneous tendon properties, e.g. collagen [21, 136, 176] and cell distribution [171, 173, 174, 177-180] during healing. Throughout healing, the core of the healing callus may be deprived of cells, blood supply and oxygen, which may biologically limit early healing in the tendon core. However, it is unknown what role mechanical loading may play in the heterogeneous restoration of tendon properties.

Clinical treatment of tendons aims to stimulate regeneration without extensive scar formation, but understanding of 'scarless' healing and scar formation is lacking [59, 181]. An interesting new animal model (MRL/MpJ mice) has shown improved healing compared to other animal models, which will allow investigation of key aspects of 'scarless' healing [182]. Studies investigating tendon healing in young and mature animals have found interesting differences in collagen properties, cell differentiation and mechanical properties [22, 183, 184]. These studies may prove vital in identifying key processes underlying scarless and regenerative healing, observed in young animals.

Overall, mechanical loading has been shown to affect tendon properties during early tendon healing in rodents. Still, a deep understanding of mechanobiology during tendon healing is lacking. This is partially related to the limited number of properties investigated by single studies and the lack of consistency in experimental protocols between studies. To create a deeper understanding of tendon mechanobiology, there is a need for generalized experimental protocols combining

multiple mechanical loading scenarios, in combination with characterization of a wide spectrum of tendon properties e.g. mechanical, histological, compositional, structural and ambulatory analysis of healing tendons. In terms of tendon function, mechanical characterization should not only address stiffness or strength, but also the evolution of viscoelastic properties (e.g. stress-relaxation, creep, and hysteresis) and fatigue properties (e.g. cycles to failure and dynamic modulus). Investigating all these different properties will give valuable insight as to which tendon properties are restored to intact values during healing, and which properties are (permanently) altered after rupture, as a function of the particular treatment. Additionally, future experiments should investigate effects of more long-term rehabilitation protocols, since multiple studies have shown that the initial effect of the mechanical loading protocols diminishes through time [21, 185].

3.5 Mechanical modeling of tendon

3.5.1 Constitutive material modeling

Computational modeling has been used to describe the mechanical properties of tendon and investigate deformation mechanisms on multiple length-scales of the tendon structure. Mechanical modeling of tendon and soft tissue has focused mainly on describing collagen on different length-scales [16, 54], i.e. on the molecule [186-193], fibril [194-198] and fiber [199-201] level as it is the main load-bearing constituent of tendon. Some studies have started to identify mechanisms of load/strain transfer between length-scales [187-189, 202-204]. Still, much work is left to be done to fully grasp the transfer of loads and deformations throughout the hierarchical tendon structure [205]. A realistic multi-scale model, that integrates structure-function relationships on all length-scales could be a key advancement in understanding biomechanics of tendon [15]. Several modeling techniques have been utilized to describe deformation of the tendon or collagen on different length scales, such as atomistic and molecular dynamic simulations, analytical or mathematical frameworks and finite element simulations. Atomistic and molecular simulations focus on describing the interactions between atoms and molecules, for example in a collagen molecule or small fibril [186-193]. These simulations are computationally costly and cannot describe the tendon deformation on the tissue level, yet these approaches are very relevant for determining deformation mechanisms on the nano- or micro-scale which are typically difficult to measure experimentally. On the other hand, analytical or mathematical frameworks allow the description of the tendon mechanics on the tissue scale, but they often assume a simplified tendon geometry

or assume homogeneity of the tendon material [52, 195, 206-216]. Both atomistic/molecular simulations and analytical/mathematical frameworks display a limited capability to describe the heterogeneous biomechanics during tendon healing. However, finite element simulations allow computational analysis of the whole tissue level and have been used to investigate the contributions of more realistic and complex tendon geometry and heterogeneous properties to the overall mechanical behaviour [199, 202, 217-225]. Furthermore, the finite element method enables the characterization of tissue-level and local deformation mechanisms and spatial distribution of various mechanical quantities such as strain, stress or fluid flow. Still, many different material models, both analytical and in finite element frameworks, have investigated different mechanical behaviours of tendon (Table 3.1).

Table 3.1. Overview of the different types of mechanical behaviours in tendon investigated by computational modeling. These studies mostly used tissue scale experimental data for validation of the model parameters.

Article	Quasi-static	Relaxation	Creep	Cyclic	Strain stiffening
Analytical models					
Ciarletta et al., 2006 [206]	x	x	x		
Ciarletta et al., 2008 [195]	x	x		x	x
DeFrate and Li, 2007 [207]	x	x			x
Duenwald et al., 2009 [208]	x	x			x
Duenwald et al., 2010 [209]		x			
Fang et al., 2014 [210]		x			
Johnson et al., 1994 [211]	x	x		x	
Kahn et al., 2010 [213]		x		x	
Kahn et al., 2013 [212]				x	
Pioletti et al., 1998 [214]	x				x
Provenzano et al., 2002 [215]		x		x	
Puxkandl et al., 2002 [52]	x				x
Sopakayang & De Vita, 2011 [216]		x	x		
Finite element models					
Ahmadzadeh et al., 2013 [217]	x				
Atkinson et al., 1997 [218]	x				
Fessel and Snedeker, 2011 [219]	x				
Herchenhan et al., 2012 [202]	x				
Khayyeri et al., 2015 [220]		x	x	x	x
Khayyeri et al., 2016 [221]		x	x	x	
Machiraju et al., 2006 [222]		x			
Obrezkov et al., 2021 [223]		x	x	x	x
Reese et al., 2010 [199]	x				
Swedberg et al., 2014 [224]	x	x			
Troyer & Shetye, 2012 [225]		x		x	

3.5.2 Microstructural tendon modeling

A fundamental effort in material modeling of soft tissues was done by the works of Lanir [226-228] which described a microstructural and thermodynamical constitutive framework for soft tissues by assuming that the total tissue mechanics is the sum of the mechanical contribution by individual fibers. Additionally, these works considered different structural and mechanical features, e.g. anisotropy, nonlinear stress-strain behaviour and viscoelasticity. This framework was expanded

by adding a statistical distribution of collagen fibers and by modeling fiber recruitment [229]. Various other material models considered structural features of the hierarchical collagen structure, e.g. fiber or fibril distributions [200, 230], crimp or recruitment [216, 226, 231-238], crosslinking [198, 239, 240], the helical superstructure of the fibrils [199], and even stiffness, viscosity, stress-relaxation and creep on the single fibril level [187-189].

3.5.3 Phenomenological tendon modeling of viscoelasticity

Several studies have modeled the viscoelastic behaviour of tendon. One of the earliest phenomenological continuum frameworks to describe viscoelasticity in soft tissues is the quasi-linear viscoelastic theory [241]. This framework divides tendon mechanics into a strain-independent and time-independent contribution. Yet, this framework has shown limited capability to predict the mechanical behaviour of tendon under multiple loading conditions [208, 225]. There are several other phenomenological models that describe elastic and dissipative contributions of tendon behaviour on the tissue scale. These material models focused on describing single fibrils [188, 242], tail [52], patellar [214], subscapularis [222], Achilles [212, 220, 221, 223, 225] and digital flexor tendon [210]. Pioletti et al. (2008)[214] used independent elastic (strain-dependent) and viscous (strain-rate dependent) stress contributions. On the other hand, several studies used a Maxwell-Weichert approach that combines an elastic contribution in parallel with one [212, 220, 221], two [210], four [225], or eight Maxwell elements [222] (Figure 3.8). The advantage of having multiple Maxwell elements is that every element may have a unique characteristic time-scale for relaxation or creep, therefore, multiple Maxwell branches may describe stress-relaxation or creep behaviour on multiple time-scales.

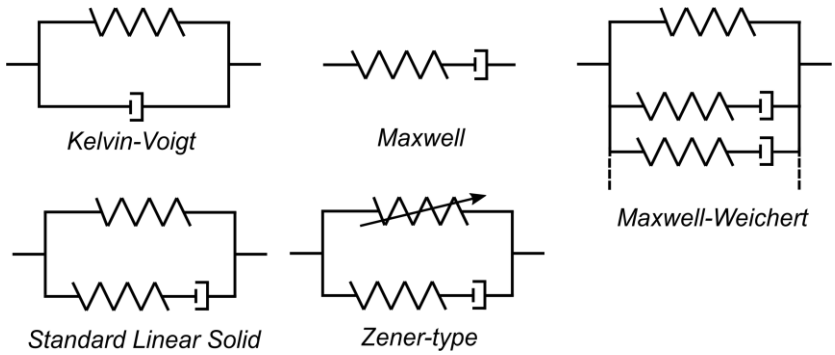

Figure 3.8. Schematic depiction of the different phenomenological models combining different elastic (spring-like) and dissipative (damper-like) contributions to constitute the time-dependent behaviour.

These phenomenological models can capture different types of loading on the tissue-level biomechanical behaviour. Although these models are easy to implement, they have limitations. For instance, this approach typically does not allow for multi-scale investigation or strain transfer, typically does not consider the interplay with the ground substance and the constitutive parameters do not always represent physiological or structural features [54]. However, some phenomenological models have described more specific structure-function relationships, e.g. by considering fiber recruitment in the elastic element in a Zener-type model (see figure 3.8) [212] or fiber dispersion [223]. Another early study implemented two Kelvin-Voigt elements in series to model the elastic and dissipative contributions for collagen and ground substance separately [52]. On the fibril level, viscoelasticity was modeled by coupling a Kelvin-Voigt element, describing intrinsic collagen fibril crosslinks, in series with two Maxwell elements that described the interfibrillar and interfiber ground substance [243]. An isolated collagen fibril was modeled in Maxwell-Weichert fashion with two Maxwell branches [188, 242]. Gautieri et al. (2013) even used molecular dynamics simulations to model creep of the collagen molecule and subsequently fitted a Kelvin-Voigt model to the simulated creep data [188].

3.5.4 Models considering ground substance and water

Some modeling studies have focused on identifying the mechanical contribution of ground substance, with a particular interest in the role for proteoglycans, to overall tendon mechanics [52, 204, 217, 219, 244-249]. For example, Fessel and Snedeker (2011)[219] and Ahmadzadeh et al. (2013)[217] investigated how

proteoglycans could crosslink discontinuous fibrils and proposed possible explanations for the experimental observation that tendon mechanics is rather insensitive to the deletion of these proteoglycan crosslinks. Predictions from these so-called shear lag models showed that interfibrillar shear load transfer between discontinuous fibrils may be responsible for strain transfer across different length scales [54], and some even see it as the main loading mechanism for tendon fibrils [247]. A shear lag model including fluid, predicted experimentally observed tendon features i.e. a high Poisson's ratio and fluid exudation tensile load [244]. Additionally, modeling efforts considered plasticity of the interfibrillar matrix upon deformation [245, 246, 250]. Also, the contribution of water to overall tendon mechanics has been heavily discussed. Some studies explicitly account for water in tendon by modeling the tendon as poroelastic [217, 218, 224, 244, 251, 252]. Smith et al. (2013)[205] proposed a need for a poro-visco elastic material model to investigate viscoelastic behaviour, observed in tendon, that is partly explained by fluid flow.

3.5.5 A representative finite element model of the tendon

To address the need for a tissue-scale viscoelastic material model with collagen, proteoglycans and water, a fibril-reinforced poro-visco-elastic material model for describing articular cartilage [253] was further refined to describe the mechanical behaviour of tendon tissue [220, 221]. Specifically, the collagen behaviour was modeled with a visco-hyper elastic standard linear solid formulation with exponential stress-strain behaviour. A poroelastic formulation with nonlinear strain-dependent permeability was implemented to model hydrostatic stress and to predict fluid flow. The ground substance was modeled as transversely isotropic hyperelastic in Khayyeri et al. (2016)[221]. The developed material model was promising as the model could capture many different mechanical features observed in tendon, i.e. strain-stiffening, creep, stress-relaxation, hysteresis during cyclic loading [220] and fluid exudation upon tensile loading [221]. Yet, a drawback of this material model is that it does not explicitly describe the mechanical contribution of specific structural features, such as collagen crimp or crosslinking, but rather describes the nonlinear, elastic and dissipative mechanical behaviour of collagen on the tissue scale.

3.5.6 Adaptive modeling in healing

There is little literature on adaptive modeling in tendon. Several overview articles expressed a need for computational modeling to reinforce experimental investigations of mechanobiology in intact and healing tendon [16, 69, 108]. Adaptive models for describing tendon homeostasis have been reviewed [205]. Another overview article discussed the broad spectrum of mathematical modeling, e.g. continuum level, partial differential equations, finite elements, agent-based modeling, lattice approach, that can be used to investigate mechanobiology during growth, remodeling and healing of tissues [254]. To address the need for adaptive modeling in tendon mechanobiology, this thesis focused on developing and exploring such a framework.

One of the first mathematical frameworks to describe mechanobiology in intact tendon described the temporal evolution of the geometry (tendon length, cross sectional area) and material properties (stiffness, ultimate stress) [255-257]. A more recent study uses a multi-scale modeling approach to predict remodeling of the tendon fiber length upon damage and repair [258]. This study used a dynamic tendon-muscle model to describe the Achilles tendon force during gait.

Only recently, two numerical frameworks for tendon healing [19, 20] investigated mechano-regulated processes underlying the temporal evolution of tendon properties (cell distribution, collagen alignment and content). Specifically, Richardson et al. (2018)[19] used an agent-based modeling approach to describe cell migration and they explored strain-dependent collagen production, degradation, damage to predict collagen content and alignment. This work identified an optimal strain-range for maximizing the collagen content and alignment. A follow-up study by Chen et al. (2018)[20] implemented a multi-scale approach to investigate the effect of mechanical loading and suture repair on temporal evolution of collagen content and alignment in rat Achilles tendon healing. First, a musculoskeletal model of the rat hindlimb was used to estimate tissue-level strains in the healing Achilles tendon during gait. Subsequently, cell alignment and collagen production rates were predicted and combined in a tissue-level agent-based model. Interestingly, this approach provided a possible mechanism for understanding complex effects of mechanical loading and the effect of suture-repair on the temporal evolution of tendon properties, e.g. cell alignment and collagen production, during healing.

Another interesting feature of tendon healing is the formation of different tissue types during tendon healing. Yet, no tendon model has investigated this. However, several computational models have been utilized to investigate mechanobiological regulation in regeneration of other musculoskeletal tissues, especially during bone

healing [259, 260]. Different finite element frameworks utilized biophysical stimuli [17, 261], in combination with angiogenesis and oxygen [262-264] to predict heterogeneous cell behaviour (differentiation, migration, proliferation, apoptosis) [263, 265], and heterogeneous production of different tissue type, e.g. cartilage, (im)mature bone, bone marrow, granulation tissue, fibrous tissue. These models considered differentiation and de-differentiation of mesenchymal stem cells into fibroblasts, chondrocyctes, osteoblasts and adipocytes. A wide range of biophysical stimuli has been considered to guide tissue differentiation and the subsequent formation of different tissue types, e.g. principal strain, octahedral shear strain, pore pressure, hydrostatic stress or fluid flow [17]. In addition to these stimuli, also considered mechano-regulated angiogenesis, local tissue stiffness and oxygen concentration to affect tissue differentiation and tissue formation in bone [262]. These aforementioned frameworks were considered in this thesis to affect the heterogeneous formation of different tissue types during tendon healing.

In summary, many different material models have been used to investigate tendon mechanical behaviour on different length scales. One finite element study [221] showed promising results by describing different aspects of complex biophysical behaviour of tendon, including fluid exudation, creep, relaxation and hysteresis, of tendon on the tissue scale (see Table 3.1), whereas other studies focused on describing only one or two types of mechanical loading. Also, the finite element method enables modeling of the tendon geometry and allows investigation of the spatial distribution of various mechanobiological stimuli, e.g. strain, stress or fluid flow, and other heterogeneously distributed properties that may govern tendon mechanobiology and healing. Additionally, a limited amount of numerical studies have investigated mechano-regulatory processes governing tendon homeostasis and tendon healing. Yet, more elaborate mechanobiological frameworks have investigated tissue- and cell-level differentiation in bone. Together, different aspects of existing adaptive mechanobiological frameworks are combined in this thesis to investigate mechanobiology in intact and healing tendon. Since only a limited number of experimental studies and no numerical studies have investigated the heterogeneous properties of tendon, the computational modelling in this thesis particularly focused on investigating spatial characterization of mechanobiological stimuli that may govern principal mechanisms and the heterogeneous nature of tendon regeneration.

4 Methods

This chapter describes the methods adopted in this thesis. The constitutive material description used to model the tendon is introduced. This material model was used to determine mechanical properties of intact tendon in Study II. Then, the adaptive framework used to study mechanobiological aspects of tendon healing, used in studies III-V, is described.

4.1 Constitutive material model

An existing fiber-reinforced poro-visco-hyperelastic formulation with a transversely isotropic matrix was used to describe the mechanical contributions of collagen fibers, ground substance and fluid in tendon mechanics (Figure 4.1) [221], according to:

$$\boldsymbol{\sigma}_{total} = \boldsymbol{\sigma}_f + \boldsymbol{\sigma}_m - p\mathbf{I} \tag{1}$$

with total stress ($\boldsymbol{\sigma}_{total}$) consisting of the stress in the collagen fibers ($\boldsymbol{\sigma}_f$) and ground substance ($\boldsymbol{\sigma}_m$) and hydrostatic pressure p with unit tensor $\mathbf{I}$ from the fluid phase.

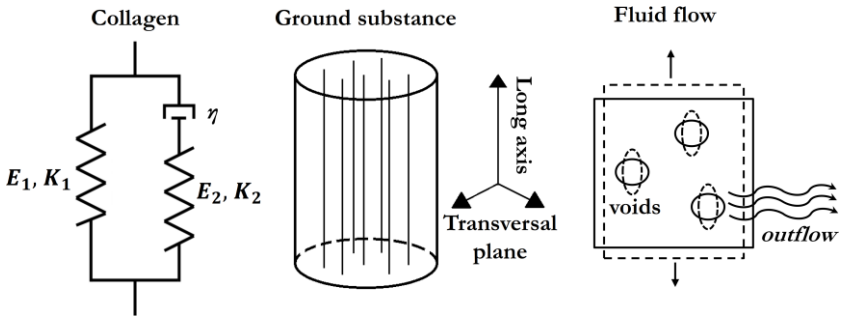

Figure 4.1. Schematic drawing of the standard linear model, consisting of an elastic spring in parallel with a Maxwell spring-dashpot, the transversely isotropic ground substance and void-ratio dependent fluid flow.

4.1.1 Collagen mechanics

The mechanical behaviour of collagen was described by a standard linear solid model (Figure 4.1) which includes one elastic (spring) and one damping (spring and damper) contribution. The springs were described with an exponential stress-strain behaviour (Eq. 2) that consisted of linear (E_1, E_2) and nonlinear (K_1, K_2) stiffness parameters, whereas the damping constant (η) described the strain-rate and time-dependent behaviour (Eq. 3). The total collagen behaviour was expressed in terms of the first Piola-Kirchhoff stress according to:

$$P_n = \begin{cases} E_n\,(e^{K_n \varepsilon_n} - 1), & \varepsilon_n > 0 \\ 0, & \varepsilon_n \leq 0 \end{cases} \quad \text{for } n = 1, 2 \tag{2}$$

$$P_\eta = \eta \frac{d\varepsilon_\eta}{dt}, \tag{3}$$

$$\varepsilon_1 = \varepsilon_2 + \varepsilon_\eta, \tag{4}$$

$$P_f = P_1 + P_2 = P_1 + \eta \frac{d\varepsilon_\eta}{dt} = P_1 + \eta \left(\frac{d\varepsilon_1}{dt} - \frac{d\varepsilon_2}{dt}\right), \tag{5}$$

where P_1, P_2, P_η and ε_1 , ε_2, ε_η refer to the first Piola-Kirchhoff stress and strain in the spring and the damper, respectively. The Cauchy stress of the collagen was then defined as:

$$\boldsymbol{\sigma}_f = \frac{\lambda}{J} P_f \overrightarrow{\boldsymbol{e}_f}\, \overrightarrow{\boldsymbol{e}_f}^{\,\mathrm{T}}, \tag{6}$$

with $\lambda = \frac{\|\overrightarrow{e_f}\|}{\|\overrightarrow{e_{f,0}}\|}$ the fiber stretch, and unit vectors ($\overrightarrow{e_f}$ and $\overrightarrow{e_{f,0}}$) describing the current and initial fiber direction respectively. The fiber strain was defined as a logarithmic function of the stretch ($\varepsilon_1 = \log(\lambda)$). Fiber orientation was updated using deformation tensor **F** according to:

$$\overrightarrow{\boldsymbol{e}_f} = \frac{\mathbf{F} \cdot \boldsymbol{e}_{f,0}}{\|\mathbf{F} \cdot \boldsymbol{e}_{f,0}\|}. \tag{7}$$

4.1.2 Ground substance

The ground substance was modeled with a transversely isotropic strain-energy formulation [266] following:

$$W_{ort} = \frac{1}{2}\sum_{i,j}^{3} a_{ij} tr(\boldsymbol{E} \cdot \boldsymbol{L}_{ii}) tr(\boldsymbol{E} \cdot \boldsymbol{L}_{jj}) + \sum_{i,j\neq 1}^{3} G_{ij} tr(\boldsymbol{E} \cdot \boldsymbol{L}_{ii} \cdot \boldsymbol{E} \cdot \boldsymbol{L}_{jj}) \ , \tag{8}$$

with Green-Lagrange strain tensor ($\boldsymbol{E}$) and $\boldsymbol{L}_{ii} = \boldsymbol{I}_i \otimes \boldsymbol{I}_i$ where i=1, 2, 3 a set of orthogonal unit base vectors with transversal (i=1, 3) and longitudinal (i=2) orientation. The stiffness tensor is a_{ij} $(i, j = 1, 2, 3)$ with components according to:

$$a_{ii} = E_i \frac{1 - \nu_{jk}\nu_{kj}}{\Delta}, \tag{9}$$

$$a_{ij} = E_i \frac{\nu_{ij} + \nu_{jk}\nu_{ik}}{\Delta}, (\mathrm{i} \neq \mathrm{j} \neq \mathrm{k}) \tag{10}$$

with $\Delta = 1 - \nu_{12}\nu_{21} - \nu_{23}\nu_{32} - \nu_{31}\nu_{13} - 2\nu_{21}\nu_{32}\nu_{13}$ and $\nu_{ij} = \nu_{ji}\frac{E_j}{E_i}$. For a transversely isotropic model the five independent material parameters were defined as:

$$E_1 = E_3 = E_p,\ E_2 = E_n,$$

$$\nu_{13} = \nu_{31} = \nu_p, \qquad \nu_{12} = \nu_{32} = \nu_{pn}, \qquad \nu_{21} = \nu_{23} = \nu_{np}$$

$$G_{12} = G_{23} = G_{pn}, \qquad G_{13} = \frac{E_p}{2(1+\nu_p)},$$

where E, G, ν represent elastic modulus, shear modulus and Poisson's ratio in the transversal (p) plane or normal (n) directions, respectively. The Cauchy stress-formulation for the ground substance was then defined as:

$$\boldsymbol{\sigma}_m = \frac{1}{J}\boldsymbol{F} \cdot \frac{\partial W}{\partial \boldsymbol{E}} \cdot \boldsymbol{F}^{\mathrm{T}}$$

$$\boldsymbol{\sigma}_m = \frac{1}{J}\boldsymbol{F} \cdot \left[\sum_{i,j}^{3} a_{ij} tr\left(\boldsymbol{E} \cdot \boldsymbol{L}_{jj}\right) \boldsymbol{L}_{ii} + 2 \sum_{i,j\neq 1}^{3} G_{ij}\, \boldsymbol{L}_{ii} \cdot \boldsymbol{E} \cdot \boldsymbol{L}_{jj} \right] \cdot \boldsymbol{F}^{\mathrm{T}}. \qquad (11)$$

4.1.3 Strain-dependent fluid flow

The permeability is dependent on the void-ratio [267], according to:

$$k = k_0 \left(\frac{1+e}{1+e_0}\right)^{M_k}, \qquad (12)$$

Where the permeability (k) and the nonlinear tuning parameter (M_k) describe the nonlinear dependency of permeability, on initial permeability (k_0) and void-ratio. In addition, the water mass fraction ($n_{f,m}$) was used to estimate the water volume fraction [268] according to:

$$n_f = \frac{\rho_s n_{f,m}}{1 - n_{f,m} + n_{f,m}\rho_s}, \qquad (13)$$

with water volume fraction (n_f), water mass fraction ($n_{f,m}$) and the mass density of the solid matrix (ρ_s).

Table 4.1. The constitutive parameters for the fluid flow parameters (k_0, M_k) and ground substance parameters ($E_p, E_n, \nu_{pn}, \nu_p, G_{pn}$) that were used in Studies II-V. The ground substance parameters were chosen to ensure numerical stability and predict fluid exudation upon tensile load whereas the fluid flow parameters were adopted from Khayyeri et al. (2016)[221].

Parameter	k_0 (mm/s)	M_k	E_p (MPa)	E_n (MPa)	ν_{pn}	ν_p	G_{pn} (MPa)
Value	1.43 10^{-9}	0.424	0.5	1.0	0.3	0.45	0.27

4.2 Intact tendon properties (II)

To model the geometry and mechanical properties of intact tendon, experimental data from Achilles tendon in rats was used [28]. In this work, female Sprague-Dawley rats (aged 16 weeks) were subjected to free cage activity (full loading). Half of the animals received an intramuscular Botox injection in the calf muscles of the right hindlimb to induce muscle paralysis, in order to reduce active loading of the Achilles tendon. After five weeks, the tendons were harvested, geometries were measured, and mechanical tests for viscoelastic properties were performed using a creep and stress-relaxation test.

- Creep: pre-load 0.1 N, rate 1.0 mm/s, hold phase: 20 N for 200 seconds
- Stress-relaxation: pre-load 0.1 N, rate 0.1 mm/s, hold phase: 2.0 mm for 200 seconds.

The constitutive material was implemented in Abaqus (v6.17-1, Dassault Systèmes, France). Two 3D quarter-cylinder geometries were created to represent the tendons undergoing full and reduced daily loading, with length 10.84 mm (1140 elements) and 13.38 mm (1254 elements) respectively, and radius 0.9mm (Figure 4.4). Eight-node trilinear displacement and pore pressure brick elements (C3D8P) were used. In terms of boundary conditions, the nodes on the bottom and top surface were constrained in all directions, symmetry conditions were used to mimic a full cylindrical geometry, and zero nodal pore pressure was prescribed on the outer surface (Figure 4.3). The in silico mechanical tests were performed to mimic the experimental creep (20N) and stress-relaxation test (~2mm displacement). The *fmincon* optimization algorithm in MATLAB (R2017a, The MathWorks, Inc., US) was used to fit the 5 collagen parameters (E_1, K_1, E_2, K_2, η) while the parameters for ground substance and fluid flow were kept constant (Table 4.1). The model was fitted using the error (Eq. 14) between experimental data (y^i_{exp}) and model output (y^i_{model}), averaged for N data points according:

$$Error = \frac{1}{N}\sum_{i=1}^{N}(y_{exp}^{i} - y_{model}^{i})^2 . \quad (14)$$

For the creep and stress-relaxation simulations, strain-time and stress-time output were fitted, respectively. The model was fitted to creep and stress-relaxation separately (unimodal fitting) and simultaneously (bimodal fitting) by combining the normalized errors of both tests according to:

$$Error_{bimodal} = \frac{Error_{creep}}{y_{exp,creep}^{max}} + \frac{Error_{stress-relaxation}}{y_{exp,stress-relaxation}^{max}}. \quad (15)$$

To assess the final quality-of-fit, the normalized root-mean-squared error (NRMSE) was computed according to:

$$NRMSE = \frac{1}{y_{exp}^{max}}\sum_{i=1}^{N}\sqrt{\frac{(y_{exp}^{i} - y_{model}^{i})^2}{N}} \quad (16)$$

with normalizing to the maximum experimental value (y_{exp}^{max}).

4.3 Framework to predict tendon healing (III-V)

4.3.1 Experimental data

In studies III-V, experimental data from Khayyeri et al. (2020)[21] was used to construct the tendon geometry and validate spatial predictions of collagen production and temporal predictions of mechanical properties (stiffness, Young's modulus, creep magnitude and ratio, and strain levels) during rat Achilles tendon healing (Figure 4.2). In the experimental study, the Achilles tendon of female Sprague-Dawley rats was transected and left to heal without surgical repair of the rupture. Subsequently, the rats were subjected to full loading (free cage activity) or received intramuscular Botox injection in the transected limb to reduce daily loading during healing. After 1, 2 and 4 weeks of healing the tendons were harvested and characterized for compositional, structural and organizational (histology and small angle x-ray scattering; SAXS), geometrical (cross-sectional area, gap distance) and mechanical (creep tests) properties. In particular, SAXS was used to visualize the heterogeneous distribution of collagen properties throughout early healing.

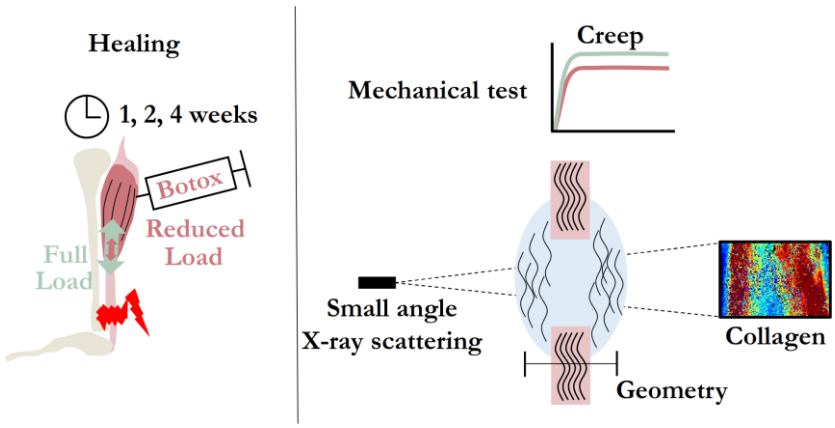

Figure 4.2. Overview of the experimental data used to design and validate the tendon model. In particular geometrical, mechanical and spatial collagen properties were determined in rat Achilles tendons healing for four weeks after transection of the tendon. The Achilles tendons were subjected to full or reduced *in vivo* loading through free cage activity or Botox injection, respectively.

4.3.2 Mechanobiological healing framework

A healing framework was developed to investigate the effect of mechanical loading and cell distribution on the heterogeneous evolution of collagen production, alignment and the temporal evolution of mechanical properties in comparison with experimental data. Mechano-regulated collagen production and collagen reorientation were simulated to mimic the healing process on a day-to-day basis (Figure 4.3). In Studies III-V, tissue production was strain-regulated and collagen was reoriented towards the direction of maximum principal strain. In Studies IV-V, cell infiltration into the healing callus was simulated and tissue production was dependent on the local cell density.

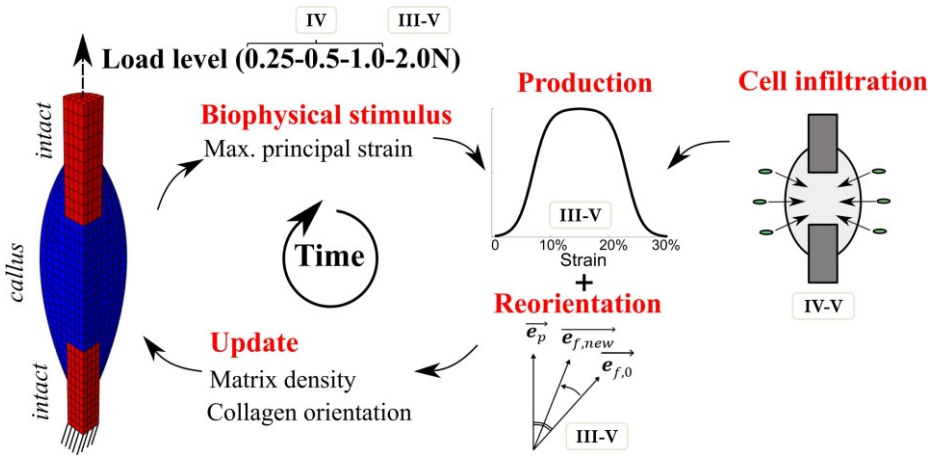

Figure 4.3. Schematic overview of the healing framework used in studies III-V. FE simulations of daily loading were performed to predict the maximum principal strain distribution in the healing callus. Tissue production was regulated by local strain magnitude (Eq. 19-20) and cell density (Eq. 23) and collagen fibrils (Eq. 21) were reoriented towards the maximum principal strain direction. Each iteration of the framework represents 1 day of healing. The tendon was stimulated with various load levels to mimic full physiological load (2.0N) and different levels of reduced loading (0.25N, 0.5N, and 1.0N).

4.3.3 Finite element meshes and boundary conditions

Two quarter-cylinder geometries (Figure 4.4) were developed for studies III-V, using the experimental data from the full and reduced loading group at 1 week post-rupture [21]. Boundary conditions describe clamping of the bottom stump, symmetry conditions to mimic a full cylinder, zero nodal pore pressure on the outer surface. Daily loading is applied on the upper end of the tendon, where nodes are only allowed to displace along the longitudinal axis. The meshes have 1206 and 876 brick elements (C3D8P) for the full and reduced load level meshes with characteristic element length of 0.298 and 0.264 mm, respectively.

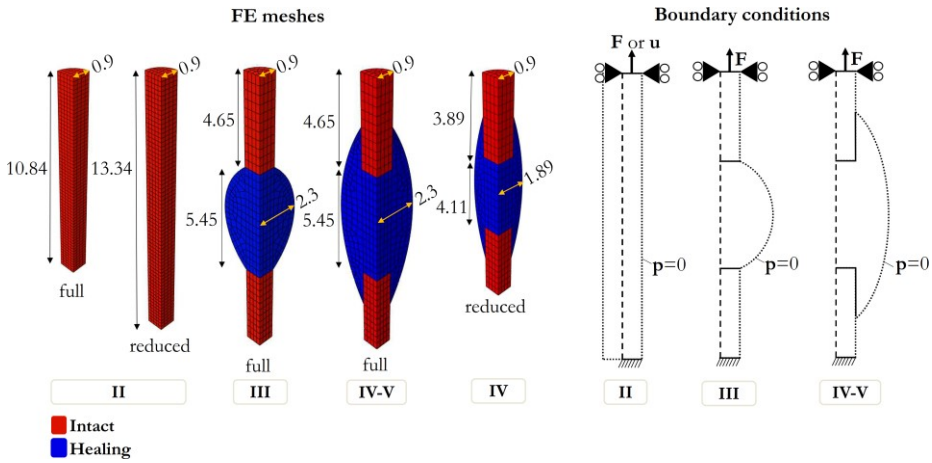

Figure 4.4. Model geometries and boundary conditions used in studies II-V for the full and reduced load level models consisting denoting intact tendon (red) and the healing callus (blue). Model dimensions (mm) are based on experimental observations in intact [28] and healing [21] Achilles tendon from rats subjected to free cage activity (full load) or Botox -treated (reduced load level). In studies II-V, an external force (F) is applied to the upper end of the tendon, where in Study II also a displacement (u) is prescribed during stress-relaxation.

Every day of healing, a mechanical load was applied to the tendon. The applied force consisted of a preload of 0.1 N (loading rate: 0.1 N/s), followed by an external tensile load (loading rate: 1.1 N/s). The 'full' loading level in studies III-V was 2.0 N tensile load, to represent the maximum ground reaction force during gait in adult female Sprague-Dawley rats [269], whereas multiple 'reduced' loading levels were tested in Study IV, 0.25 N, 0.5 N, and 1.0 N, representing 12.5-50% of the physiological loading during gait. For all load scenarios, the applied loading is 0.25N at day 1 post-rupture and incrementally increased towards the final load level to avoid excessive deformation (>60% strain) during the first days of healing (Figure 4.5).

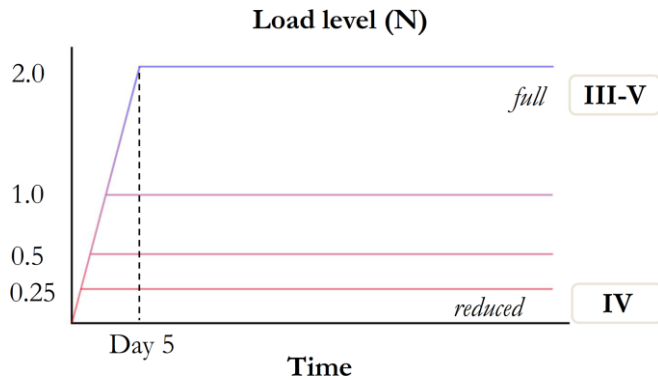

Figure 4.5. Different load levels explored in studies III-V to mimic physiological loading during gait and reduced load, comparable to certain unloading or immobilization techniques such as intramuscular Botox injection [21].

4.3.4 Density implementation

In studies III and IV, a density function ρ was implemented to scale the Cauchy stress exerted by the collagen and ground substance in intact tendon to callus properties according to:

$$\sigma_{\text{callus}}^{\text{collagen}} = \rho * \sigma_{\text{intact}}^{\text{collagen}} \tag{17}$$

$$\sigma_{\text{callus}}^{\text{ground substance}} = \rho * \sigma_{\text{intact}}^{\text{ground substance}} \tag{18}$$

The initial callus density (collagen and ground substance) was set to 1% to match experimental measurements of the tendon stiffness reported at the third day of healing [149].

4.3.5 Strain-regulated tissue production laws

Tissue production was implemented similarly to earlier work of Richardson et al. (2018)[19] and Chen et al. (2018)[20] where tissue production modeled to be strain-regulated (Law 1 in Figure 4.5). However, a thorough literature study of strain-regulated collagen type 1 and 3 gene expression and production in fibroblasts showed that there is little experimental data for high strain magnitudes (>10%) and that they have mixed results. *In vitro* studies showed that collagen production was highest for strain levels around 10% and decreased for strain levels above 10% [270-272]. Considering these experimental results, a second production law was proposed that describes the initial increase of production in response to increasing strain (as seen in production law 1), followed by a decrease

of collagen production upon 'overstimulation' by strains over 15% (Figure 4.5). The strain-regulated production laws were defined similarly to Richardson et al. (2018)[19] according to:

$$\text{Production Factor} = \frac{1}{1 + e^{-k_{\text{sig}}\left(\varepsilon_{\text{prin}}^{\max} - C_1\right)}} \quad \text{for } \varepsilon_{\text{prin}}^{\max} < \varepsilon_{\text{prin}}^{\max,\ \text{transition}} \tag{19}$$

$$\text{Production Factor} = 1 - \frac{1}{1 + e^{-k_{\text{sig}}\left(\varepsilon_{\text{prin}}^{\max} - C_2\right)}} \quad \text{for } \varepsilon_{\text{prin}}^{\max} > \varepsilon_{\text{prin}}^{\max,\ \text{transition}} \tag{20}$$

leading to the following production laws (Figure 4.6), with different shape parameters (k_{sig}: 75, C_1: 7%, C_2: 3%, $\varepsilon_{\text{prin}}^{\max,\ \text{transition}}$: 15%), depending on the maximum principal strain ($\varepsilon_{\text{prin}}^{\max}$). In Study III, production law 1 and 2 were explored, whereas in Studies IV-V only production law 2 was used.

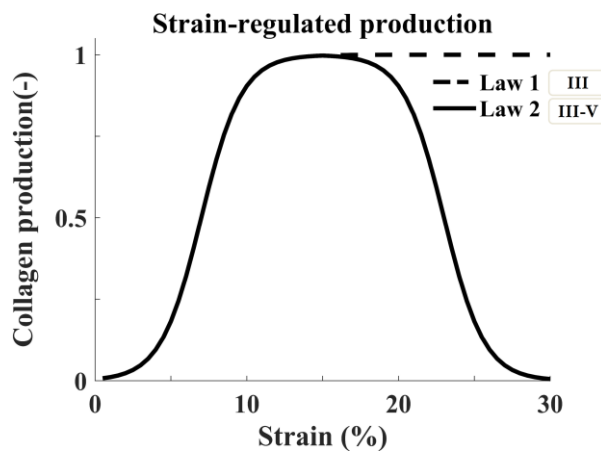

Figure 4.6. Strain-dependent collagen production laws estimated based on literature [111, 112, 117, 121, 273-277], where strain is the maximum principal strain. The production law 2 was used in Studies III-V.

4.3.6 Tissue production rates

During tendon healing, restoration of the extracellular matrix depends mainly on the timely restoration of the collagen architecture. Several experimental studies in rodents reported that the bulk of collagen production occurred in the first four to six weeks of healing [129, 149, 154, 172, 175, 278-282], implying a production rate of 2-4% per day. Based on this, a maximum amount of collagen produced per day of 2% of the intact collagen content was assumed. In Study V, the maximum production rate for tendon-, cartilage- and fat-like tissue was 2%/day and 1.2%/day for bone-like tissue according earlier frameworks in bone healing [17]. Additionally, as one tissue type is produced, the other tissue types are degraded at the same rate of the particular tissue type that is produced. In studies III-V, inflammatory-driven collagen production was considered during the first 4 days of healing [283]. To model this, mechano-regulated production (maximum 1%/day) was combined with a fixed inflammatory-driven baseline production rate of 1% per day, to maintain a total production of 2% per day. Subsequently, from day 5 on, daily production rate was purely dependent on mechano-regulated production (maximum 2%/day). Additionally, the ground substance was assumed to be produced at a similar rate as collagen, thus the spatio-temporal evolution of collagen and ground substance occur similarly.

4.3.7 Collagen reorientation and alignment

Throughout healing, the alignment of the collagen matrix evolves from a random isotropic matrix into a highly aligned organization. For intact tendon and tendon stumps in studies II-V, collagen was assumed to be perfectly aligned in the longitudinal direction. However, for the healing callus in studies III-V, a collagen organization with 13 different collagen fibrils with random orientations was implemented [18, 253] to capture the initially disorganized matrix during early healing. These fibrils were reoriented towards the local maximum principal strain throughout healing, inspired by an existing implementation in articular cartilage [18] according to:

$$\overrightarrow{\boldsymbol{e}_{f,new}} = \exp(\kappa\alpha\boldsymbol{R})\overrightarrow{\boldsymbol{e}_{f,0}} \tag{21}$$

with the angle (α) between the current fibril direction ($\overrightarrow{\boldsymbol{e}_{f,0}}$) and the direction of maximum principal strain, reorientation rate parameter (κ), new fibril orientation ($\overrightarrow{\boldsymbol{e}_{f,new}}$) and a rotation matrix ($\boldsymbol{R}$) that rotates the fibril towards the direction of maximum principal strain. The reorientation rate (κ) was set to 0.06 to ensure that the collagen network is fully aligned in the longitudinal direction by four weeks of healing [135, 136]. To quantify the collagen alignment an established criterion [20] was used:

$$S = \frac{1}{N}\sum_{i=1}^{N}\cos(2\alpha) \qquad \text{for N fibrils.} \tag{22}$$

4.3.8 Cell infiltration and density dependent tissue production

To investigate the effect of cells on tendon healing, cell infiltration from the extrinsic compartment into the healing callus was considered in studies IV-V, depicting both migration and proliferation, similar to Isaksson et al. (2006)[17]. Cell infiltration was modeled using a diffusive process, where the diffusion constant in Fick's law describes the rate of cell infiltration and the nodes on the outer surface of the callus were set as constant cell sources. The value of the diffusion constant was set such that the average cell density in the callus reached 95% after 2 weeks (Figure 4.7). This reflects measurements on the temporal evolution of cell density and proliferation in tendon healing. These studies identified maximum cell density and proliferation rate at 1-2 weeks post-rupture [171-175].

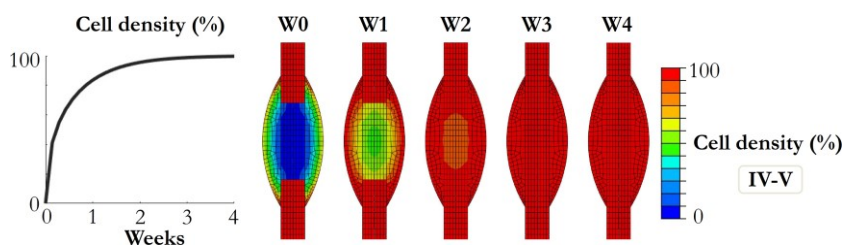

Figure 4.7. Spatio-temporal evolution of cell density as a result of cell infiltration, reported weekly during healing. Mean cell density reached 95% after 2 weeks. Used in studies IV-V.

In Studies IV-V, cell density-dependent tissue production was implemented by scaling the mechano-regulated production ($P_{mechanical}$) to the local cell density (ρ_{cell}; ranging from 0-100%) according:

$$P_{total} = \rho_{cell} * P_{mechanical} \tag{23}$$

Hence, no tissue production occurs if there are no cells present, regardless of the mechanical cue, and tissue production can occur to the full extent if there is 100% local cell density (ρ_{cell}= 100%).

4.3.9 Tissue differentiation frameworks

To investigate the formation of different tissue types during tendon healing, the developed healing framework (Studies III-IV) was extended by incorporating the mechanobiological production and considering the material properties of cartilage-, bone- and fat-like tissue, in addition to tendon (Figure 4.8). A range of existing frameworks considered multiple ranges and combinations of biophysical stimuli, i.e. principal strain, hydrostatic stress, pore pressure, octahedral shear strain, fluid flow, oxygen concentration or angiogenesis (blood vessel presence), to govern the formation of different tissue types (Table 4.2). The hydrostatic stress and octahedral shear strains were calculated according to:

$$\sigma_{hydrostatic} = \frac{tr(\boldsymbol{\sigma})}{3} = \frac{(\sigma_{11} + \sigma_{22} + \sigma_{33})}{3} \tag{24}$$

$$\varepsilon_{os} = \frac{1}{3}\sqrt{\left(\varepsilon_{\text{prin}}^{\text{max}} - \varepsilon_{\text{prin}}^{\text{min}}\right)^2 + \left(\varepsilon_{\text{prin}}^{\text{max}} - \varepsilon_{\text{prin}}^{\text{mid}}\right)^2 + \left(\varepsilon_{\text{prin}}^{\text{mid}} - \varepsilon_{\text{prin}}^{\text{min}}\right)^2} \tag{25}$$

where hydrostatic stress ($\sigma_{hydrostatic}$) is defined as the trace of the stress tensor ($\boldsymbol{\sigma}$) in cartesian format and octahedral shear strain (ε_{os}) depends on the maximum ($\varepsilon_{\text{prin}}^{\text{max}}$), mid ($\varepsilon_{\text{prin}}^{\text{mid}}$) and minimum ($\varepsilon_{\text{prin}}^{\text{min}}$) principal strains.

Table 4.2. Overview of thresholds and daily production rates used for the tissue production of tendon-, cartilage-, fat- and bone-like tissue, depending on different biophysical stimuli, i.e. maximum principal strain (PE, %), hydrostatic stress (HS, MPa), pore pressure (PP, MPa), octahedral shear strain (OSS, %), fluid flow (FF, µm/s), oxygen concentration (OXY, %) and angiogenesis (%), from [262, 284-286]. The octahedral shear strain and fluid flow algorithm is based on a general stimulus (i) that is calculated according: i = OSS/3.75 + FF/3 [286]. The asterisk (*) denotes that these models produced tendon according to the strain-dependent production law 2 presented in Figure 4.6.

Biophysical stimuli:	**Princ. strain Hydrostatic stress**	**Princ. strain Pore pressure**	**Octahedral shear strain Fluid flow**	**Princ. strain**	**Princ. strain Oxygen Angiogenesis**
Abbreviation:	**PE-HS**	**PE-PP**	**OSS-FF**	**PE**	**PE-OXY**
Reference:	Carter et al. (1988) [284]	Claes and Heigele (1999) [285]	Lacroix and Prendergast (2002) [286]	-	Burke et al. (2012) [262]
Tendon	>5 ; <0.2	>15 ; >0.15 >5; <-0.15 or >0.15	i > 3	>4*	- ; 3 ; <90* 2-25 ; >3 ; >90*
Cartilage	<5 ; >0.2	<15 ; >0.15	1 < i < 3	2-4	- ; <3 ; -
Bone	<5 ; <0.2	<5 ; <±0.15	i >1	<2	<2 ; - ; >90
Fat	-	-	-	-	>25 ; - ; >90

To model the material properties for fat-, cartilage-, tendon- and bone-like tissue, a new tissue type-dependent material behaviour was defined (Eq. 26). This implementation allowed the scaling of different stiffness properties for the fat-, cartilage- and bone-like tissue compared to the intact tendon properties defined in Study II. To ensure a decrease in stiffness for fat-like tissue [262], compared to tendon, a scaling coefficient for fat-like tissue (0.5 in Eq. 26) was implemented. The scaling coefficients were determined to ensure that the cartilage- and bone-like materials were 5 and 500 times stiffer than the tendon, respectively. The ratio of the stiffness for the different tissue types follows from an earlier computational framework for predicting tissue differentiation in bone healing [17]. The material behaviour also included a density-dependency for all tissue types, defining the local material properties in the healing callus as:

$$M_{\text{tissue}}^{Callus} = (\rho^F * 0.5 + \rho^T + \rho^C * 2.62 + \rho^B * 40.40) * M_{\text{Tendon}}^{intact}$$
$$\text{for M} = E_1, E_2, K_1, K_2, E_p, E_n, G_{pn} \quad (26)$$

where the generalized material parameter (M) in the healing callus depends on the local fat (ρ^F) tendon (ρ^T), cartilage (ρ^C) and bone (ρ^B) density. The densities affected the stiffness properties in our model for both the collagen ($E_1, E_2, K_1, K_2; Eq.2$) and for the transversely isotropic matrix ($E_p, E_n, G_{pn}; Eq.9-11$).

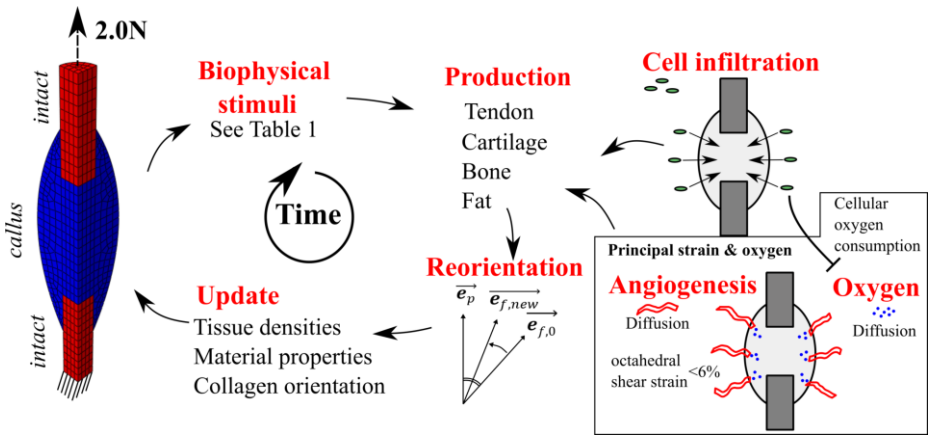

Figure 4.8. Overview of the iterative healing framework that predicts the formation of different tissue types (Study V). Every iteration of healing, a 2N mechanical load was applied and a wide range of biophysical stimuli (see Table 4.2) were calculated to predict tendon-, cartilage-, bone- and fat-like tissue production. Similar to Study IV, cell infiltration occurred in two weeks, affecting tissue production (Eq. 23). For the principal strain and oxygen framework, according Burke et al. (2012)[262], simulations of angiogenesis and oxygen diffusion were utilized to predict oxygen-dependent tissue formation. Angiogenesis was only allowed in elements with less than 6% octahedral shear strain, and oxygen was consumed by cells.

The previous mechanobiological algorithms predicted bone-like tissue formation based on local mechanical stimuli or the presence of blood supply. However, bone formation during tendon healing has been claimed to occur only through endochondral ossification [24], i.e. bone formation that occurs through the ossification of cartilage or further ossification of existing bone. Therefore, this hypothesis was explored using the principal strain model (PE). In particular, bone-like tissue formation was only allowed to occur if the two following requirements were met:

- Maximum principal strain < 2%
- Threshold value of cartilage (ρ^C >20%; ρ^C >25%) or bone ($\rho^B > 0\%$)

tissue densities where two different threshold values for the cartilage density (20% and 25%) were explored. This algorithm was referred to as PE-ENDO.

Following the mechanobiological framework of Burke et al. (2012)[262], angiogenesis (blood vessel formation) and oxygen concentrations were predicted in the healing callus. At the start of healing, the callus was completely deprived of blood vessels and oxygen. Subsequently, every iteration of the healing framework (~1 day) angiogenesis and oxygen diffusion were simulated similarly to the cell infiltration simulations presented in Figure 4.7. Thus, all nodes on the external surface of the callus were sources for angiogenesis and oxygen. Angiogenesis was allowed to occur in elements where the octahedral shear strain was lower than a threshold value (default value: A-OSS = 6%; from [262, 287]). When the angiogenesis concentration reached 90%, the material point was considered an 'established blood supply', and this location was added as an additional source for oxygen diffusion. Furthermore, cellular oxygen consumption was considered (C = 0.5; maximum 50% of oxygen was consumed at 100% cell density).

The predicted angiogenesis and oxygen distributions then affected tissue formation (see PE-OXY in Table 4.2). In particular, cartilage production was predicted under hypoxic conditions (<3% oxygen concentration), whereas presence of a blood supply (>90% angiogenesis) was a prerequisite for either bone-like (<2% strain) or fat-like (>25% strain) tissue formation. Tendon formation was predicted in the non-hypoxic environment (oxygen concentration >3%) and for the strain levels (2-25%) if a blood supply was present.

A parameter sensitivity analysis was performed to determine the sensitivity of the temporal formations of the different tissue types with regards to different angiogenesis- and oxygen-related parameters, i.e. the diffusion constant for angiogenesis (A = 0.25 - 0.5 - 1.0) and oxygen (O = 0.25 - 0.5 - 1.0), the extent of cellular oxygen-consumption (C = 0.25 - 0.5 - 0.75) and the octahedral shear strain-threshold for angiogenesis (A-OSS = 3 - 6 - 12 %), performed similarly to the original framework [262].

4.3.10 Validation of predicted mechanical properties

Predicted mechanical properties of the healing tendon tissue were compared directly with experimental data from Khayyeri et al. (2017 and 2020)[21, 28]. In Studies III and V, stiffness values were validated at 2N load. In Study IV, a creep test was simulated (load rate: 1.1N/s, holding load: 5N) to determine creep magnitude and ratio, strain (at 2N load), stiffness and Young's modulus (at 4-4.5N) identical to the mechanical analysis in the experimental study.

5 Results

5.1 Mechanobiological changes in intact collagen properties (II)

The existing material model was utilized to determine the change of viscoelastic mechanical properties upon a period of reduced daily loading in intact tendon. The collagen material parameters (E_1, E_2, K_1, K_2, η) were successfully fitted (NRMSE: 1.03 - 2.65%, Table 5.1) to the creep and/or stress-relaxation data (Figure 5.1) from rats subjected to five weeks of full (free cage activity) or reduced (Botox-treated) daily loading. For the unimodal optimization strategy (considering only creep or stress-relaxation data), collagen material parameters both increased and decreased for the reduced loading data compared to the full loading data. Also, these optimized parameter sets showed a low predictive power when simulating the test that the model was not calibrated to, i.e. running the creep test with the parameters fitted to stress-relaxation and vice versa. For the bimodal optimization strategy (considering both creep and stress-relaxation data simultaneously), the identified collagen material parameter sets were different from the resulting parameter sets obtained using unimodal optimization. Interestingly, an overall increase in all collagen properties was observed for the reduced loading model compared to the full loading model.

Table 5.1. Collagen parameters fitted to group-averaged creep (CR) and/or stress-relaxation (SR) data from rats subjected to five weeks of full (free cage activity) or reduced (Botox-treated) daily loading. The Δ denotes the relative change (%) in parameter value for the reduced compared to the full loading parameter set. The quality-of-fit is expressed as NRMSE (%) for the different models. Adapted and reprinted from Study II with permission from Elsevier.

	Creep			Stress-Relaxation			Creep & Stress-Relaxation		
	Full	Reduced	Δ	Full	Reduced	Δ	Full	Reduced	Δ
E_1	0.589	2.72	361	5.73	1.53	-73	0.0122	0.0271	122
K_1	10.2	7.76	-24	0.783	6.67	752	25.8	33.7	30
E_2	0.853	0.705	-17	0.200	0.244	22	0.315	0.516	63
K_2	8.50	13.8	62	18.2	22.4	23	16.9	20.5	21
η	490	506	3	531	924	74	460	690	50
CR NRMSE	1.79	1.78		-	-		2.35	2.65	
SR NRMSE	-	-		1.03	1.09		1.39	1.85	

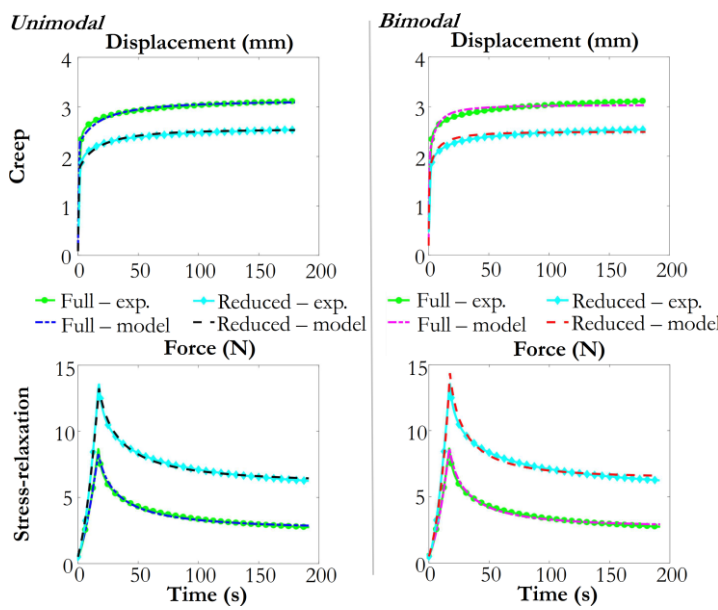

Figure 5.1. Overview of the fitted creep and stress-relaxation behaviour for the unimodal (fitted to creep or stress-relaxation data) and bimodal (fitted to both creep and stress-relaxation data) optimization strategies. The experimental data was obtained from rat Achilles tendon that was subjected to five weeks of full (free cage activity) or reduced (Botox-treated) daily loading. Adapted and reprinted from Study II with permission from Elsevier.

5.2 Mechanobiological mechanism underlying tendon healing (III-V)

5.2.1 Principal mechanisms of tendon healing (III)

A mechanobiological framework was developed to investigate heterogeneous tissue production and temporal evolution of collagen alignment and mechanical properties during tendon healing after rupture. The finite element model predicted high strain levels (>15%) that were heterogeneously distributed, i.e. higher in the tendon core compared to periphery (Figure 5.2A). Also, high strain levels were observed at the stump interface throughout healing. Early tissue production was predicted to occur predominantly in the core between the tendon stumps and at the stump interface (production law 1; Figure 4.6) or predominantly in the periphery of the callus (production law 2; Figure 4.6) (Figure 5.2B). The high strains at the stump interface and in the tendon core prevented early collagen production at these locations in simulations with production law 2. The majority of collagen alignment occurred within 4 weeks of healing (Figure 5.2C) and this prediction did not depend on the production law. The predicted evolution of stiffness was well within the range of experimental data at all timepoints (Figure 5.3D), yet the healing model with production law 1 predicted a higher stiffness throughout the first weeks of healing. The healing model with production law 2 predicted heterogeneous recovery of collagen content, similar to the experimental data in Khayyeri et al. (2020)[21], by predicting that early tissue production mainly occurs in the periphery of the callus and not in the callus core. Therefore, the models in Studies IV and V all utilized production law 2.

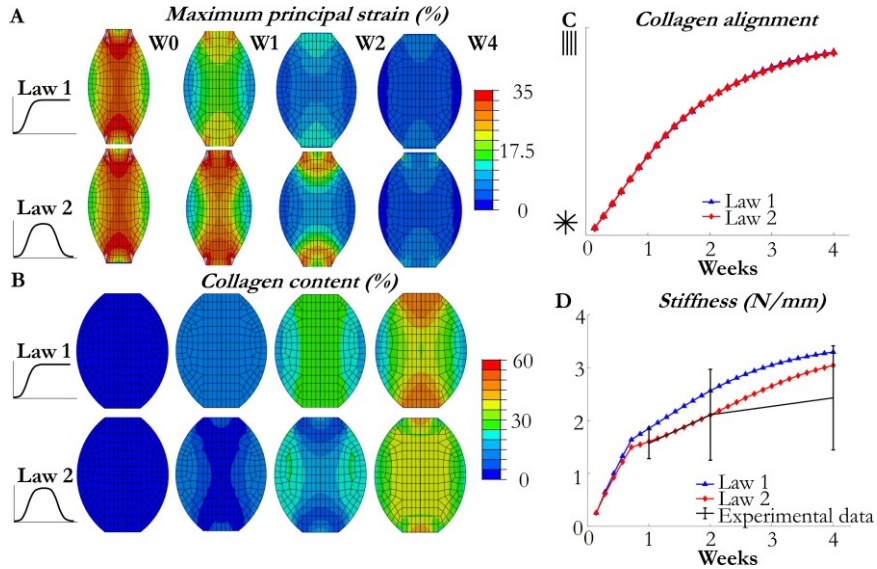

Figure 5.2. Overview of the predicted tendon properties during early healing for a tendon stimulated with full load level (2.0N) and the two strain-regulated production laws. The spatial prediction of maximum principal strain (A), collagen content in the undeformed state (B), the temporal evolution of collagen alignment (C) the evolution of stiffness (D) compared to experimental data (mean±standard deviation) [21]. Adapted and reprinted from Study III licensed under CC BY 4.0.

5.2.2 Effect of reduced load level and cell infiltration (IV)

The developed mechanobiological framework was characterized and validated by investigating the effect of reduced load levels and cell infiltration on spatio-temporal predictions of tendon healing. The main effect of a reduced daily load level in combination with production law 2 (Figure 4.6) was that the model predicted reduced strain levels, which allowed more tissue production throughout the initial healing stage (<2 weeks of healing), yet it predicted less tissue production between two and four weeks of healing (Figure 5.3). Similar to Study III, strains were persistently higher in tendon core compared to the periphery in all models, regardless of the load level. The main effect of including cell infiltration during tendon healing was that the predicted tissue production was higher in the periphery of the tendon callus, versus the tendon core, throughout four weeks of healing for all load levels (Figure 5.3-5.4). Including cell infiltration in our healing framework strengthened the prediction for the spatio-temporal evolution of collagen properties measured by Khayyeri et al. (2020)[21], where collagen production occured in the callus periphery first, for rats subjected to either full (free cage activity) or reduced daily load (intramuscular Botox injection).

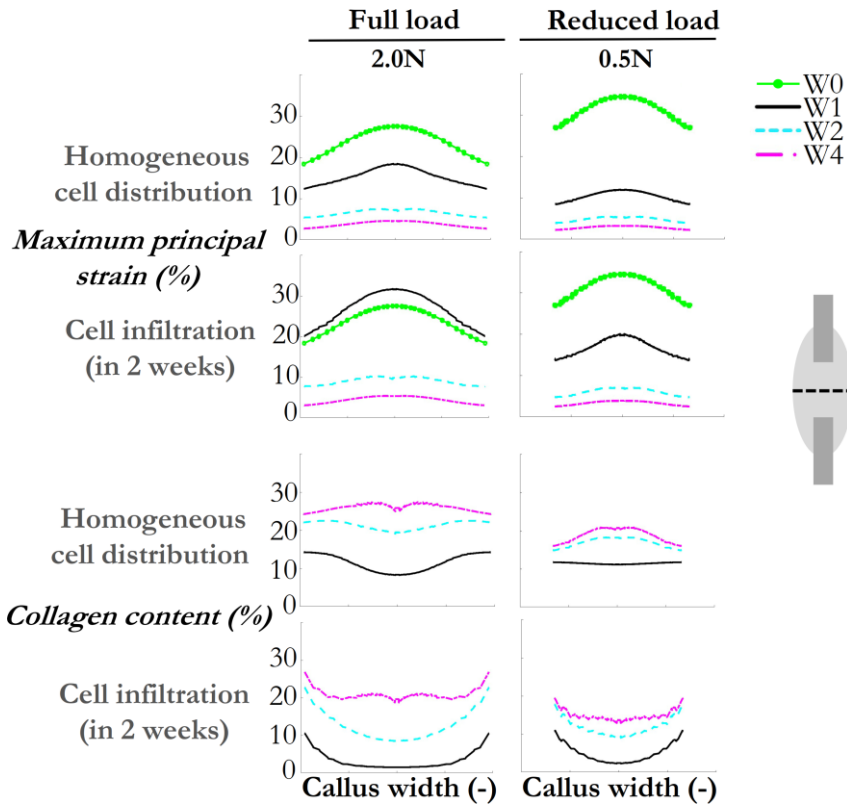

Figure 5.3. Spatio-temporal evolution of maximum principal strain and tissue production with production law 2 for tendon models with full (2.0N) or reduced (0.5N) load level. The values are plotted along a whole-width profile at the midtendon cross-section only. Simulation output is from healing simulations with homogeneous cell distributions or cells infiltrating for 2 weeks.

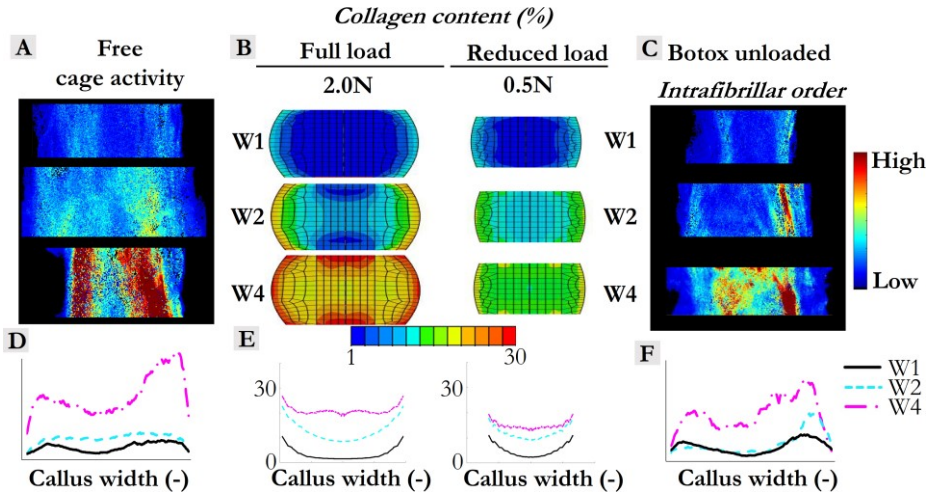

Figure 5.4. Spatio-temporal evolution of tissue production with production law 2 for tendon models with full (2.0N) or reduced (0.5N) load level in the whole callus (B) or a whole-width profile at the midtendon cross-section only (E). Simulation output is from healing simulations with cells infiltrating for 2 weeks (B, E). Model predictions are compared to the spatio-temporal evolution of the SAXS imaging data (A, C, D, F) from rats subjected to free cage activity (A, D) or Botox-treated (C, F) healing tendon [21], where intrafibrillar order reflects the collagen matrix. The spatial maps (A, C) are unique samples, where the midtendon profiles (D, F) are group-averaged at 1, 2 and 4 weeks of healing.

The healing simulations predicted most mechanical properties (stiffness, Young's modulus, strain level, creep magnitude and ratio) within 1 standard deviation of the experimental data in Khayyeri et al. (2020)[21] or at least captured the trends in the experimental data when comparing the full (free cage activity) and reduced load level (Botox unloaded). (Figure 5.5). Interestingly, the predicted stiffness resulting from the healing models with a reduced daily load level was increased compared to the full load models throughout the initial stage of healing, similar to experimental data. The different reduced load models predicted rather similar evolution of the mechanical properties.

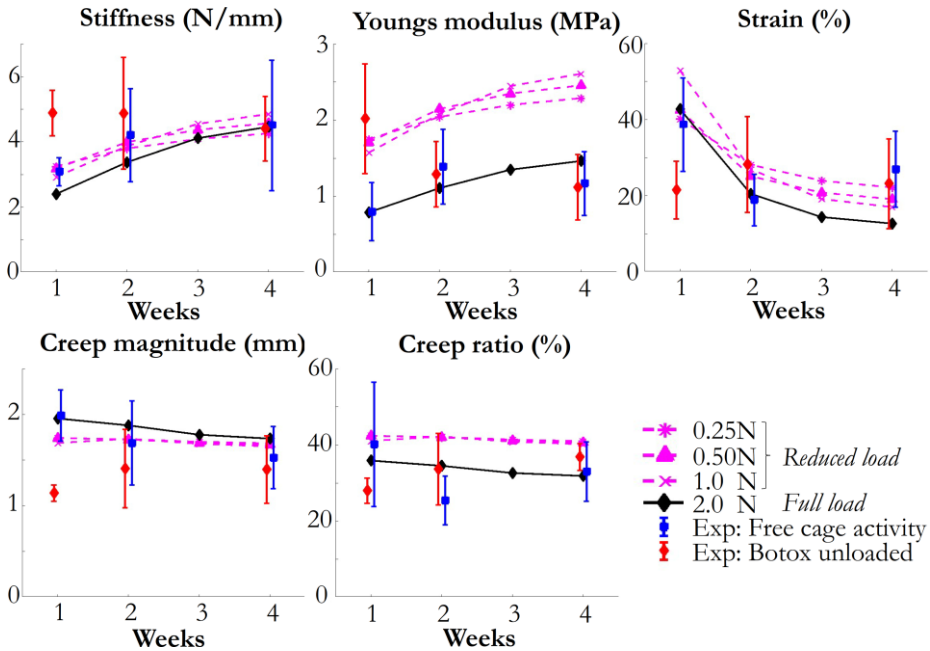

Figure 5.5. Temporal evolution of mechanical properties (stiffness, Young's modulus, strain level, creep magnitude and ratio) for the models with production law 2, cell infiltration for 2 weeks and full (2.0N) or reduced (0.25; 0.5; 1.0N) load level. Predicted mechanical data is compared to experimental data (mean ± standard deviation) from free cage activity loaded and Botox unloaded tendons [21].

5.2.3 Formation of different tissue types (V)

The different mechanobiological algorithms predicted a sequential evolution of tendon-, cartilage- and bone-like tissue formation throughout the first 20 weeks of healing (Figure 5.6). All frameworks predicted an initial production of tendon-like tissue, and ended with a significant production of bone-like tissue. The principal strain and oxygen algorithm (PE-OXY) predicted that the healing callus was predominantly tendon-like for the longest time, with the latest occurrence of production of bone-like tissue. Oppositely, octahedral shear strain and fluid flow algorithm (OSS-FF) predicted the shortest time span of tendon formation and the earliest bone formation of all models. Principal strain combined with hydrostatic stress (PE-HS) or pore pressure (PE-PP) predicted slow but gradual cartilage production throughout healing. On the other hand, the other algorithms (PE; PE-OXY; OSS-FF) predicted a cartilage production over a shorter time span.

With the production of tendon-, cartilage- and bone-like tissue, the stiffness of the healing tendon progressively increased throughout the first weeks of healing, followed by an asymptotic flattening. The principal strain and oxygen stimulus (PE-OXY) displayed the slowest stiffness evolution, yet the predicted stiffness in this model was within the experimental data within the first weeks of healing and reached intact levels of stiffness at 20 weeks of healing. The other mechanobiological algorithms (PE; PE-HS; PE-PP; OSS-FF) predicted that intact levels of stiffness would be reached within four to twelve weeks of healing.

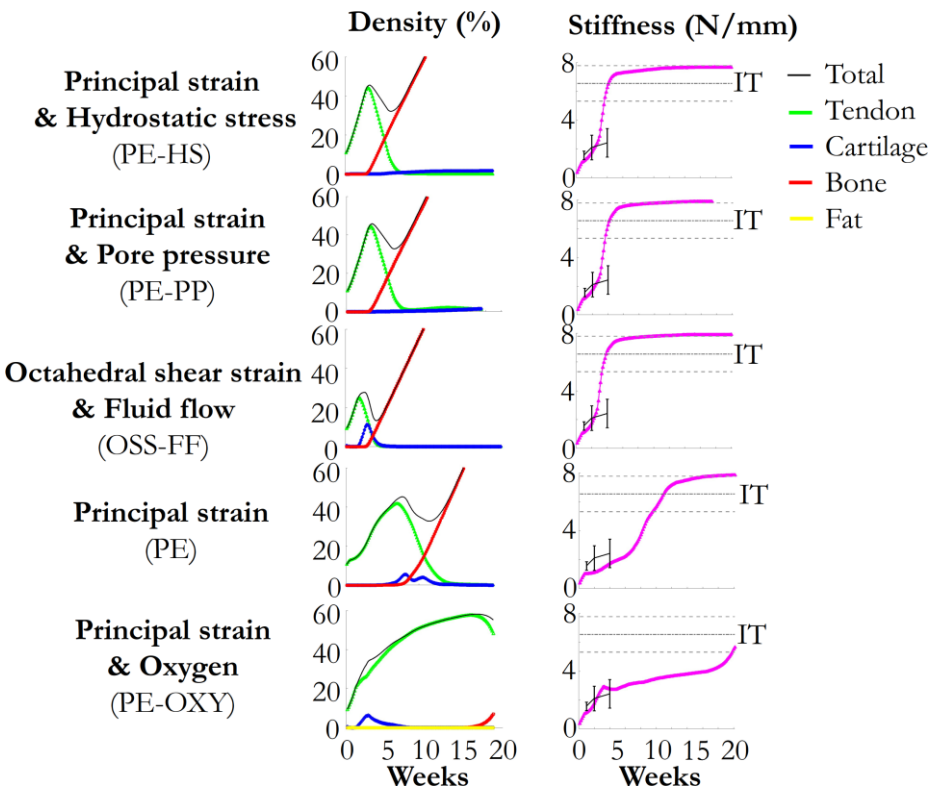

Figure 5.6. Evolution of tendon, cartilage and bone tissue density and overall stiffness throughout 20 weeks of healing. The stiffness data is compared with experimental measurements (mean ± standard deviation) from intact (IT) [28] and post-transection healing rats subjected to free cage activity loading [21] after 1, 2 and 4 weeks of healing.

All mechanobiological algorithms predicted heterogeneous tissue formation throughout 20 weeks of healing (Figure 5.7). The initial production of tendon-like tissue was predicted to occur in the periphery of the callus (similar to study IV), followed by a homogeneous production. Most algorithms (PE-HS; PE-PP; PE; OSS-FF) only predicted a rather short time span of tendon-like tissue formation. However, the principal strain and oxygen algorithm (PE-OXY) predicted that the typical heterogeneous initial formation of tendon, with increased tendon-like tissue in the callus periphery, was maintained for over 10 weeks of healing.

Cartilage-like tissue production was less prominent than either tendon- or bone-like tissue production for all mechanobiological algorithms. The principal strain and pore pressure (PE-PP) algorithm predicted long term cartilage production at the stump interface. The principal strain and oxygen (PE-OXY) algorithm was the only algorithm to predict cartilage production in the callus core. Production of bone-like tissue generally started in the periphery of the callus, before spreading to the callus core and throughout the whole callus. Yet, for the principal strain and oxygen (PE-OXY) algorithm, bone-like tissue production was predicted rather late and did not spread throughout the whole callus at 20 weeks.

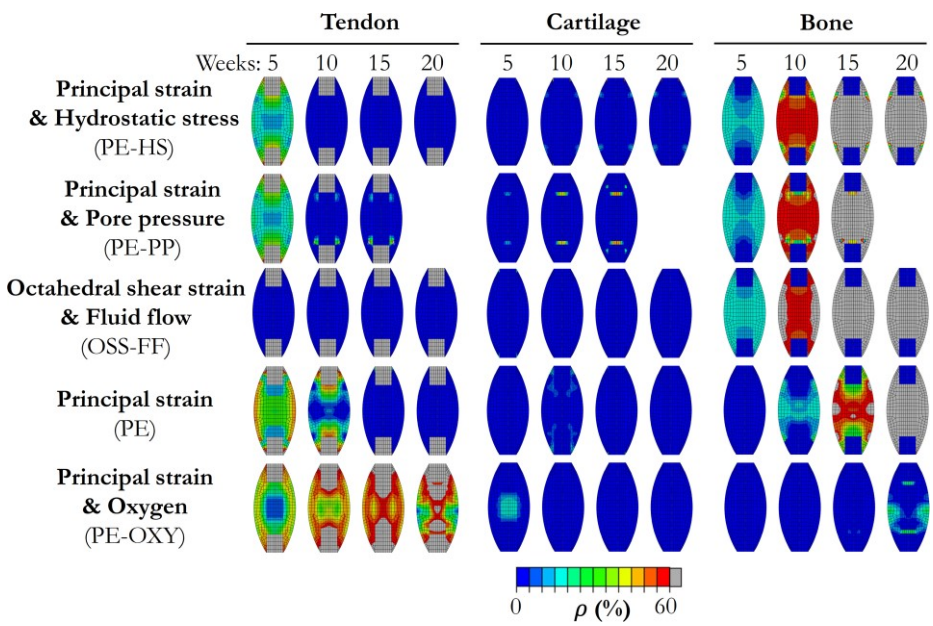

Figure 5.7. Evolution of tendon, cartilage and bone tissue density for the different mechanobiological algorithms at 5, 10, 15 and 20 weeks of healing.

Allowing bone-like tissue formation only to occur endochondrally (PE-ENDO 20% and 25%), decreased the formation of bone-like tissue, and increased the long-term presence of both tendon- and cartilage-like tissue, compared to the default principal strain model (Figure 5.8). The endochondral algorithm is the only one to predict co-existence of tendon-, cartilage- and bone-like tissue at 20 weeks of healing.

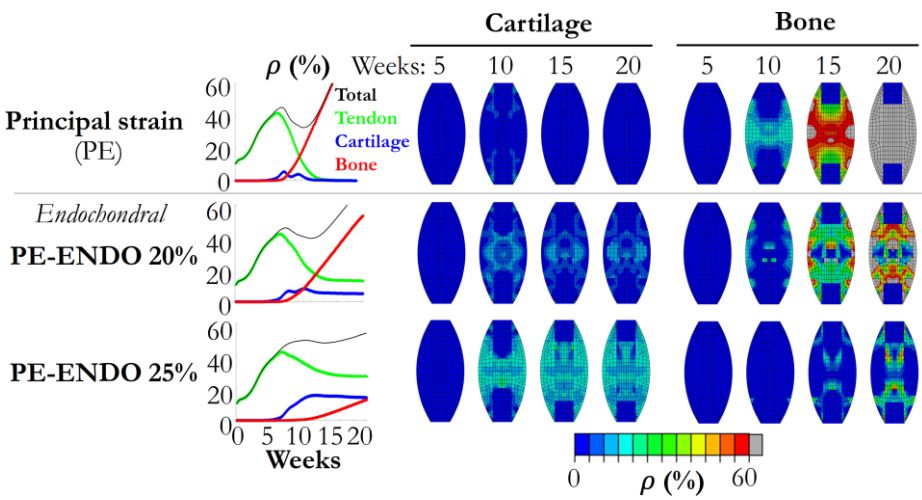

Figure 5.8. The effect of allowing production of bone-like tissue only through the endochondral pathway (PE-ENDO) in combination with the strain-dependent algorithm (PE). Two cartilage density threshold values (20% and 25%) were explored to observe the effect of allowing bone-like tissue formation only via endochondral ossification on the spatio-temporal evolution of the different tissue types throughout twenty weeks of healing.

The parameter sensitivity study performed for the algorithm regulated by principal strain and oxygen (PE-OXY) showed large variations in the predicted temporal evolution of tendon-, cartilage-, bone- and fat-like tissue production throughout 20 weeks of healing (Figure 5.9). Parameter perturbations that increased the process of angiogenesis or oxygen concentration (A=1.0, A-OSS = 12%, C = 0.25, O = 1.0), generally predicted less cartilage formation, whereas all perturbations that created more hypoxic conditions (A = 0.25, A-OSS = 3%, C = 0.75, O = 0.25) predicted more cartilage formation. Different perturbations, both increasing and decreasing blood vessel formation and oxygen levels or decreasing these, led to increased levels of predicted bone-like tissue formation. Only one parameter set (A-OSS = 12%) predicted early production of fat-like tissue.

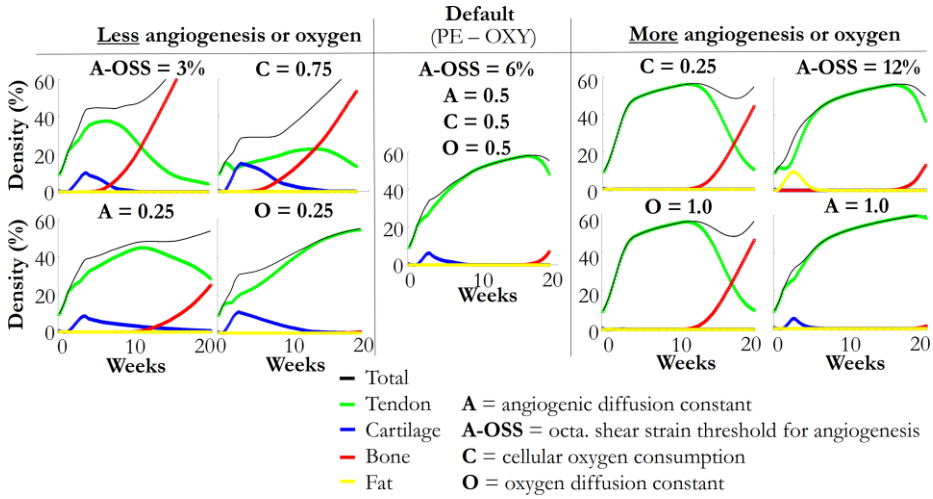

Figure 5.9. Overview of the results of the parameter sensitivity study for the principal strain and oxygen framework (PE-OXY) and the temporal evolution of the tendon, cartilage, bone and fat density, throughout the first 20 weeks of healing.

The principal strain and oxygen (PE-OXY) algorithm predicted spatio-temporal evolution of angiogenesis (blood vessel formation) and oxygen levels (Figure 5.10). The spatial maps displayed the gradual infiltration of blood vessels and oxygen saturation from the periphery of the callus into the callus core, within four weeks of healing. The angiogenesis and oxygen levels saturated (100% angiogenesis and oxygen levels) in the whole callus within the first 8 weeks of healing.

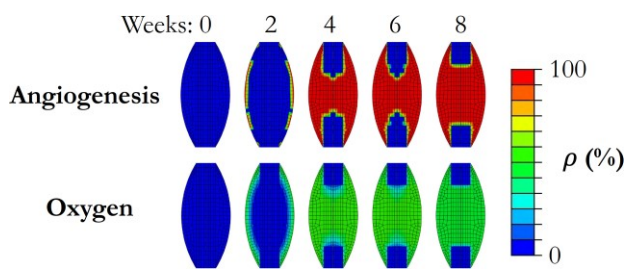

Figure 5.10. The spatio-temporal evolution of angiogenesis (blood vessel formation) and oxygen levels in the strain and oxygen framework (PE-OXY) throughout the first eight weeks of healing.

6 Discussion

6.1 General

The aim of this thesis was to investigate mechanobiological mechanisms in intact and healing tendon by using and developing computational models. Towards this aim, the thesis summarized important (mechanobiological) features of tendon healing (Study I), validated an existing tendon material model with mechanobiological data from intact tendon (Study II) and utilized this material model to develop an adaptive mechanobiological healing framework (Studies III-V). Extensive experimental data, i.e. geometrical, mechanical, structural properties, from rat Achilles tendon was used to design and validate the intact and healing tendon models [21, 28]. In particular, the experimentally observed changes in viscoelastic properties upon reduced daily loading in intact tendon could be captured by a combination of elastic and dissipative collagen properties (Study II). Subsequently, the developed healing framework with strain-regulated tissue production in combination with cell infiltration and collagen alignment, predicted heterogeneous evolution of collagen properties and the evolution of mechanical properties as observed experimentally in tendons subjected to full (Studies III-IV) and reduced (Study IV) daily load levels. Finally, the predictive capability to reproduce experimental observations of tissue formation with the healing framework was explored by developing and adopting existing mechano-regulatory tissue differentiation schemes for tendon-, cartilage-, bone- and fat-like tissue formation (Study V).

In Study II, the material model was successfully utilized to capture mechanical behaviour of intact rat Achilles tendon subjected to full or reduced daily loading (through intramuscular Botox injection). The material model was able to describe creep and stress-relaxation behaviour independently and simultaneously. Also, our

results displayed the capability of the material model for describing mechanobiological adaptation of mechanical properties in rat Achilles tendon. In particular, reduced daily loading affected the elastic (linear E_1 and exponential K_1 stiffness; Section 4.1, Eq. 2) and damping properties (linear E_2, exponential K_2 and damping time-constant η; Section 4.1, Eq. 3). The increase in elastic properties represents an increase in stiffness and elastic energy storage. The increase in damping properties (linear, exponential and damping time-constant) described an increase in dissipated energy that is dissipated over a longer time span. The differences in elastic properties may be related to different structural changes in the ECM such as the crosslinking density or collagen content, whereas the prolonged viscoelastic response could be related to decreased collagen organization, increased crimp or slower fiber recruitment. The mechanical properties were identified by using a group-averaged tendon geometry that was fitted to group-averaged mechanical data. This approach allowed us to look at general differences between the two groups, yet it did not allow us to study subject-specific differences in tendon behaviour. In summary, Study II provided a validated material model for intact rat Achilles tendon that could be utilized when investigating the tissue response to external mechanical loading in rats. Additionally, the material model showed the capability to describe the mechanobiological changes in mechanical properties for rat Achilles tendon after a period of reduced loading.

Study I summarized and generalized literature findings regarding temporal and spatial evolution of tendon properties during tendon healing in rodents. Additionally, the effects of different mechanical loading protocols, gender and suture-repair were investigated. The study also identified that there is a limited understanding of long-term recovery of the tendon properties and how the loading protocols can affect this. In addition, it is rather unknown whether mechanobiology plays an important role in cell and tissue differentiation and subsequent formation of different tissue types that is observed during tendon healing. Furthermore, it is unknown how the formation of fat-, cartilage- and bone-like tissue affects the outcome of the healing process and how these tissues affect the local, heterogeneous and overall biomechanical function of the tendon. Also, a wide range of cell populations have been identified to be present in the callus tendon healing, yet the exact function and spatio-temporal distribution of many cell populations is rather unknown [128]. Recently, different experimental works have observed heterogeneity during tendon healing in terms of collagen features, cell populations and their distributions, or different tissue types, i.e. formation of fat-like, cartilage-like or bone-like regions in the tendon during healing. It is unknown to what extent mechanobiology plays a role in the heterogeneous recovery of tendon properties during tendon healing. Spatial

changes in biophysical stimuli may affect tendon mechanobiology in a heterogeneous manner, yet no experimental or numerical study has investigated the spatial distribution of mechanical stimuli during tendon healing. To address some of the aforementioned gaps in knowledge, this thesis investigated the heterogeneous evolution of tendon properties (collagen production, alignment and mechanical properties) during tendon healing as function of mechanical loading. To achieve this, a numerical framework was developed (in Studies III-V) that could predict and investigate some of the main processes of tendon healing that were identified in Study I.

The main focus of this work was to develop a computational healing framework that could describe and investigate the evolution of tendon properties with a particular focus on identifying mechanobiological mechanisms observed in experimental data. Interestingly, recent experimental work showed early recovery of collagen properties in the periphery of the healing tendon, and not in the tendon core [21]. The developed healing model incorporated a mechanobiological mechanism predicting this experimental observation. In short, the combination of finite element predictions of high levels of (principal) strain in the tendon core, combined with a strain-regulated production law that predicts decreased collagen production for high strain levels, predicted decreased collagen production in the tendon core during early healing. Future experimental measurements of the spatio-temporal evolution of strains in the healing callus, combined with spatial measurements of collagen formation can validate or scrutinize this hypothesis. Another interesting observation of the investigated strain-dependent collagen production was that healing tendons subjected to reduced daily loading displayed increased early collagen production compared to the fully loaded tendons. This was predicted because the reduced load levels resulted in lower strain levels, thereby avoiding high strain levels where collagen production was predicted to be decreased (production law 2). More elaborate spatio-temporal measurements of collagen or tissue production throughout early healing, for tendons subjected to different mechanical load levels, could provide valuable data for validation or redesigning of the implemented strain-regulated production laws.

In addition to strain-regulated tissue production, the spatial distribution of matrix-producing cells may affect spatial tissue production. Therefore, cell infiltration from the periphery into the empty tendon core was considered to contribute to early tissue production in the tendon periphery throughout the first two weeks of healing. Implementing this cell activity strengthened the prediction that collagen production occurs first in the tendon periphery, regardless of the load level. This was similar to observations in experimental data, where rats showed early collagen production occurring first in the tendon periphery, both for rats

subjected to full (free cage activity) or reduced daily loading (through intramuscular Botox injections) [21]. Future experiments should combine spatial measurements of tissue production and cell distribution to determine the importance of accounting for the distribution of matrix-producing cells to healing.

The healing framework was further developed in Study V to explore a range of existing mechanobiological frameworks for predicting the formation of different tissue types. Different biophysical stimuli, e.g. principal strain, hydrostatic stress, pore pressure, octahedral shear strain and fluid flow, angiogenesis and oxygen concentration were considered, according to earlier work in bone healing [17, 262, 265]. The developed framework was able to predict experimentally observations of cartilage-like [22, 23, 139] and bone-like tissues [24, 138, 288, 289] throughout the first 20 weeks of tendon healing. This work supported that mechanobiology may play a role in tissue differentiation during tendon healing, as proposed in Huber et al. (2020)[25].

The healing framework predicted heterogeneous evolution of different tissue types throughout healing. Generally, initial tendon-like tissue formation was followed by temporal production and degradation of cartilage-like tissue and progressive production of bone-like tissue. Tendon- and bone-like tissue production started mostly in the periphery of the callus and spread later throughout the callus. Similar to Studies III and IV, tendon-like tissue production occurred early in the periphery due to production law 2 and as a result of cell infiltration. Formation of bone-like tissue was predicted in the periphery of the callus since the strain levels are lower in the periphery than in the tendon core and low strain levels are required for bone formation. Typically, there was less cartilage-like tissue formation predicted, compared to bone- or tendon-like tissue. Allowing bone-like tissue formation to only occur endochondrally (PE-ENDO), as suggested by experimental data from Lin et al. (2010)[24], increased the predicted formation and persistence of tendon and cartilage. On the other hand, it limited the predicted bone-like tissue formation, compared to the default strain model. This prediction of tissue formation was deemed more realistic since it reproduced the experimental observations of long-term (>15 weeks) presence of cartilage [139] in co-existence with more isolated islands of bone-like tissue [290], instead of a fully ossified callus without any cartilage present. Yet, two long-term healing studies showed that the bone-like volumes may span the full length of the tendon and may take up a large volume of the tendon after 15 [289] and 16 weeks [138] of healing. In agreement with these experimental observations, most mechanobiological algorithms in Study V predicted a vast amount of bone formation in the whole callus.

In addition to purely mechanical stimuli, the potential role of angiogenesis and oxygen levels in formation of different tissue types was explored. The principal strain and oxygen-dependent algorithm (PE-OXY), similar to Burke et al. (2012)[262], predicted less excessive bone-like tissue formation, and predicted significant cartilage production in the callus core. This algorithm captured the experimental observations that cartilage production (chondrogenesis) is likely to occur under hypoxic conditions [24] whereas bone-like areas have been found to be surrounded by blood vessels [290]. However, the predicted bone-like tissue production occurred at a late stage of healing (>15 weeks) and potentially underpredicted the amount of bone-like tissue formation observed in experimental data. Yet, the parameter sensitivity analysis showed significant variation of the predicted formation of the different tissue types with changes in different parameters that remain uncertain. Future experimental studies should perform spatio-temporal measurements on oxygen concentrations, and blood vessels formation, to enable validation of these frameworks, similar to Burke et al. (2012)[262].

In summary, different mechanobiological mechanisms were identified in Study V to contribute to heterogeneous tissue formation and differentiation. Similar to Studies III-IV, cell infiltration may contribute to early (tendon) tissue production in the periphery and the finite element simulations predicted higher strain levels in the core and lower strains in the periphery. Lower strain levels in the periphery will allow earlier cartilage- and bone-like tissue formation in the periphery. Additionally, the heterogeneous process of angiogenesis and the oxygen distribution may regulate spatial patterns of tissue formation. In particular, hypoxic conditions promotes cartilage formation whereas blood supply has to be present for formation of bone- and fat-like tissue. Therefore, early cartilage formation was predicted in the hypoxic tendon core. The superposition of the oxygen and strain field imply that bone formation may occur earlier in the periphery given the lower strains and the presence of blood supply. On the other hand, high strain levels combined with blood supply may relate to fat formation. Yet, the strain and oxygen framework predicted very little fat formation, as it takes a while for blood supply to establish, and the high strain levels associated with fat formation are only predicted during very early healing.

Other than tissue production, also the gradual alignment of the collagen structure throughout the first month of healing was considered to affect the global and local mechanical behaviour of the tendon in Studies III-V. The implementation predicted a strong alignment of the tendon in the direction of principal strain. This implementation reproduced the typical tendon organization with mainly parallel collagen fibers along the principal loading direction of the

tendon. In terms of reorientation, in accordance with experimental observations [135, 136] the majority of collagen reorientation occurred gradually within four weeks in all models since the maximum strain directions are very similar between the models, due to the uniaxial loading of the tendon. There is very limited experimental data on mechano-regulated control over collagen alignment in healing tendons, but future implementations of the framework could consider different mechanoregulated collagen alignment mechanisms, as explored by Richardson et al. (2018)[19] and Chen et al. (2018)[20].

In addition to predictions of tissue production and collagen alignment, the healing models predicted temporal evolution of a range of mechanical properties such as the overall stiffness, Young's modulus, creep ratio and magnitude and strain levels. The predicted mechanical properties were compared with available experimental data. In general, the healing models were able to predict the experimental data at most timepoints throughout the first four weeks of healing. Interestingly, the finite element simulations in Studies III-V displayed supraphysiological strains (>15%) during early healing. Mechanical data from healing rat Achilles tendons, one week post-rupture, also showed that the overall tissue strain during a load-to-failure [149] or creep test [21] is well over 15%. However, no experimental data was available to validate the spatio-temporal evolution of the strain fields during healing. Study III showed that the initial healing framework was capable of predicting experimental stiffness data during healing [21] that the framework was not fitted to. Additionally, reduced loading affected some mechanical properties as observed in experimental data [21]. Study IV showed that healing tendons stimulated with reduced loading displayed an increased stiffness, Young's modulus and decreased creep magnitude compared to the fully loaded model, at the first week of healing, similar to experimental data [21]. However, the opposite trend was observed for mechanical data from load-to-failure test in healing rat tendon. Specifically, Eliasson et al. (2009)[149] and Khayyeri et al. (2020)[21] showed that tendons subjected to intramuscular Botox treatment display a lower stiffness than tendons subjected to free cage activity. One underlying mechanism to explain these results could be that tendons subjected to free cage activity display a longer toe region in their stress-strain response, and require more force to be fully recruited and aligned. The material model used in this thesis does not incorporate the crimp behaviour or fiber recruitment explicitly, thus we cannot capture these behaviours. On a different note, Study IV showed that the inclusion of cell infiltration in the healing model had a marginal effect on the temporal evolution of the mechanical properties. Parameter sensitivity analysis of the cell infiltration rate showed that slower cell infiltration predicted slower tissue production and thus slower recovery of stiffness. The healing models in Study IV predicted a marginal evolution of creep properties. This may be explained

by the fact that in the material modeling of the healing callus, the time-constant for the damping property (η) was not density-dependent. Yet, the available experimental data [21] does not show a very conclusive evolution of these properties throughout the first weeks of healing either. In Study V, different mechanobiological algorithms predicted a temporal evolution of stiffness that was roughly within experimental data [21] throughout the first four weeks of healing while predicting that intact levels of stiffness [28] would be recovered within four to twenty weeks. These results largely agree with the findings of the literature study (Study I) where it was shown that intact levels of stiffness are recovered within two to eight weeks of healing (Figure 3.7).

6.2 Limitations

The main limitations of this thesis are: (i) the phenomenological material model, (ii) unknown *in vivo* load levels, tissue deformation and strain transfer during tendon healing, (iii) the limited amount of mechanoregulated processes that were considered, (iv) tissue production due to biological and inflammatory processes, (v) assuming continuum level mechanics in the healing tendon. These limitations are explored and discussed below.

The phenomenological material model

The choice of the standard linear solid model had implications for the fitting procedure in Study II. The damping constant is in the order of minutes, as the bulk of relaxation or creep occurs in the time-scale of minutes. Thus, the dissipative behaviour of the Maxwell branch for quick deformations (<10 seconds) is rather limited. Hence, there is a considerable overlap in the sensitivity of the overall stress-strain response to the linear (E_1, E_2) and exponential (K_1, K_2) stiffness parameters in the elastic and Maxwell branch for quick deformations. This similarity may contribute to the fact that the parameter fitting procedure (*fmincon* in Matlab) often found local minima, instead of the global minimum. To improve the robustness of the parameter identification method, a bimodal fitting strategy was implemented, i.e. fitting the material parameters to both stress-relaxation and creep data simultaneously. The 'optimal' parameter sets using this approach were different to the parameter sets found by the individual fitting procedures (Table 5.1). Interestingly, the bimodal fitting approach identified an increase in all material properties comparing the Botox-treated rats to the fully loaded rats, whereas the fitting to one mechanical test led to mixed results. Still, the identified differences in phenomenological material parameters are difficult to interpret as they do not represent discrete structure-function relationships in the tendon, but

rather describe different contributions to the overall stress-strain response of tendon in various mechanical loading scenarios.

Although the mechanical behaviour of the ground substance is highly disputed, Khayyeri et al. (2016)[221] stated that the transversely isotropic matrix was essential to predict fluid exudation upon tensile loading. Fluid exudation has not been investigated elaborately in numerical modeling or experimental work, but has been reported in experimental observations [85, 291]. Future experimental studies should investigate fluid flow velocities and flux to enable thorough validation of this aspect in material modeling frameworks. Additionally, future material models also may consider the role of elastin or elastic fibers in tendon mechanics [292].

In vivo load, nonuniform deformation and strain transfer

There is almost no experimental data quantifying the magnitude, rate, duration or frequency of *in vivo* mechanical loading for intact and healing (rat) Achilles tendon. One of the main unknowns in this thesis is the applied mechanical load during healing. Experimental measurements found a ~2N peak ground reaction force in Sprague-Dawley rats aged 12-16 weeks [269]. Additionally, the rats used in in Khayyeri et al. (2020)[21] weighed ~200g, which represents a 2N force. Applying a 2.0N load in the intact tendon model induced physiological levels of strain (~4.5%), which were deemed reasonable. Thus, in Studies III-V, a maximum physiological load of 2.0N was applied during tendon healing to reflect the maximum load during gait. Thorough experimental validation of the forces and strains in the Achilles tendon will be key to develop and validate mechanobiological frameworks, similar to the ones presented in this thesis.

For the mechanobiological experiments in rats, it is unknown to what extent the different techniques (intramuscular Botox injection, tail suspension, immobilization by cast or orthosis) affect the mechanical loading of the Achilles tendon compared to normal physiological loading during gait or free cage activity. Different levels of reduced load (12.5 – 25 - 50% of full physiological load) were explored to mimic the intramuscular Botox treatment that was used in rat experiments of Khayyeri et al. (2020)[21]. Recently, a musculoskeletal model of the rat hindlimb was used to get estimates of tissue and cell-level strains in loaded, unloaded, suture-repaired and nonrepaired Achilles tendon [20]. Recent measurements of strain and forces in the human Achilles tendon observed during different rehabilitation exercises, e.g. walking, running, heel raises, hopping, squatting, can be utilized to explore more realistic loading patterns in computational healing frameworks for different loading regimens [293, 294].

Additionally, it is known that the magnitude and spatial distribution of deformation of the human Achilles tendon may vary considerably, yet there are almost no spatial and/or temporal measurements of tissue-level or cell-level deformation or strain throughout healing in rats. Yet, human data implies higher deformation in the tendon core for intact human Achilles tendon [295-297], similar to the strain maps predicted by finite element simulations during healing (Studies III-V). Experimental measurements of deformation could help to validate the finite element simulations. This is a vital step in identifying how certain rehabilitation regimens are related to impaired healing through local mechanical over- or unloading. Moreover, the identification of loading-induced damage or microtrauma may help identifying appropriate levels of physical loading throughout healing.

Also, the different subtendons that connect the Achilles tendon to the three calf muscles (medial and lateral gastrocnemius and soleus) were not considered in the finite element simulations. However, the three muscles may induce heterogeneous loading of the tendon by exerting different forces during contraction, inducing different deformations and loads in the subtendons [298]. Also, the subtendons may display different structural and mechanical properties. In intact human tendon, the subtendons display different viscoelastic properties [299] and these differences may contribute to the nonuniform displacements observed in human Achilles tendon [295-298]. These factors may also contribute to heterogeneities found during tendon healing, as suggested in Khayyeri et al. (2020)[21]. Another process that may affect *in vivo* tendon loading throughout healing is the temporal change in muscle-tendon dynamics or gait during healing. For example, different features of gait, e.g. joint angles, speed, and swing time, were found to change throughout the first three weeks of healing in rats [300].

Other mechanoregulated processes

In the healing framework (Studies III-IV), only mechanoregulated production and realignment of collagen were considered to describe the initial repair of the tendon. However, recent modeling studies also described constant or strain-regulated degradation or damage of collagen [19]. These mechanisms of matrix degradation are more important in predictions of long-term homeostasis. Yet, in our healing model, the bulk (>95%) of production, reorientation and stiffening occurs within the first four to six weeks of healing. Future development of the healing framework may also entail modeling the accumulation of microdamage during fatigue loading or identifying mechanisms of tendon failure in intact or healing tendons. Healing studies in rat Achilles tendon showed that early loading may induce considerable microdamage, which may induce additional growth of the healing callus [97, 170]. Additionally, the collagen dispersion or speed of alignment in our healing

framework did not depend on the magnitude of strain, only on the direction of maximum principal strain. However, more disorganized collagen has been found in tendons that are more unloaded. Huber et al. (2020)[25] even suggested that this unorganized collagen matrix may affect cell spreading and TAZ signaling to regulate fat and bone differentiation during healing.

Only one type of collagen was considered in the material model. The mechanical behaviour of collagen in the material model probably resembled collagen type 1 since the intact data from Study II contains mostly collagen type 1. However, during early healing there are considerable amounts of collagen type 3 being produced, yet many questions remain on its properties and function. Collagen type 3 has been described as having thinner and longer fibrils, with less crosslinks and lower level of organization, which together results in decreased mechanical properties compared to collagen type 1 [57, 166, 301, 302]. Most probably, collagen type 3 is produced in the early healing phase in an unorganized manner to establish an initial stable matrix network that allows cellular processes such as *migration* and *mechanosensing* [131, 132]. We capture this initial behavior in our model by creating an initial collagen network with random/isotropic organization and with decreased mechanical properties (more collagen type 3 like) that develops into an aligned and stiff matrix (more collagen type 1 like). Future experimental and modeling efforts may distinguish between the production, degradation and mechanical properties of the different collagen types.

The size (length and width) of the callus in healing Achilles tendon has been shown to be affected by mechanical loading [21, 95, 97, 149]. The tendon geometry is an important feature of the finite element model. One larger and one smaller tendon geometry were designed using the geometrical measurements from Khayyeri et al. (2020)[21] for the full and reduced load models in Studies III-IV. Yet, we did not consider the temporal adaptation of the tendon geometry during healing. Future computational studies could investigate the mechano-regulated growth of the healing callus domain.

Biological and inflammatory processes

In addition to mechanobiology, purely biological and inflammatory processes also regulate tissue production and differentiation [303]. Different biological or inflammatory processes were explored in this thesis. The implemented healing framework considered how the local cell density can regulate tissue production and how acute inflammation can stimulate tissue production during the first days of healing. Including cell infiltration during early tendon healing strengthened the prediction of early tissue production in the periphery of the callus, similar to observations from experimental data [21]. Inflammatory-driven tissue production

ensured a baseline of early tissue production and recovery of mechanical stability throughout the first days of acute inflammation, regardless of mechano-regulated production. The initial wound healing response is presumably regulated by predominantly biological (nonmechanical) processes. The healing framework in Study V also considered mechanoregulated angiogenesis and oxygen diffusion. However, extensive experimental data on all the aforementioned processes and the extent of mechano-regulation and heterogeneity of these processes is limited. For example, many different cell populations have been identified during healing [128], yet the spatial and temporal evolution of cells that contribute to tissue production and differentiation remains rather unknown. Yet, a prolonged presence of cells, e.g. myofibroblasts, may contribute to scar formation [22]. In Study V, only the production of different tissue types was considered and not the differentiation on the cellular level. However, previous computational frameworks in bone healing considered actual differentiation of stem cells or pluripotent cells into different cell populations with distinct cellular properties, e.g. migration, differentiation, apoptosis, production, degradation [263, 265]. In tendon, the experimental evidence for tissue differentiation on the cell-level during tendon healing is limited. Future mechanobiological frameworks investigating tissue differentiation in tendon may also consider these distinct cell-level features in a similar fashion.

Continuum level mechanics

Our finite element implementation is a continuum tissue level model that assumes full mechanical connectivity between all material points. However, for a healing tendon, it can be questioned whether this is a reasonable assumption. For example, during the first days of healing, the stump and the callus are probably not fully mechanically connected. However, microscopic images have observed that the stumps are well integrated into the healing callus matrix by 15 days of healing in rat Achilles tendon [141]. Additionally, more established load-bearing parts of the callus are likely to take most of the mechanical load, or they can possibly slide, with respect to less developed parts of the callus, thereby unloading other parts of the callus. These regional differences in load-bearing and mechanical stimulation, are likely to be even more prominent when considering the formation of different tissue types with different mechanical properties. For instance, it remains unknown whether newly formed fat-, cartilage- and bone-like regions contribute to load-bearing in the healing tendon. Some preliminary in-house data from high-resolution 3D imaging has implied that bone-like tissue occurs within fibers that are well-integrated in the fibrillar matrix. This suggests that these bone-like regions can carry load, thereby contributing to overall load-bearing of the tendon and potentially unloading other parts of the tendon. Many questions on the formation of different tissue types during tendon healing remain unanswered but future

research can investigate if, for example, bone-like regions play a role in the risk of re-rupture or long-term loss of tendon function or associated pain.

A different aspect of the tissue-scale finite element modeling approach is that tissue-scale strains were used to govern mechanoregulatory mechanisms, while strain transfer between different length scales of the tendon was not modeled or investigated. This is questionable since the literature data used for the design of our strain-dependent collagen production law was based on *in vitro* experiments that apply strains to cells. Yet, different levels of *in vivo* strain transfer have been observed in soft tissues, e.g. tendon [304] and meniscus [305] and in *in vitro* experiments that apply strains to cells on a flexible substrate [306]. The only available 'multiscale' model on Achilles tendon healing implemented a constant strain transfer of 28% between tissue and cell-level strains [20]. However, since a thorough characterization of strain transfer across multiple length scales is lacking, and the available data implied similar strain attenuation in *in vitro* and *in vivo* experiments, it was assumed reasonable to couple the local tissue strains to cellular production of collagen.

6.3 Future perspectives

Computational investigations of mechanobiology in small animal models may prove important to unravel mechanisms underlying tendon healing. Yet, developed tendon models must be validated in synergy with experimental studies such that the model has a strong predictive capacity to a certain experimental model and can be used to design new experimental setups or ultimately to find optimal rehabilitation regimens that can be tested in the experimental studies. For instance, the developed mechanobiological model can help identify optimal timing for incremental steps in daily load level. For example, preliminary investigations using the healing framework in this thesis showed that one week of reduced level of daily loading, followed by full loading, displayed superior recovery of tissue content and stiffness throughout the first eight weeks of healing, compared to tendons subjected to continuous reduced or full daily loading. These results were similar to the experimental data in small animal studies, where they observed improved recovery of quasi-static, dynamic and fatigue mechanical properties following early mobilization (after 1 week of cast immobilization) compared to prolonged immobilization [96, 167, 185]. The simulations also predicted the experimental observation that the tendon properties would become more similar throughout time, as observed after six [167] and 16 weeks of healing [185], regardless of the rehabilitation regimen. These preliminary results exemplify the role that the developed healing framework can play in identifying optimal rehabilitation regimens, and how the framework contributes to create a better

understanding of the benefits or drawbacks of particular loading regimens during healing.

In terms of the evolution of tendon structure and function during healing, it will be important to collect more elaborate mechanical data on viscoelastic (e.g. creep, stress-relaxation, hysteresis) and fatigue properties (e.g. cycles to failure, dynamic modulus) while identifying distinct structure-function relationships for structural features throughout the multiscale tendon structure. Also, the recent experimental and numerical findings described in this thesis started identifying possibly mechanisms that may explain heterogeneous patterns of tendon healing. Experimental studies have recently started to consider the spatial distribution of collagen properties by, for example, doing spatial characterization of tendon gene production and high resolution imaging of the collagen matrix. In addition, the characterization of the heterogeneous deformation of healing tendon and strain transfer may provide valuable information to validate computational models of the healing tendon. Most of the aforementioned experimental investigations are not possible in humans due to various reasons such as ethical consideration, lack of compliance to rehabilitation regimens, availability of representative and young subjects. Therefore, the majority of experimental and numerical investigations of tendon mechanobiology will, can and should first be done on small animals before transferring this knowledge to the human scale. One example of this is the identification of different multiscale structure-function relationships related to the hierarchical collagen structure and its interaction with other proteins should be transferable to the human scale.

In terms of modeling tendon healing and mechanobiology, there are numerous interesting processes that may be investigated and considered in future works, such as load-dependent adaptation of the tendon geometry, considering different muscle forces combined with the three subtendons, investigating the mechanical role of the interfascicular matrix, considering other (mechano) biological stimuli (e.g. blood vessel formation, oxygen concentrations, inflammatory cells and signaling), the role of contractile myofibroblasts and scar formation, separating collagen type 1 and 3 production, damage and degradation, and more elaborate mechanical characterization. An important first step for the rat Achilles tendon models will be to mimic physiological loading, considering realistic strain and force-levels in the whole tendon and the subtendons during normal gait and for the different rehabilitation treatments, e.g. intramuscular Botox injection, immobilization by cast or orthosis.

In recent years, there has been a strong progression in the development of finite element models of the human Achilles tendon [307-314]. Some of these models

considered the three different subtendons and even investigated the effect of the interfascicular matrix on overall Achilles tendon mechanics and deformation. However, none of the studies considered viscoelastic properties in their material model. Future finite element models of the human Achilles tendon may consider modeling the different viscoelastic properties (stiffness, hysteresis and relaxation) measured in the three subtendons on the human scale [299]. The existing viscoelastic material model in this thesis may be valuable here, but also the developed mechanobiological healing framework may provide a good starting point for validating mechano-regulated tissue healing or differentiation processes on the human scale. There is also quite an extensive literature available on finite element analysis of the supraspinatus tendon that focus on modeling the tendon-to-bone insertion [315-320]. Similar methods may also be employed to consider the complex structure and different tissue types (tendon, cartilage, bone) that comprise the Achilles tendon insertion at the calcaneus. Other recent human modeling approaches have considered whole foot models [321], muscle-tendon dynamics [322-325] and even a whole leg model [326]. These models may be of value to consider the interaction of the Achilles tendon with different surrounding tissues, i.e. model physiological loading or muscle-tendon interactions.

Current treatments of the ruptured Achilles tendon are not optimal. To address this, computational modeling efforts investigating the human Achilles tendon have developed rapidly over the last few years. In addition, this thesis considered the first 3D mechanobiological framework in tendon healing. Together, these numerical frameworks and extensive development and validation of these models may lead to key insights involved in tendon biomechanics and mechanobiology. Hopefully, these models will help designing better treatments for diseased or ruptured tendon.

7 Summary and conclusions

The overall aim of this thesis was to investigate mechanobiological mechanisms in intact and healing tendon by using and developing computational models. The presented mechanobiological tendon framework was able to capture and predict a range of experimental observations in intact and healing tendon, such as spatio-temporal evolution of collagen production and the formation of different tissue types, collagen alignment, and viscoelastic mechanical properties.

- Study I: There is a limited understanding on the effect of different mechanical loading protocols, gender and suture-repair on Achilles tendon healing in rodents. Literature findings have described the heterogeneous evolution of different tissue features during healing such as tissue production, tissue differentiation and cell distribution. This study found that mechanical loading has been found to play a role in recovery of mechanical properties, yet it remains unclear what role mechanobiology exactly plays during tendon healing.
- Study II: An existing material model for tendon was further validated by determining the viscoelastic properties of collagen in rat Achilles tendon by incorporating creep and stress-relaxation behaviour. Creep and stress-relaxation behaviour were described simultaneously with high accuracy using a single material parameter set. This study found that the mechanical properties of tendon undergoing reduced daily loading displayed different elastic and viscoelastic properties.
- Study III: A mechanobiological framework was developed to describe the evolution of collagen content, alignment and overall mechanical properties during early tendon healing. The finite element simulations displayed heterogeneous distributions of strain, and

supraphysiological strain levels (>15%) during early tendon healing. This study suggests that decreased collagen production for high strain levels could explain why tendon properties heal in a heterogeneous fashion as observed in experimental data.

- Study IV: The mechanobiological healing framework was characterized and validated by investigating the effect of reduced daily loading on tissue production, collagen alignment, mechanical properties (stiffness and creep). This study identified that the combination of the explored strain-regulated collagen production law and reduced loading predicted improved collagen production and stiffness recovery during early healing. On the other hand, long-term prolongation of reduced loading may impair the recovery of tendon properties.
- Study IV: Cell infiltration during early tendon healing was found to be a potential mechanism contributing to heterogeneous collagen and overall tissue production that was observed experimentally. The tendon core has a low cell density after rupture, thus early tissue production may be very limited, regardless of mechanical loading, as observed in experimental data. If the process of cell infiltration (migration and proliferation) is mechano-regulated, this may lead to further heterogeneity of cell distribution and tissue distribution during healing.
- Study V: A mechanobiological framework was developed for predicting the formation of different tissue types (tendon-, fat-, cartilage-, bone-like) during tendon healing. This framework explored a wide range of biophysical stimuli, the process of endochondral bone formation and the potential role of angiogenesis and oxygen in the formation of different tissue types. The mechanobiological algorithms predicted spatio-temporal formation of tendon, cartilage and bone-like tissue formation. Additionally, the heterogeneous process of angiogenesis and the oxygen distribution may regulate spatial patterns of tissue formation. In particular, hypoxic conditions promoted cartilage formation in the tendon core whereas blood supply had to be present for formation of bone-like tissue. Allowing only endochondral bone formation predicted more realistic long-term tissue formation with prolonged tendon-like and cartilage-like tissue presence and more limited bone-like tissue formation. This was the first framework to predict temporal and spatial formation of fat-, tendon-, cartilage- and bone-like tissue formation during tendon healing, similar to experimental observations.

References

1. Ganestam A, Kallemose T, Troelsen A, Barfod KW. Increasing incidence of acute Achilles tendon rupture and a noticeable decline in surgical treatment from 1994 to 2013. A nationwide registry study of 33,160 patients. Knee Surgery, Sports Traumatology, Arthroscopy. 2016;24(12):3730-7.
2. Huttunen TT, Kannus P, Rolf C, Felländer-Tsai L, Mattila VM. Acute Achilles tendon ruptures: incidence of injury and surgery in Sweden between 2001 and 2012. The American journal of sports medicine. 2014;42(10):2419-23.
3. Nyyssönen T, Lüthje P, Kröger H. The increasing incidence and difference in sex distribution of Achilles tendon rupture in Finland in 1987–1999. Scandinavian Journal of Surgery. 2008;97(3):272-5.
4. Lantto I, Heikkinen J, Flinkkilä T, Ohtonen P, Leppilahti J. Epidemiology of A chilles tendon ruptures: Increasing incidence over a 33-year period. Scandinavian journal of medicine & science in sports. 2015;25(1):e133-e8.
5. Lemme NJ, Li NY, DeFroda SF, Kleiner J, Owens BD. Epidemiology of Achilles tendon ruptures in the United States: athletic and nonathletic injuries from 2012 to 2016. Orthopaedic journal of sports medicine. 2018;6(11):2325967118808238.
6. Reito A, Logren H-L, Ahonen K, Nurmi H, Paloneva J. Risk factors for failed nonoperative treatment and rerupture in acute Achilles tendon rupture. Foot & ankle international. 2018;39(6):694-703.
7. Park YH, Kim TJ, Choi GW, Kim HJ. Age is a risk factor for contralateral tendon rupture in patients with acute Achilles tendon rupture. Knee Surgery, Sports Traumatology, Arthroscopy. 2019:1-6.
8. Holm C, Kjaer M, Eliasson P. A chilles tendon rupture–treatment and complications: A systematic review. Scandinavian journal of medicine & science in sports. 2015;25(1):e1-e10.

9. Ochen Y, Beks RB, van Heijl M, Hietbrink F, Leenen LP, van der Velde D, et al. Operative treatment versus nonoperative treatment of Achilles tendon ruptures: systematic review and meta-analysis. bmj. 2019;364:k5120.
10. Egger AC, Berkowitz MJ. Achilles tendon injuries. Current reviews in musculoskeletal medicine. 2017;10(1):72-80.
11. Reda Y, Farouk A, Abdelmonem I, El Shazly OA. Surgical versus non-surgical treatment for acute Achilles' tendon rupture. A systematic review of literature and meta-analysis. Foot and Ankle Surgery. 2020;26(3):280-8.
12. Carvalho FA, Kamper SJ. Effects of early rehabilitation following operative repair of Achilles tendon rupture (PEDro synthesis). Br J Sports Med. 2016;50(13):829-30.
13. El-Akkawi AI, Joanroy R, Barfod KW, Kallemose T, Kristensen SS, Viberg B. Effect of Early Versus Late Weightbearing in Conservatively Treated Acute Achilles Tendon Rupture: A Meta-Analysis. The Journal of Foot and Ankle Surgery. 2018;57(2):346-52. doi: https://doi.org/10.1053/j.jfas.2017.06.006.
14. Kjaer M. Role of extracellular matrix in adaptation of tendon and skeletal muscle to mechanical loading. Physiological reviews. 2004;84(2):649-98.
15. Wang JH-C. Mechanobiology of tendon. Journal of biomechanics. 2006;39(9):1563-82.
16. Thompson MS, Bajuri MN, Khayyeri H, Isaksson H. Mechanobiological modelling of tendons: review and future opportunities. Proceedings of the Institution of Mechanical Engineers, Part H: Journal of Engineering in Medicine. 2017;231(5):369-77.
17. Isaksson H, Van Donkelaar CC, Huiskes R, Ito K. Corroboration of mechanoregulatory algorithms for tissue differentiation during fracture healing: comparison with in vivo results. Journal of Orthopaedic Research. 2006;24(5):898-907.
18. Tanska P, Julkunen P, Korhonen RK. A computational algorithm to simulate disorganization of collagen network in injured articular cartilage. Biomechanics and Modeling in Mechanobiology. 2018;17(3):689-99.
19. Richardson WJ, Kegerreis B, Thomopoulos S, Holmes JW. Potential strain-dependent mechanisms defining matrix alignment in healing tendons. Biomechanics and modeling in mechanobiology. 2018:1-12.
20. Chen K, Hu X, Blemker SS, Holmes JW. Multiscale computational model of Achilles tendon wound healing: Untangling the effects of repair and loading. PLoS computational biology. 2018;14(12):e1006652.
21. Khayyeri H, Hammerman M, Turunen MJ, Blomgran P, Notermans T, Guizar-Sicairos M, et al. Diminishing effects of mechanical loading over time during rat Achilles tendon healing. PloS one. 2020;15(12):e0236681.

22. Howell K, Chien C, Bell R, Laudier D, Tufa SF, Keene DR, et al. Novel model of tendon regeneration reveals distinct cell mechanisms underlying regenerative and fibrotic tendon healing. Scientific reports. 2017;7:45238.
23. Korntner S, Kunkel N, Lehner C, Gehwolf R, Wagner A, Augat P, et al. A high-glucose diet affects Achilles tendon healing in rats. Scientific reports. 2017;7(1):1-12.
24. Lin L, Shen Q, Xue T, Yu C. Heterotopic ossification induced by Achilles tenotomy via endochondral bone formation: expression of bone and cartilage related genes. Bone. 2010;46(2):425-31.
25. Huber AK, Patel N, Pagani CA, Marini S, Padmanabhan KR, Matera DL, et al. Immobilization after injury alters extracellular matrix and stem cell fate. The Journal of clinical investigation. 2020;130(10):5444-60.
26. Chen G, Jiang H, Tian X, Tang J, Bai X, Zhang Z, et al. Mechanical loading modulates heterotopic ossification in calcific tendinopathy through the mTORC1 signaling pathway. Molecular medicine reports. 2017;16(5):5901-7.
27. Palmes D, Spiegel H, Schneider T, Langer M, Stratmann U, Budny T, et al. Achilles tendon healing: long-term biomechanical effects of postoperative mobilization and immobilization in a new mouse model. Journal of orthopaedic research. 2002;20(5):939-46.
28. Khayyeri H, Blomgran P, Hammerman M, Turunen MJ, Löwgren A, Guizar-Sicairos M, et al. Achilles tendon compositional and structural properties are altered after unloading by botox. Scientific reports. 2017;7(1):13067.
29. Taye N, Karoulias SZ, Hubmacher D. The “Other” 15–40%: the role of non-collagenous extracellular matrix proteins and minor collagens in tendon. Journal of Orthopaedic Research®. 2020;38(1):23-35.
30. Kastelic J, Galeski A, Baer E. The multicomposite structure of tendon. Connective tissue research. 1978;6(1):11-23.
31. Ottani V, Martini D, Franchi M, Ruggeri A, Raspanti M. Hierarchical structures in fibrillar collagens. Micron. 2002;33(7-8):587-96.
32. Kadler KE, Holmes DF, Trotter JA, Chapman JA. Collagen fibril formation. Biochemical Journal. 1996;316(1):1-11.
33. Silver FH, Kato YP, Ohno M, Wasserman AJ. Analysis of mammalian connective tissue: relationship between hierarchical structures and mechanical properties. Journal of long-term effects of medical implants. 1992;2(2-3):165-98.
34. Silver F, Christiansen D, Snowhill P, Chen Y, Landis W. The role of mineral in the viscoelasticity of turkey tendons. Biomacromolecules. 2000;1(180):180-5.
35. Silver FH, Christiansen DL, Snowhill PB, Chen Y. Role of storage on changes in the mechanical properties of tendon and self-assembled collagen fibers. Connective tissue research. 2000;41(2):155-64.

36. Petruska JA, Hodge AJ. A subunit model for the tropocollagen macromolecule. Proceedings of the National Academy of Sciences of the United States of America. 1964;51(5):871.

37. Ottani V, Raspanti M, Ruggeri A. Collagen structure and functional implications. Micron. 2001;32(3):251-60.

38. Eyre DR, Paz MA, Gallop PM. Cross-linking in collagen and elastin. Annual review of biochemistry. 1984;53(1):717-48.

39. Wess TJ, Hammersley A, Wess L, Miller A. Molecular packing of type I collagen in tendon. Journal of molecular biology. 1998;275(2):255-67.

40. Abrahams M. Mechanical behaviour of tendonIn vitro. Medical and Biological Engineering. 1967;5(5):433-43.

41. Diamant J, Keller A, Baer E, Litt M, Arridge R. Collagen; ultrastructure and its relation to mechanical properties as a function of ageing. Proceedings of the Royal Society of London Series B Biological Sciences. 1972;180(1060):293-315.

42. Rigby BJ, Hirai N, Spikes JD, Eyring H. The mechanical properties of rat tail tendon. The Journal of general physiology. 1959;43(2):265-83.

43. Hedbom E, Heinegård D. Binding of fibromodulin and decorin to separate sites on fibrillar collagens. Journal of Biological Chemistry. 1993;268(36):27307-12.

44. Raspanti M, Congiu T, Guizzardi S. Structural aspects of the extracellular matrix of the tendon: an atomic force and scanning electron microscopy study. Archives of histology and cytology. 2002;65(1):37-43.

45. Scott J. Structure and function in extracellular matrices depend on interactions between anionic glycosaminoglycans. Pathologie Biologie. 2001;49(4):284-9.

46. Scott JE. Proteoglycan-fibrillar collagen interactions. Biochemical Journal. 1988;252(2):313.

47. Svensson L, Heineg D. Decorin-binding sites for collagen type I are mainly located in leucine-rich repeats 4-5. Journal of Biological Chemistry. 1995;270(35):20712-6.

48. Svensson L, Närlid I, Oldberg Å. Fibromodulin and lumican bind to the same region on collagen type I fibrils. FEBS letters. 2000;470(2):178-82.

49. Cribb A, Scott J. Tendon response to tensile stress: an ultrastructural investigation of collagen: proteoglycan interactions in stressed tendon. Journal of anatomy. 1995;187(Pt 2):423.

50. Scott JE. Proteodermatan and proteokeratan sulfate (decorin, lumican/fibromodulin) proteins are horseshoe shaped. Implications for their interactions with collagen. Biochemistry. 1996;35(27):8795-9.

51. Pins GD, Christiansen DL, Patel R, Silver FH. Self-assembly of collagen fibers. Influence of fibrillar alignment and decorin on mechanical properties. Biophysical journal. 1997;73(4):2164-72.

52. Puxkandl R, Zizak I, Paris O, Keckes J, Tesch W, Bernstorff S, et al. Viscoelastic properties of collagen: synchrotron radiation investigations and structural model. Philosophical Transactions of the Royal Society of London Series B: Biological Sciences. 2002;357(1418):191-7.
53. Robinson PS, Lin TW, Jawad AF, Iozzo RV, Soslowsky LJ. Investigating tendon fascicle structure–function relationships in a transgenic-age mouse model using multiple regression models. Annals of biomedical engineering. 2004;32(7):924-31.
54. Fang F, Lake SP. Modelling approaches for evaluating multiscale tendon mechanics. Interface focus. 2016;6(1):20150044.
55. Jozsa L, Kannus P. Histopathological findings in spontaneous tendon ruptures. Scandinavian journal of medicine & science in sports. 1997;7(2):113-8.
56. Nourissat G, Berenbaum F, Duprez D. Tendon injury: from biology to tendon repair. Nature Reviews Rheumatology. 2015;11(4):223.
57. Snedeker JG, Foolen J. Tendon injury and repair–a perspective on the basic mechanisms of tendon disease and future clinical therapy. Acta biomaterialia. 2017.
58. Kendal AR, Layton T, Al-Mossawi H, Appleton L, Dakin S, Brown R, et al. Multi-omic single cell analysis resolves novel stromal cell populations in healthy and diseased human tendon. Scientific reports. 2020;10(1):1-14.
59. Galatz LM, Gerstenfeld L, Heber-Katz E, Rodeo SA. Tendon regeneration and scar formation: The concept of scarless healing. Journal of Orthopaedic Research. 2015;33(6):823-31.
60. Stauber T, Blache U, Snedeker JG. Tendon tissue microdamage and the limits of intrinsic repair. Matrix Biology. 2019.
61. Tempfer H, Traweger A. Tendon vasculature in health and disease. Frontiers in physiology. 2015;6:330.
62. Grant TM, Thompson MS, Urban J, Yu J. Elastic fibres are broadly distributed in tendon and highly localized around tenocytes. Journal of anatomy. 2013;222(6):573-9.
63. Thorpe CT, Peffers MJ, Simpson D, Halliwell E, Screen HR, Clegg PD. Anatomical heterogeneity of tendon: Fascicular and interfascicular tendon compartments have distinct proteomic composition. Scientific reports. 2016;6:20455.
64. Godinho MS, Thorpe CT, Greenwald SE, Screen HR. Elastin is localised to the interfascicular matrix of energy storing tendons and becomes increasingly disorganised with ageing. Scientific reports. 2017;7(1):1-11.
65. Lee AH, Elliott DM. Comparative multi-scale hierarchical structure of the tail, plantaris, and Achilles tendons in the rat. Journal of anatomy. 2019;234(2):252-62.

66. Sasaki N, Odajima S. Stress-strain curve and Young's modulus of a collagen molecule as determined by the X-ray diffraction technique. Journal of biomechanics. 1996;29(5):655-8.

67. Silver FH, Freeman JW, Seehra GP. Collagen self-assembly and the development of tendon mechanical properties. Journal of biomechanics. 2003;36(10):1529-53.

68. VANBROCKLIN JD, Ellis DG. A study of the mechanical behavior of toe extensor tendons under applied stress. Archives of physical medicine and rehabilitation. 1965;46:369-73.

69. Thompson MS. Tendon mechanobiology: experimental models require mathematical underpinning. Bulletin of mathematical biology. 2013;75(8):1238-54.

70. Franchi M, Fini M, Quaranta M, De Pasquale V, Raspanti M, Giavaresi G, et al. Crimp morphology in relaxed and stretched rat Achilles tendon. Journal of anatomy. 2007;210(1):1-7.

71. Cheng VW, Screen HR. The micro-structural strain response of tendon. Journal of Materials Science. 2007;42(21):8957-65.

72. Fratzl P, Misof K, Zizak I, Rapp G, Amenitsch H, Bernstorff S. Fibrillar structure and mechanical properties of collagen. Journal of structural biology. 1998;122(1-2):119-22.

73. Fallon J, Blevins FT, Vogel K, Trotter J. Functional morphology of the supraspinatus tendon. Journal of orthopaedic research. 2002;20(5):920-6.

74. Screen HR. Hierarchical approaches to understanding tendon mechanics. Journal of Biomechanical Science and Engineering. 2009;4(4):481-99.

75. Snedeker JG, Pelled G, Zilberman Y, Arav AB, Huber E, Müller R, et al. An analytical model for elucidating tendon tissue structure and biomechanical function from in vivo cellular confocal microscopy images. Cells Tissues Organs. 2009;190(2):111-9.

76. Screen H, Lee D, Bader D, Shelton J. An investigation into the effects of the hierarchical structure of tendon fascicles on micromechanical properties. Proceedings of the Institution of Mechanical Engineers, Part H: Journal of Engineering in Medicine. 2004;218(2):109-19.

77. Fang F, Lake SP. Experimental evaluation of multiscale tendon mechanics. Journal of Orthopaedic Research. 2017;35(7):1353-65.

78. Thorpe CT, Udeze CP, Birch HL, Clegg PD, Screen HR. Specialization of tendon mechanical properties results from interfascicular differences. Journal of the Royal Society Interface. 2012;9(76):3108-17.

79. Wang T, Chen P, Zheng M, Wang A, Lloyd D, Leys T, et al. In vitro loading models for tendon mechanobiology. Journal of Orthopaedic Research®. 2018;36(2):566-75.

80. Benjamin M, Kaiser E, Milz S. Structure-function relationships in tendons: a review. Journal of anatomy. 2008;212(3):211-28.

81. Elliott DM, Robinson PS, Gimbel JA, Sarver JJ, Abboud JA, Iozzo RV, et al. Effect of altered matrix proteins on quasilinear viscoelastic properties in transgenic mouse tail tendons. Annals of biomedical engineering. 2003;31(5):599-605.

82. Butler DL, Grood ES, Noyes FR, Zernicke RE. Biomechanics of ligaments and tendons. Exercise and sport sciences reviews. 1978;6(1):125-82.

83. Danto MI, Woo SLY. The mechanical properties of skeletally mature rabbit anterior cruciate ligament and patellar tendon over a range of strain rates. Journal of Orthopaedic Research. 1993;11(1):58-67.

84. Screen H, Seto J, Krauss S, Boesecke P, Gupta H. Extrafibrillar diffusion and intrafibrillar swelling at the nanoscale are associated with stress relaxation in the soft collagenous matrix tissue of tendons. Soft Matter. 2011;7(23):11243-51.

85. Hannafin JA, Arnoczky SP. Effect of cyclic and static tensile loading on water content and solute diffusion in canine flexor tendons: an in vitro study. Journal of Orthopaedic Research. 1994;12(3):350-6.

86. Lanir Y, Salant E, Foux A. Physico-chemical and microstructural changes in collagen fiber bundles following stretch in-vitro. Biorheology. 1988;25(4):591-603.

87. Folkhard W, Mosler E, Geercken W, Knörzer E, Nemetschek-Gansler H, Nemetschek T, et al. Quantitative analysis of the molecular sliding mechanisms in native tendon collagen—time-resolved dynamic studies using synchrotron radiation. International Journal of Biological Macromolecules. 1987;9(3):169-75.

88. Han WM, Heo S-J, Driscoll TP, Smith LJ, Mauck RL, Elliott DM. Macro-to microscale strain transfer in fibrous tissues is heterogeneous and tissue-specific. Biophysical journal. 2013;105(3):807-17.

89. Li LJ, Zhang YX, editors. Biomechanical simulation of Achilles tendon strains during hurdling. Advanced Materials Research; 2013: Trans Tech Publ.

90. Thorpe CT, Klemt C, Riley GP, Birch HL, Clegg PD, Screen HR. Helical sub-structures in energy-storing tendons provide a possible mechanism for efficient energy storage and return. Acta biomaterialia. 2013;9(8):7948-56.

91. Torp S, Arridge R, Armeniades CD, Baer E. Structure-property relationships in tendon as a function of age. Butterworths, London; 1975.

92. Buchanan CI, Marsh RL. Effects of exercise on the biomechanical, biochemical and structural properties of tendons. Comparative Biochemistry and Physiology Part A: Molecular & Integrative Physiology. 2002;133(4):1101-7.

93. Freedman BR, Bade ND, Riggin CN, Zhang S, Haines PG, Ong KL, et al. The (dys) functional extracellular matrix. Biochimica Et Biophysica Acta (BBA)-Molecular Cell Research. 2015;1853(11):3153-64.

94. Eliasson P, Fahlgren A, Pasternak B, Aspenberg P. Unloaded rat Achilles tendons continue to grow, but lose viscoelasticity. Journal of applied physiology. 2007;103(2):459-63.

95. Andersson T, Eliasson P, Aspenberg P. Tissue memory in healing tendons: short loading episodes stimulate healing. Journal of applied physiology. 2009;107(2):417-21.

96. Freedman BR, Gordon JA, Bhatt PR, Pardes AM, Thomas SJ, Sarver JJ, et al. Nonsurgical treatment and early return to activity leads to improved Achilles tendon fatigue mechanics and functional outcomes during early healing in an animal model. Journal of Orthopaedic Research. 2016;34(12):2172-80.

97. Hammerman M, Dietrich-Zagonel F, Blomgran P, Eliasson P, Aspenberg P. Different mechanisms activated by mild versus strong loading in rat Achilles tendon healing. PloS one. 2018;13(7):e0201211.

98. Michna H. Morphometric analysis of loading-induced changes in collagen-fibril populations in young tendons. Cell and tissue research. 1984;236(2):465-70.

99. Michna H, Hartmann G. Adaptation of tendon collagen to exercise. International orthopaedics. 1989;13(3):161-5.

100. Heinemeier KM, Skovgaard D, Bayer ML, Qvortrup K, Kjaer A, Kjaer M, et al. Uphill running improves rat Achilles tendon tissue mechanical properties and alters gene expression without inducing pathological changes. Journal of applied physiology. 2012;113(5):827-36.

101. Tipton CM, Matthes RD, Vailas AC, Schnoebelen CL. The response of the galago senegalensis to physical training. Comparative Biochemistry and Physiology Part A: Physiology. 1979;63(1):29-36.

102. Almeida-Silveira MI, Lambertz D, Pérot C, Goubel F. Changes in stiffness induced by hindlimb suspension in rat Achilles tendon. European journal of applied physiology. 2000;81(3):252-7.

103. Majima T, Yasuda K, Fujii T, Yamamoto N, Hayashi K, Kaneda K. Biomechanical effects of stress shielding of the rabbit patellar tendon depend on the degree of stress reduction. Journal of orthopaedic research. 1996;14(3):377-83.

104. Yamamoto N, Ohno K, Hayashi K, Kuriyama H, Yasuda K, Kaneda K. Effects of stress shielding on the mechanical properties of rabbit patellar tendon. 1993.

105. Amiel D, Woo SL, Harwood FL, Akeson WH. The effect of immobilization on collagen turnover in connective tissue: a biochemical-biomechanical correlation. Acta Orthopaedica Scandinavica. 1982;53(3):325-32.

106. Müllner T, Kwasny O, Reihsner R, Löhnert V, Schabus R. Mechanical properties of a rat patellar tendon stress-shielded in situ. Archives of orthopaedic and trauma surgery. 2000;120(1-2):70-4.

107. Muellner T, Kwasny O, Loehnert V, Mallinger R, Unfried G, Schabus R, et al. Light and electron microscopic study of stress-shielding effects on rat patellar tendon. Archives of orthopaedic and trauma surgery. 2001;121(10):561-5.

108. Lavagnino M, Wall ME, Little D, Banes AJ, Guilak F, Arnoczky SP. Tendon mechanobiology: current knowledge and future research opportunities. Journal of Orthopaedic Research. 2015;33(6):813-22.

109. Wang JH, Li Z, Yang G, Khan M. Repetitively stretched tendon fibroblasts produce inflammatory mediators. Clinical Orthopaedics and Related Research®. 2004;422:243-50.

110. Yang G, Crawford RC, Wang JH. Proliferation and collagen production of human patellar tendon fibroblasts in response to cyclic uniaxial stretching in serum-free conditions. Journal of biomechanics. 2004;37(10):1543-50.

111. Atance J, Yost MJ, Carver W. Influence of the extracellular matrix on the regulation of cardiac fibroblast behavior by mechanical stretch. Journal of cellular physiology. 2004;200(3):377-86.

112. Butt RP, Bishop JE. Mechanical load enhances the stimulatory effect of serum growth factors on cardiac fibroblast procollagen synthesis. Journal of molecular and cellular cardiology. 1997;29(4):1141-51.

113. Carver W, Nagpal M, Nachtigal M, Borg T, Terracio L. Collagen expression in mechanically stimulated cardiac fibroblasts. Circulation research. 1991;69(1):116-22.

114. Husse B, Briest W, Homagk L, Isenberg G, Gekle M. Cyclical mechanical stretch modulates expression of collagen I and collagen III by PKC and tyrosine kinase in cardiac fibroblasts. American Journal of Physiology-Regulatory, Integrative and Comparative Physiology. 2007;293(5):R1898-R907.

115. Kim JJ, Musson DS, Matthews BG, Cornish J, Anderson IA, Shim VB. Applying Physiologically Relevant Strains to Tenocytes in an In Vitro Cell Device Induces In Vivo Like Behaviors. Journal of Biomechanical Engineering. 2016;138(12):121003.

116. Papakrivopoulou J, Lindahl GE, Bishop JE, Laurent GJ. Differential roles of extracellular signal-regulated kinase 1/2 and p38MAPK in mechanical load-induced procollagen α1 (I) gene expression in cardiac fibroblasts. Cardiovascular research. 2004;61(4):736-44.

117. Liu J, Yu W, Liu Y, Chen S, Huang Y, Li X, et al. Mechanical stretching stimulates collagen synthesis via down-regulating SO 2/AAT1 pathway. Scientific reports. 2016;6:21112.

118. Loesberg W, Walboomers X, Van Loon J, Jansen J. The effect of combined cyclic mechanical stretching and microgrooved surface topography on the behavior of fibroblasts. Journal of Biomedical Materials Research Part A: An Official Journal of The Society for Biomaterials, The Japanese Society for Biomaterials, and The

Australian Society for Biomaterials and the Korean Society for Biomaterials. 2005;75(3):723-32.

119. Maeda E, Fleischmann C, Mein CA, Shelton JC, Bader DL, Lee DA. Functional analysis of tenocytes gene expression in tendon fascicles subjected to cyclic tensile strain. Connective tissue research. 2010;51(6):434-44.
120. Maeda E, Shelton JC, Bader DL, Lee DA. Time dependence of cyclic tensile strain on collagen production in tendon fascicles. Biochemical and biophysical research communications. 2007;362(2):399-404.
121. Screen HR, Shelton JC, Bader DL, Lee DA. Cyclic tensile strain upregulates collagen synthesis in isolated tendon fascicles. Biochemical and biophysical research communications. 2005;336(2):424-9.
122. Fu L, Wei C-C, Powell PC, Bradley WE, Collawn JF, Dell'Italia LJ. Volume overload induces autophagic degradation of procollagen in cardiac fibroblasts. Journal of molecular and cellular cardiology. 2015;89:241-50.
123. Galie P, Russell M, Westfall M, Stegemann J. Interstitial fluid flow and cyclic strain differentially regulate cardiac fibroblast activation via AT1R and TGF-β1. Experimental cell research. 2012;318(1):75-84.
124. Hsiao M-Y, Lin P-C, Liao W-H, Chen W-S, Hsu C-H, He C-K, et al. The effect of the repression of oxidative stress on tenocyte differentiation: a preliminary study of a rat cell model using a novel differential tensile strain bioreactor. International journal of molecular sciences. 2019;20(14):3437.
125. Lindahl GE, Chambers RC, Papakrivopoulou J, Dawson SJ, Jacobsen MC, Bishop JE, et al. Activation of fibroblast procollagen α1 (I) transcription by mechanical strain is transforming growth factor-β-dependent and involves increased binding of CCAAT-binding factor (CBF/NF-Y) at the proximal promoter. Journal of Biological Chemistry. 2002;277(8):6153-61.
126. Nakamura T, Liu M, Mourgeon E, Slutsky A, Post M. Mechanical strain and dexamethasone selectively increase surfactant protein C and tropoelastin gene expression. American Journal of Physiology-Lung Cellular and Molecular Physiology. 2000;278(5):L974-L80.
127. Roche PL, Nagalingam RS, Bagchi RA, Aroutiounova N, Belisle BM, Wigle JT, et al. Role of scleraxis in mechanical stretch-mediated regulation of cardiac myofibroblast phenotype. American Journal of Physiology-Cell Physiology. 2016;311(2):C297-C307.
128. Nichols AE, Best KT, Loiselle AE. The cellular basis of fibrotic tendon healing: challenges and opportunities. Translational Research. 2019;209:156-68.
129. Sugg KB, Lubardic J, Gumucio JP, Mendias CL. Changes in macrophage phenotype and induction of epithelial-to-mesenchymal transition genes following acute Achilles tenotomy and repair. Journal of Orthopaedic Research. 2014;32(7):944-51.

130. Hammerman M, Blomgran P, Dansac A, Eliasson P, Aspenberg P. Different gene response to mechanical loading during early and late phases of rat Achilles tendon healing. Journal of applied physiology. 2017;123(4):800-15.

131. Keane TJ, Horejs C-M, Stevens MM. Scarring vs. functional healing: Matrix-based strategies to regulate tissue repair. Advanced Drug Delivery Reviews. 2018;129:407-19. doi: https://doi.org/10.1016/j.addr.2018.02.002.

132. Liu SH, Yang R-S, Al-Shaikh R, Lane JM. Collagen in tendon, ligament, and bone healing. A current review. Clinical orthopaedics and related research. 1995;(318):265-78.

133. Kueckelhaus M, Philip J, Kamel RA, Canseco JA, Hackl F, Kiwanuka E, et al. Sustained release of amnion-derived cellular cytokine solution facilitates achilles tendon healing in rats. Eplasty. 2014;14.

134. Svärd A, Hammerman M, Eliasson P. Elastin levels are higher in healing tendons than in intact tendons and influence tissue compliance. The FASEB Journal. 2020;34(10):13409-18.

135. Burssens P, Steyaert A, Forsyth R, van Ovost EJ, De Paepe Y, Verdonk R. Exogenously administered substance P and neutral endopeptidase inhibitors stimulate fibroblast proliferation, angiogenesis and collagen organization during Achilles tendon healing. Foot & ankle international. 2005;26(10):832-9.

136. Sasaki K, Yamamoto N, Kiyosawa T, Sekido M. The role of collagen arrangement change during tendon healing demonstrated by scanning electron microscopy. Journal of electron microscopy. 2012;61(5):327-34.

137. Oshima J, Sasaki K, Yamamoto N, Kiyosawa T, Sekido M. Visualization of microstructural change affected by mechanical stimulation in tendon healing with a novel tensionless model. Microscopy. 2021;70(2):186-91.

138. Hsieh C-F, Alberton P, Loffredo-Verde E, Volkmer E, Pietschmann M, Müller P, et al. Scaffold-free Scleraxis-programmed tendon progenitors aid in significantly enhanced repair of full-size Achilles tendon rupture. Nanomedicine. 2016;11(9):1153-67.

139. da Silva FS, Abreu BJ, Eriksson BI, Ackermann PW. Complete mid-portion rupture of the rat achilles tendon leads to remote and time-mismatched changes in uninjured regions. Knee Surgery, Sports Traumatology, Arthroscopy. 2020:1-10.

140. Hillin CD, Fryhofer GW, Freedman BR, Choi DS, Weiss SN, Huegel J, et al. Effects of Immobilization Angle on Tendon Healing after Achilles Rupture in a Rat Model. Journal of Orthopaedic Research®. 2019.

141. Best TM, Collins A, Lilly EG, Seaber AV, Goldner R, Murrell GA. Achilles tendon healing: a correlation between functional and mechanical performance in the rat. Journal of orthopaedic research. 1993;11(6):897-906.

142. Murrell G, Szabo C, Hannafin J, Jang D, Dolan M, Deng X-H, et al. Modulation of tendon healing by nitric oxide. Inflammation Research. 1997;46(1):19-27.

143. Kurtz CA, Loebig TG, Anderson DD, DeMeo PJ, Campbell PG. Insulin-like growth factor I accelerates functional recovery from Achilles tendon injury in a rat model. The American journal of sports medicine. 1999;27(3):363-9.

144. Staresinic M, Sebecic B, Patrlj L, Jadrijevic S, Suknaic S, Perovic D, et al. Gastric pentadecapeptide BPC 157 accelerates healing of transected rat Achilles tendon and in vitro stimulates tendocytes growth. Journal of orthopaedic research. 2003;21(6):976-83.

145. Wieloch P, Buchmann G, Roth W, Rickert M. A cryo-jaw designed for in vitro tensile testing of the healing Achilles tendons in rats. Journal of biomechanics. 2004;37(11):1719-22.

146. Bolt P, Clerk AN, Luu HH, Kang Q, Kummer JL, Deng Z-L, et al. BMP-14 gene therapy increases tendon tensile strength in a rat model of Achilles tendon injury. JBJS. 2007;89(6):1315-20.

147. Majewski M, Betz O, Ochsner P, Liu F, Porter R, Evans CH. Ex vivo adenoviral transfer of bone morphogenetic protein 12 (BMP-12) cDNA improves Achilles tendon healing in a rat model. Gene therapy. 2008;15(16):1139-46.

148. Murrell GA, Tang G, Appleyard RC, Del Soldato P, Wang M-X. Addition of nitric oxide through nitric oxide-paracetamol enhances healing rat achilles tendon. Clinical orthopaedics and related research. 2008;466(7):1618-24.

149. Eliasson P, Andersson T, Aspenberg P. Rat Achilles tendon healing: mechanical loading and gene expression. Journal of applied physiology. 2009;107(2):399-407.

150. Schizas N, Li J, Andersson T, Fahlgren A, Aspenberg P, Ahmed M, et al. Compression therapy promotes proliferative repair during rat Achilles tendon immobilization. Journal of Orthopaedic Research. 2010;28(7):852-8.

151. Ahmed AS, Schizas N, Li J, Ahmed M, Östenson C-G, Salo P, et al. Type 2 diabetes impairs tendon repair after injury in a rat model. Journal of applied physiology. 2012;113(11):1784-91.

152. Black DA, Tucci M, Puckett A, Benghuzzi H. Histopathological and biomechanical parameters of repaired rat achilles tendons treated with and without mannose-6-phosphate. Biomedical sciences instrumentation. 2012;48:43-8.

153. Kaux JF, Drion PV, Colige A, Pascon F, Libertiaux V, Hoffmann A, et al. Effects of platelet-rich plasma (PRP) on the healing of A chilles tendons of rats. Wound Repair and Regeneration. 2012;20(5):748-56.

154. Majewski M, Porter RM, Betz OB, Betz VM, Clahsen H, Flückiger R, et al. Improvement of tendon repair using muscle grafts transduced with TGF-β1 cDNA. European cells & materials. 2012;23:94.

155. Müller SA, Dürselen L, Heisterbach P, Evans C, Majewski M. Effect of a simple collagen type I sponge for Achilles tendon repair in a rat model. The American journal of sports medicine. 2016;44(8):1998-2004.

156. Komatsu I, Wang JH, Iwasaki K, Shimizu T, Okano T. The effect of tendon stem/progenitor cell (TSC) sheet on the early tendon healing in a rat Achilles tendon injury model. Acta biomaterialia. 2016;42:136-46.

157. Usman MA, Nakasa T, Shoji T, Kato T, Kawanishi Y, Hamanishi M, et al. The effect of administration of double stranded MicroRNA-210 on acceleration of Achilles tendon healing in a rat model. Journal of Orthopaedic Science. 2015;20(3):538-46.

158. Majewski M, Heisterbach P, Jaquiéry C, Dürselen L, Todorov A, Martin I, et al. Improved tendon healing using bFGF, BMP-12 and TGFβ1 in a rat model. European cells & materials. 2018;35:318-34.

159. Müller SA, Evans CH, Heisterbach PE, Majewski M. The role of the paratenon in Achilles tendon healing: a study in rats. The American journal of sports medicine. 2018;46(5):1214-9.

160. Devana SK, Kelley BV, McBride OJ, Kabir N, Jensen AR, Park SJ, et al. Adipose-derived human perivascular stem cells may improve achilles tendon healing in rats. Clinical orthopaedics and related research. 2018;476(10):2091.

161. Genç E, Beytemur O, Yuksel S, Eren Y, Çağlar A, Küçükyıldırım BO, et al. Investigation of the biomechanical and histopathological effects of autologous conditioned serum on healing of Achilles tendon. Acta orthopaedica et traumatologica turcica. 2018;52(3):226-31.

162. Misir A, Kizkapan TB, Arikan Y, Akbulut D, Onder M, Yildiz KI, et al. Repair within the first 48 h in the treatment of acute Achilles tendon ruptures achieves the best biomechanical and histological outcomes. Knee Surgery, Sports Traumatology, Arthroscopy. 2019:1-10.

163. Weng C-J, Lee D, Ho J, Liu S-J. Doxycycline-Embedded Nanofibrous Membranes Help Promote Healing of Tendon Rupture. International journal of nanomedicine. 2020;15:125.

164. Eliasson P, Andersson T, Aspenberg P. Influence of a single loading episode on gene expression in healing rat Achilles tendons. Journal of applied physiology. 2011;112(2):279-88.

165. Eliasson P, Andersson T, Aspenberg P. Achilles tendon healing in rats is improved by intermittent mechanical loading during the inflammatory phase. Journal of Orthopaedic Research. 2012;30(2):274-9.

166. Fryhofer GW, Freedman BR, Hillin CD, Salka NS, Pardes AM, Weiss SN, et al. Postinjury biomechanics of Achilles tendon vary by sex and hormone status. Journal of applied physiology. 2016;121(5):1106-14.

167. Freedman BR, Salka NS, Morris TR, Bhatt PR, Pardes AM, Gordon JA, et al. Temporal healing of Achilles tendons following injury in rodents depends on surgical treatment and activity. The Journal of the American Academy of Orthopaedic Surgeons. 2017;25(9):635.

168. Huegel J, Boorman-Padgett JF, Nuss CA, Minnig MCC, Chan PY, Kuntz AF, et al. Quantitative comparison of three rat models of Achilles tendon injury: A multidisciplinary approach. Journal of Biomechanics. 2019;88:194-200.

169. Andersson T, Eliasson P, Hammerman M, Sandberg O, Aspenberg P. Low-level mechanical stimulation is sufficient to improve tendon healing in rats. Journal of applied physiology. 2012;113(9):1398-402.

170. Hammerman M, Aspenberg P, Eliasson P. Microtrauma stimulates rat Achilles tendon healing via an early gene expression pattern similar to mechanical loading. Journal of applied physiology. 2014;116(1):54-60.

171. Ackerman JE, Nichols AE, Studentsova V, Best KT, Knapp E, Loiselle AE. Cell non-autonomous functions of S100a4 drive fibrotic tendon healing. Elife. 2019;8:e45342.

172. Chamberlain CS, Duenwald-Kuehl SE, Okotie G, Brounts SH, Baer GS, Vanderby R. Temporal healing in rat achilles tendon: ultrasound correlations. Annals of biomedical engineering. 2013;41(3):477-87.

173. Dyment NA, Liu C-F, Kazemi N, Aschbacher-Smith LE, Kenter K, Breidenbach AP, et al. The paratenon contributes to scleraxis-expressing cells during patellar tendon healing. PloS one. 2013;8(3):e59944.

174. Dyment NA, Hagiwara Y, Matthews BG, Li Y, Kalajzic I, Rowe DW. Lineage tracing of resident tendon progenitor cells during growth and natural healing. PloS one. 2014;9(4).

175. Galatz LM, Sandell LJ, Rothermich SY, Das R, Mastny A, Havlioglu N, et al. Characteristics of the rat supraspinatus tendon during tendon-to-bone healing after acute injury. Journal of Orthopaedic Research. 2006;24(3):541-50.

176. Cury DP, Schäfer BT, de Almeida SRY, Righetti MMdS, Watanabe I-s. Application of a Purified Protein From Natural Latex and the Influence of Suture Type on Achilles Tendon Repair in Rats. The American journal of sports medicine. 2019:0363546518822836.

177. Ackerman JE, Best KT, O'Keefe RJ, Loiselle AE. Deletion of EP4 in S100a4-lineage cells reduces scar tissue formation during early but not later stages of tendon healing. Scientific reports. 2017;7(1):1-11.

178. Best KT, Loiselle AE. Scleraxis lineage cells contribute to organized bridging tissue during tendon healing and identify a subpopulation of resident tendon cells. The FASEB Journal. 2019;33(7):8578-87.

179. Best KT, Lee FK, Knapp E, Awad HA, Loiselle AE. Deletion of NFKB1 enhances canonical NF-κB signaling and increases macrophage and myofibroblast content during tendon healing. Scientific reports. 2019;9(1):1-11.

180. Best KT, Mora KE, Buckley MR, Loiselle AE. Scleraxis-Lineage Cell Depletion Improves Tendon Healing. bioRxiv. 2020.

181. Andarawis-Puri N, Sereysky JB, Sun HB, Jepsen KJ, Flatow EL. Molecular response of the patellar tendon to fatigue loading explained in the context of the initial induced damage and number of fatigue loading cycles. Journal of Orthopaedic Research. 2012;30(8):1327-34.

182. George N, Bell R, Paredes J, Taub P, Andarawis-Puri N. Superior mechanical recovery in male and female MRL/MpJ tendons is associated with a unique genetic profile. Journal of Orthopaedic Research®. 2020.

183. Ansorge HL, Hsu JE, Edelstein L, Adams S, Birk DE, Soslowsky LJ. Recapitulation of the Achilles tendon mechanical properties during neonatal development: a study of differential healing during two stages of development in a mouse model. Journal of Orthopaedic Research. 2012;30(3):448-56.

184. Beredjiklian PK, Favata M, Cartmell JS, Flanagan CL, Crombleholme TM, Soslowsky LJ. Regenerative versus reparative healing in tendon: a study of biomechanical and histological properties in fetal sheep. Annals of biomedical engineering. 2003;31(10):1143-52.

185. Freedman BR, Fryhofer GW, Salka NS, Raja HA, Hillin CD, Nuss CA, et al. Mechanical, histological, and functional properties remain inferior in conservatively treated Achilles tendons in rodents: Long term evaluation. Journal of biomechanics. 2017;56:55-60.

186. in 't Veld P, Stevens M. Simulation of the mechanical strength of a single collagen molecule. Biophysical journal. 2008;95(1):33-9.

187. Gautieri A, Pate MI, Vesentini S, Redaelli A, Buehler MJ. Hydration and distance dependence of intermolecular shearing between collagen molecules in a model microfibril. Journal of biomechanics. 2012;45(12):2079-83.

188. Gautieri A, Vesentini S, Redaelli A, Ballarini R. Modeling and measuring viscoelastic properties: From collagen molecules to collagen fibrils. International Journal of Non-Linear Mechanics. 2013;56:25-33.

189. Gautieri A, Vesentini S, Redaelli A, Buehler MJ. Viscoelastic properties of model segments of collagen molecules. Matrix Biology. 2012;31(2):141-9.

190. Buehler MJ. Nature designs tough collagen: explaining the nanostructure of collagen fibrils. Proceedings of the National Academy of Sciences. 2006;103(33):12285-90.

191. Buehler MJ. Nanomechanics of collagen fibrils under varying cross-link densities: atomistic and continuum studies. Journal of the mechanical behavior of biomedical materials. 2008;1(1):59-67.

192. Buehler MJ. Atomistic and continuum modeling of mechanical properties of collagen: elasticity, fracture, and self-assembly. Journal of Materials Research. 2006;21(8):1947-61.

193. Varma S, Orgel JP, Schieber JD. Nanomechanics of type I collagen. Biophysical journal. 2016;111(1):50-6.

194. Freed AD, Doehring TC. Elastic model for crimped collagen fibrils. 2005.

195. Ciarletta P, Dario P, Micera S. Pseudo-hyperelastic model of tendon hysteresis from adaptive recruitment of collagen type I fibrils. Biomaterials. 2008;29(6):764-70.

196. Parkinson J, Brass A, Canova G, Brechet Y. The mechanical properties of simulated collagen fibrils. Journal of biomechanics. 1997;30(6):549-54.

197. Shearer T, Parnell WJ, Lynch B, Screen HR, David Abrahams I. A Recruitment Model of Tendon Viscoelasticity That Incorporates Fibril Creep and Explains Strain-Dependent Relaxation. Journal of Biomechanical Engineering. 2020;142(7).

198. Tang Y, Ballarini R, Buehler MJ, Eppell SJ. Deformation micromechanisms of collagen fibrils under uniaxial tension. Journal of The Royal Society Interface. 2010;7(46):839-50.

199. Reese SP, Maas SA, Weiss JA. Micromechanical models of helical superstructures in ligament and tendon fibers predict large Poisson's ratios. Journal of biomechanics. 2010;43(7):1394-400.

200. Gasser TC, Ogden RW, Holzapfel GA. Hyperelastic modelling of arterial layers with distributed collagen fibre orientations. Journal of the royal society interface. 2006;3(6):15-35.

201. Marino M, Wriggers P. Finite strain response of crimped fibers under uniaxial traction: an analytical approach applied to collagen. Journal of the Mechanics and Physics of Solids. 2017;98:429-53.

202. Herchenhan A, Kalson NS, Holmes DF, Hill P, Kadler KE, Margetts L. Tenocyte contraction induces crimp formation in tendon-like tissue. Biomechanics and modeling in mechanobiology. 2012;11(3):449-59.

203. Maceri F, Marino M, Vairo G. A unified multiscale mechanical model for soft collagenous tissues with regular fiber arrangement. Journal of biomechanics. 2010;43(2):355-63.

204. Redaelli A, Vesentini S, Soncini M, Vena P, Mantero S, Montevecchi FM. Possible role of decorin glycosaminoglycans in fibril to fibril force transfer in relative mature tendons—a computational study from molecular to microstructural level. Journal of biomechanics. 2003;36(10):1555-69.

205. Smith DW, Rubenson J, Lloyd D, Zheng M, Fernandez J, Besier T, et al. A conceptual framework for computational models of Achilles tendon homeostasis. Wiley Interdisciplinary Reviews: Systems Biology and Medicine. 2013;5(5):523-38.

206. Ciarletta P, Micera S, Accoto D, Dario P. A novel microstructural approach in tendon viscoelastic modelling at the fibrillar level. Journal of biomechanics. 2006;39(11):2034-42.

207. DeFrate L, Li G. The prediction of stress-relaxation of ligaments and tendons using the quasi-linear viscoelastic model. Biomechanics and Modeling in Mechanobiology. 2007;6(4):245-51.

208. Duenwald SE, Vanderby R, Lakes RS. Viscoelastic relaxation and recovery of tendon. Annals of biomedical engineering. 2009;37(6):1131-40.

209. Duenwald SE, Vanderby R, Lakes RS. Stress relaxation and recovery in tendon and ligament: experiment and modeling. Biorheology. 2010;47(1):1-14.

210. Fang F, Sawhney AS, Lake SP. Different regions of bovine deep digital flexor tendon exhibit distinct elastic, but not viscous, mechanical properties under both compression and shear loading. Journal of biomechanics. 2014;47(12):2869-77.

211. Johnson GA, Tramaglini DM, Levine RE, Ohno K, Choi NY, L-Y. Woo S. Tensile and viscoelastic properties of human patellar tendon. Journal of orthopaedic research. 1994;12(6):796-803.

212. Kahn CJ, Dumas D, Arab-Tehrany E, Marie V, Tran N, Wang X, et al. Structural and mechanical multi-scale characterization of white New-Zealand rabbit Achilles tendon. Journal of the mechanical behavior of biomedical materials. 2013;26:81-9.

213. Kahn CJ, Wang X, Rahouadj R. Nonlinear model for viscoelastic behavior of Achilles tendon. Journal of biomechanical engineering. 2010;132(11):111002.

214. Pioletti DP, Rakotomanana L, Benvenuti J-F, Leyvraz P-F. Viscoelastic constitutive law in large deformations: application to human knee ligaments and tendons. Journal of biomechanics. 1998;31(8):753-7.

215. Provenzano P, Lakes R, Corr D, Vanderby R. Application of nonlinear viscoelastic models to describe ligament behavior. Biomechanics and modeling in mechanobiology. 2002;1(1):45-57.

216. Sopakayang R, De Vita R. A mathematical model for creep, relaxation and strain stiffening in parallel-fibered collagenous tissues. Medical engineering & physics. 2011;33(9):1056-63.

217. Ahmadzadeh H, Connizzo BK, Freedman BR, Soslowsky LJ, Shenoy VB. Determining the contribution of glycosaminoglycans to tendon mechanical properties with a modified shear-lag model. Journal of biomechanics. 2013;46(14):2497-503.

218. Atkinson T, Haut R, Altiero N. A poroelastic model that predicts some phenomenological responses of ligaments and tendons. 1997.

219. Fessel G, Snedeker JG. Equivalent stiffness after glycosaminoglycan depletion in tendon—an ultra-structural finite element model and corresponding experiments. Journal of theoretical biology. 2011;268(1):77-83.

220. Khayyeri H, Gustafsson A, Heuijerjans A, Matikainen MK, Julkunen P, Eliasson P, et al. A fibre-reinforced poroviscoelastic model accurately describes the biomechanical behaviour of the rat achilles tendon. PloS one. 2015;10(6):e0126869.

221. Khayyeri H, Longo G, Gustafsson A, Isaksson H. Comparison of structural anisotropic soft tissue models for simulating Achilles tendon tensile behaviour. Journal of the mechanical behavior of biomedical materials. 2016;61:431-43.

222. Machiraju C, Phan A-V, Pearsall A, Madanagopal S. Viscoelastic studies of human subscapularis tendon: relaxation test and a Wiechert model. Computer methods and programs in biomedicine. 2006;83(1):29-33.

223. Obrezkov L, Eliasson P, Harish AB, Matikainen MK. Usability of finite elements based on the absolute nodal coordinate formulation for deformation analysis of the Achilles tendon. International Journal of Non-Linear Mechanics. 2021;129:103662.

224. Swedberg AM, Reese SP, Maas SA, Ellis BJ, Weiss JA. Continuum description of the Poisson′ s ratio of ligament and tendon under finite deformation. Journal of biomechanics. 2014;47(12):3201-9.

225. Troyer KL, Shetye SS, Puttlitz CM. Experimental characterization and finite element implementation of soft tissue nonlinear viscoelasticity. Journal of biomechanical engineering. 2012;134(11).

226. Lanir Y. A structural theory for the homogeneous biaxial stress-strain relationships in flat collagenous tissues. Journal of biomechanics. 1979;12(6):423-36.

227. Lanir Y. Constitutive equations for fibrous connective tissues. Journal of biomechanics. 1983;16(1):1-12.

228. Lanir Y, Lichtenstein O, Imanuel O. Optimal design of biaxial tests for structural material characterization of flat tissues. 1996.

229. Sacks MS. Incorporation of experimentally-derived fiber orientation into a structural constitutive model for planar collagenous tissues. J Biomech Eng. 2003;125(2):280-7.

230. Holzapfel GA, Gasser TC, Ogden RW. A new constitutive framework for arterial wall mechanics and a comparative study of material models. Journal of elasticity and the physical science of solids. 2000;61(1):1-48.

231. Beskos D, Jenkins J. A mechanical model for mammalian tendon. 1975.

232. Comninou M, Yannas IV. Dependence of stress-strain nonlinearity of connective tissues on the geometry of collagen fibres. Journal of Biomechanics. 1976;9(7):427-33.

233. Buckley C, Lloyd D, Konopasek M. On the deformation of slender filaments with planar crimp: theory, numerical solution and applications to tendon collagen and textile materials. Proceedings of the Royal Society of London A Mathematical and Physical Sciences. 1980;372(1748):33-64.

234. Stouffer D, Butler D, Hosny D. The relationship between crimp pattern and mechanical response of human patellar tendon-bone units. 1985.

235. Belkoff SM, Haut R. Microstructurally based model analysis of γ-irradiated tendon allografts. Journal of orthopaedic research. 1992;10(3):461-4.

236. Hurschler C, Loitz-Ramage B, Vanderby Jr R. A structurally based stress-stretch relationship for tendon and ligament. 1997.

237. Shearer T. A new strain energy function for the hyperelastic modelling of ligaments and tendons based on fascicle microstructure. Journal of biomechanics. 2015;48(2):290-7.

238. Kastelic J, Palley I, Baer E. A structural mechanical model for tendon crimping. Journal of biomechanics. 1980;13(10):887-93.

239. Siegmund T, Allen MR, Burr DB. Failure of mineralized collagen fibrils: modeling the role of collagen cross-linking. Journal of biomechanics. 2008;41(7):1427-35.

240. Depalle B, Qin Z, Shefelbine SJ, Buehler MJ. Influence of cross-link structure, density and mechanical properties in the mesoscale deformation mechanisms of collagen fibrils. Journal of the mechanical behavior of biomedical materials. 2015;52:1-13.

241. Fung Y. Biomechanics: Motion, Flow, Stress, and Growth, Edwards Brothers. Inc, Ann Arbor. 1990.

242. Shen ZL, Kahn H, Ballarini R, Eppell SJ. Viscoelastic properties of isolated collagen fibrils. Biophysical journal. 2011;100(12):3008-15.

243. Gupta H, Seto J, Krauss S, Boesecke P, Screen H. In situ multi-level analysis of viscoelastic deformation mechanisms in tendon collagen. Journal of structural biology. 2010;169(2):183-91.

244. Ahmadzadeh H, Freedman BR, Connizzo BK, Soslowsky LJ, Shenoy VB. Micromechanical poroelastic finite element and shear-lag models of tendon predict large strain dependent Poisson's ratios and fluid expulsion under tensile loading. Acta biomaterialia. 2015;22:83-91.

245. Ciarletta P, Ben Amar M. A finite dissipative theory of temporary interfibrillar bridges in the extracellular matrix of ligaments and tendons. Journal of The Royal Society Interface. 2009;6(39):909-24.

246. Goh KL, Meakin JR, Aspden RM, Hukins DW. Stress transfer in collagen fibrils reinforcing connective tissues: effects of collagen fibril slenderness and relative stiffness. Journal of theoretical biology. 2007;245(2):305-11.

247. Szczesny SE, Elliott DM. Interfibrillar shear stress is the loading mechanism of collagen fibrils in tendon. Acta biomaterialia. 2014;10(6):2582-90.

248. Vesentini S, Redaelli A, Montevecchi FM. Estimation of the binding force of the collagen molecule-decorin core protein complex in collagen fibril. Journal of biomechanics. 2005;38(3):433-43.

249. Wu J, Yuan H, Li L, Fan K, Qian S, Li B. Viscoelastic shear lag model to predict the micromechanical behavior of tendon under dynamic tensile loading. Journal of theoretical biology. 2018;437:202-13.

250. Szczesny SE, Elliott DM. Incorporating plasticity of the interfibrillar matrix in shear lag models is necessary to replicate the multiscale mechanics of tendon fascicles. Journal of the mechanical behavior of biomedical materials. 2014;40:325-38.

251. Holmes M, Mow VC. The nonlinear characteristics of soft gels and hydrated connective tissues in ultrafiltration. Journal of biomechanics. 1990;23(11):1145-56.

252. Natali A, Pavan P, Carniel E, Lucisano M, Taglialavoro G. Anisotropic elasto-damage constitutive model for the biomechanical analysis of tendons. Medical engineering & physics. 2005;27(3):209-14.

253. Wilson W, Van Donkelaar C, Van Rietbergen B, Ito K, Huiskes R. Stresses in the local collagen network of articular cartilage: a poroviscoelastic fibril-reinforced finite element study. Journal of biomechanics. 2004;37(3):357-66.

254. Sree VD, Tepole AB. Computational systems mechanobiology of growth and remodeling: Integration of tissue mechanics and cell regulatory network dynamics. Current Opinion in Biomedical Engineering. 2020;15:75-80.

255. Wren TA, Beaupre GS, Carter DR. A model for loading-dependent growth, development, and adaptation of tendons and ligaments. Journal of biomechanics. 1997;31(2):107-14.

256. Wren TA, Beaupré GS, Carter DR. Tendon and ligament adaptation to exercise, immobilization, and remobilization. Journal of rehabilitation research and development. 2000;37(2):217-24.

257. Wren TA. A computational model for the adaptation of muscle and tendon length to average muscle length and minimum tendon strain. Journal of biomechanics. 2003;36(8):1117-24.

258. Young SR, Gardiner B, Mehdizadeh A, Rubenson J, Umberger B, Smith DW. Adaptive remodeling of achilles tendon: a multi-scale computational model. PLoS computational biology. 2016;12(9):e1005106.

259. Isaksson H. Recent advances in mechanobiological modeling of bone regeneration. Mechanics Research Communications. 2012;42:22-31.

260. Khayyeri H, Isaksson H, Prendergast PJ. Corroboration of computational models for mechanoregulated stem cell differentiation. Computer methods in biomechanics and biomedical engineering. 2015;18(1):15-23.

261. Isaksson H, Wilson W, van Donkelaar CC, Huiskes R, Ito K. Comparison of biophysical stimuli for mechano-regulation of tissue differentiation during fracture healing. Journal of biomechanics. 2006;39(8):1507-16.

262. Burke DP, Kelly DJ. Substrate stiffness and oxygen as regulators of stem cell differentiation during skeletal tissue regeneration: a mechanobiological model. PloS one. 2012;7(7):e40737.

263. Geris L, Gerisch A, Vander Sloten J, Weiner R, Van Oosterwyck H. Angiogenesis in bone fracture healing: a bioregulatory model. Journal of theoretical biology. 2008;251(1):137-58.

264. Checa S, Byrne DP, Prendergast PJ. Predictive modelling in mechanobiology: combining algorithms for cell activities in response to physical stimuli using a lattice-modelling approach. Computer methods in mechanics: Springer; 2010. p. 423-35.

265. Isaksson H, van Donkelaar CC, Huiskes R, Yao J, Ito K. Determining the most important cellular characteristics for fracture healing using design of experiments methods. Journal of Theoretical Biology. 2008;255(1):26-39.

266. Itskov M. A generalized orthotropic hyperelastic material model with application to incompressible shells. International Journal for Numerical Methods in Engineering. 2001;50(8):1777-99.

267. Van der Voet A. A comparison of finite element codes for the solution of biphasic poroelastic problems. Proceedings of the Institution of Mechanical Engineers Part H, Journal of engineering in medicine. 1997;211(2):209.

268. Wilson W, Huyghe J, Van Donkelaar C. Depth-dependent compressive equilibrium properties of articular cartilage explained by its composition. Biomechanics and modeling in mechanobiology. 2007;6(1-2):43-53.

269. Song H, Polk JD, Kersh ME. Rat bone properties and their relationship to gait during growth. Journal of Experimental Biology. 2019;222(18):jeb203554.

270. Lee AA, Delhaas T, McCulloch AD, Villarreal FJ. Differential responses of adult cardiac fibroblasts to in vitro biaxial strain patterns. Journal of molecular and cellular cardiology. 1999;31(10):1833-43.

271. Morita Y, Watanabe S, Ju Y, Xu B. Determination of optimal cyclic uniaxial stretches for stem cell-to-tenocyte differentiation under a wide range of mechanical stretch conditions by evaluating gene expression and protein synthesis levels. Acta of bioengineering and biomechanics. 2013;15(3).

272. Sun L, Qu L, Zhu R, Li H, Xue Y, Liu X, et al. Effects of mechanical stretch on cell proliferation and matrix formation of mesenchymal stem cell and anterior cruciate ligament fibroblast. Stem cells international. 2016;2016.

273. Parsons M, Kessler E, Laurent G, Brown R, Bishop J. Mechanical load enhances procollagen processing in dermal fibroblasts by regulating levels of procollagen C-proteinase. Experimental cell research. 1999;252(2):319-31.

274. He Y, Macarak EJ, Korostoff JM, Howard PS. Compression and tension: differential effects on matrix accumulation by periodontal ligament fibroblasts in vitro. Connective tissue research. 2004;45(1):28-39.

275. Goodman S, May S, Heinegård D, Smith R. Tenocyte response to cyclical strain and transforming growth factor beta is dependent upon age and site of origin. Biorheology. 2004;41(5):613-28.

276. Riboh J, Chong AK, Pham H, Longaker M, Jacobs C, Chang J. Optimization of flexor tendon tissue engineering with a cyclic strain bioreactor. The Journal of hand surgery. 2008;33(8):1388-96.

277. Huisman E, Lu A, McCormack RG, Scott A. Enhanced collagen type I synthesis by human tenocytes subjected to periodic in vitro mechanical stimulation. BMC musculoskeletal disorders. 2014;15(1):386.

278. Freedman BR, Gordon JA, Soslowsky LJ. The Achilles tendon: fundamental properties and mechanisms governing healing. Muscles, ligaments and tendons journal. 2014;4(2):245.

279. Jelinsky SA, Li L, Ellis D, Archambault J, Li J, St. Andre M, et al. Treatment with rhBMP12 or rhBMP13 increase the rate and the quality of rat Achilles tendon repair. Journal of Orthopaedic Research. 2011;29(10):1604-12.

280. Lin TW, Cardenas L, Glaser DL, Soslowsky LJ. Tendon healing in interleukin-4 and interleukin-6 knockout mice. Journal of biomechanics. 2006;39(1):61-9.

281. Omachi T, Sakai T, Hiraiwa H, Hamada T, Ono Y, Nakashima M, et al. Expression of tenocyte lineage-related factors in regenerated tissue at sites of tendon defect. Journal of Orthopaedic Science. 2015;20(2):380-9.

282. Scott A, Sampaio A, Abraham T, Duronio C, Underhill TM. Scleraxis expression is coordinately regulated in a murine model of patellar tendon injury. Journal of Orthopaedic Research. 2011;29(2):289-96.

283. Enwemeka CS. Inflammation, cellularity, and fibrillogenesis in regenerating tendon: implications for tendon rehabilitation. Physical therapy. 1989;69(10):816-25.

284. Carter DR, Beaupré GS, Giori NJ, Helms JA. Mechanobiology of skeletal regeneration. Clinical Orthopaedics and Related Research (1976-2007). 1998;355:S41-S55.

285. Claes L, Heigele C. Magnitudes of local stress and strain along bony surfaces predict the course and type of fracture healing. Journal of biomechanics. 1999;32(3):255-66.

286. Lacroix D, Prendergast P. A mechano-regulation model for tissue differentiation during fracture healing: analysis of gap size and loading. Journal of biomechanics. 2002;35(9):1163-71.

287. Simon U, Augat P, Utz M, Claes L. A numerical model of the fracture healing process that describes tissue development and revascularisation. Computer methods in biomechanics and biomedical engineering. 2011;14(01):79-93.

288. Asai S, Otsuru S, Candela ME, Cantley L, Uchibe K, Hofmann TJ, et al. Tendon Progenitor Cells in Injured Tendons Have Strong Chondrogenic Potential: The CD 105-Negative Subpopulation Induces Chondrogenic Degeneration. Stem cells. 2014;32(12):3266-77.

289. Sakabe T, Sakai K, Maeda T, Sunaga A, Furuta N, Schweitzer R, et al. Transcription factor scleraxis vitally contributes to progenitor lineage direction in wound healing of adult tendon in mice. Journal of Biological Chemistry. 2018:jbc. RA118. 001987.

290. Darrieutort-Laffite C, Arnolfo P, Garraud T, Adrait A, Couté Y, Louarn G, et al. Rotator Cuff Tenocytes Differentiate into Hypertrophic Chondrocyte-Like Cells to Produce Calcium Deposits in an Alkaline Phosphatase-Dependent Manner. Journal of Clinical Medicine. 2019;8(10):1544.

291. Han S, Gemmell S, Helmer K, Grigg P, Wellen J, Hoffman A, et al. Changes in ADC caused by tensile loading of rabbit achilles tendon: evidence for water transport. Journal of Magnetic Resonance. 2000;144(2):217-27.

292. Hill JR, Eekhoff JD, Brophy RH, Lake SP. Elastic fibers in orthopedics: Form and function in tendons and ligaments, clinical implications, and future directions. Journal of Orthopaedic Research®. 2020;38(11):2305-17.

293. Kharazi M, Bohm S, Theodorakis C, Mersmann F, Arampatzis A. Quantifying mechanical loading and elastic strain energy of the human Achilles tendon during walking and running. Scientific Reports. 2021;11(1):1-13.

294. Baxter JR, Corrigan P, Hullfish TJ, O'Rourke P, Silbernagel KG. Exercise Progression to Incrementally Load the Achilles Tendon. Medicine and Science in Sports and Exercise. 2020.

295. Arndt A, Bengtsson A-S, Peolsson M, Thorstensson A, Movin T. Non-uniform displacement within the Achilles tendon during passive ankle joint motion. Knee Surgery, Sports Traumatology, Arthroscopy. 2012;20(9):1868-74.

296. M. Khair Ra, Stenroth L, Péter A, Cronin NJ, Reito A, Paloneva J, et al. Non-uniform displacement within ruptured Achilles tendon during isometric contraction. Scandinavian Journal of Medicine & Science in Sports. 2021.

297. Slane LC, Thelen DG. Non-uniform displacements within the Achilles tendon observed during passive and eccentric loading. Journal of biomechanics. 2014;47(12):2831-5.

298. Finni T, Bernabei M, Baan GC, Noort W, Tijs C, Maas H. Non-uniform displacement and strain between the soleus and gastrocnemius subtendons of rat Achilles tendon. Scandinavian journal of medicine & science in sports. 2018;28(3):1009-17.

299. Ekiert M, Tomaszewski KA, Mlyniec A. The differences in viscoelastic properties of subtendons result from the anatomical tripartite structure of human Achilles tendon-ex vivo experimental study and modeling. Acta Biomaterialia. 2021.

300. Liang J-I, Chen M-Y, Hsieh T-H, Liu C-Y, Lam C-F, Chen J-JJ, et al. Video-based gait analysis for functional evaluation of healing achilles tendon in rats. Annals of biomedical engineering. 2012;40(12):2532-40.

301. Eriksen HA, Pajala A, Leppilahti J, Risteli J. Increased content of type III collagen at the rupture site of human Achilles tendon. Journal of Orthopaedic Research. 2002;20(6):1352-7.

302. Sandrey MA. Acute and chronic tendon injuries: factors affecting the healing response and treatment. Journal of Sport Rehabilitation. 2003;12(1):70-91.

303. Blomgran P, Blomgran R, Ernerudh J, Aspenberg P. A possible link between loading, inflammation and healing: Immune cell populations during tendon healing in the rat. Scientific reports. 2016;6:29824.

304. Screen H, Lee D, Bader D, Shelton J. Development of a technique to determine strains in tendons using the cell nuclei. Biorheology. 2003;40(1, 2, 3):361-8.

305. Han WM, Heo S-J, Driscoll TP, Delucca JF, McLeod CM, Smith LJ, et al. Microstructural heterogeneity directs micromechanics and mechanobiology in native and engineered fibrocartilage. Nature materials. 2016;15(4):477-84.

306. Wall ME, Dyment NA, Bodle J, Volmer J, Loboa E, Cederlund A, et al. Cell signaling in tenocytes: response to load and ligands in health and disease. Metabolic Influences on Risk for Tendon Disorders: Springer; 2016. p. 79-95.

307. Shim VB, Fernandez JW, Gamage PB, Regnery C, Smith DW, Gardiner BS, et al. Subject-specific finite element analysis to characterize the influence of geometry and material properties in Achilles tendon rupture. Journal of biomechanics. 2014;47(15):3598-604.

308. Shim VB, Handsfield GG, Fernandez JW, Lloyd DG, Besier TF. Combining in silico and in vitro experiments to characterize the role of fascicle twist in the Achilles tendon. Scientific reports. 2018;8(1):1-12.

309. Shim VB, Hansen W, Newsham-West R, Nuri L, Obst S, Pizzolato C, et al. Influence of altered geometry and material properties on tissue stress distribution

under load in tendinopathic Achilles tendons–A subject-specific finite element analysis. Journal of biomechanics. 2019;82:142-8.

310. Handsfield GG, Greiner J, Madl J, Rog-Zielinska EA, Hollville E, Vanwanseele B, et al. Achilles Subtendon Structure and Behavior as Evidenced From Tendon Imaging and Computational Modeling. Frontiers in Sports and Active Living. 2020;2.
311. Handsfield GG, Inouye JM, Slane LC, Thelen DG, Miller GW, Blemker SS. A 3D model of the Achilles tendon to determine the mechanisms underlying nonuniform tendon displacements. Journal of biomechanics. 2017;51:17-25.
312. Gains CC, Correia JC, Baan GC, Noort W, Screen HR, Maas H. Force transmission between the gastrocnemius and soleus sub-tendons of the Achilles tendon in rat. Frontiers in Bioengineering and Biotechnology. 2020;8.
313. Gerasimyuk B, Lazarev I, Movchan O, Skyban M. Insertional Achilles tendinopathy in patients with Haglund's syndrome: results of computer modeling and biomechanical research. Journal of Education, Health and Sport. 2020;10(7):396-420.
314. Sadeghi S, Taghizadeh H. Microstructural modeling of Achilles Tendon biomechanics focusing on bone insertion site. Medical Engineering & Physics. 2020.
315. Inoue A, Chosa E, Goto K, Tajima N. Nonlinear stress analysis of the supraspinatus tendon using three-dimensional finite element analysis. Knee Surgery, Sports Traumatology, Arthroscopy. 2013;21(5):1151-7.
316. Sano H, Wakabayashi I, Itoi E. Stress distribution in the supraspinatus tendon with partial-thickness tears: an analysis using two-dimensional finite element model. Journal of shoulder and elbow surgery. 2006;15(1):100-5.
317. Seki N, Itoi E, Shibuya Y, Wakabayashi I, Sano H, Sashi R, et al. Mechanical environment of the supraspinatus tendon: three-dimensional finite element model analysis. Journal of Orthopaedic Science. 2008;13(4):348.
318. Wakabayashi I, Itoi E, Sano H, Shibuya Y, Sashi R, Minagawa H, et al. Mechanical environment of the supraspinatus tendon: a two-dimensional finite element model analysis. Journal of shoulder and elbow surgery. 2003;12(6):612-7.
319. Engelhardt C, Ingram D, Müllhaupt P, Farron A, Becce F, Pioletti D, et al. Effect of partial-thickness tear on loading capacities of the supraspinatus tendon: a finite element analysis. Computer methods in biomechanics and biomedical engineering. 2016;19(8):875-82.
320. Quental C, Folgado J, Monteiro J, Sarmento M. Full-thickness tears of the supraspinatus tendon: A three-dimensional finite element analysis. Journal of biomechanics. 2016;49(16):3962-70.

321. Morales-Orcajo E, Souza TR, Bayod J, de Las Casas EB. Non-linear finite element model to assess the effect of tendon forces on the foot-ankle complex. Medical engineering & physics. 2017;49:71-8.

322. Chatzistefani N, Chappell M, Hutchinson C, Kletzenbauer S, Evans N. A mathematical model characterising Achilles tendon dynamics in flexion. Mathematical biosciences. 2017;284:92-102.

323. Spyrou L, Aravas N. Muscle-driven finite element simulation of human foot movements. Computer methods in biomechanics and biomedical engineering. 2012;15(9):925-34.

324. Choi H, Peters KM, MacConnell MB, Ly KK, Eckert ES, Steele KM. Impact of ankle foot orthosis stiffness on Achilles tendon and gastrocnemius function during unimpaired gait. Journal of biomechanics. 2017;64:145-52.

325. Kay AD, Husbands-Beasley J, Blazevich AJ. Effects of contract–relax, static stretching, and isometric contractions on muscle–tendon mechanics. Medicine & Science in Sports & Exercise. 2015;47(10):2181-90.

326. Jalali P, Noorani MS, Hassannejad R, Ettefagh MM, editors. An active model for gastrocnemius muscle activity to predict the impact force during running. 2016 4th international conference on robotics and mechatronics (ICROM); 2016: IEEE.